Final Scientific/Technical Report

Reporting Period: October 1, 2011 to June 30, 2017

Report Submission Date: March 22, 2018

Federal Agency & Org:	U.S. Department of Energy, Vehicle Technologies Office
Award Number:	DE-EE0005547
Project Title:	Industrial Scale-Up of Low-Cost Zero-Emissions Magnesium by INFINIUM Electrolysis
Project Period:	October 1, 2011 – June 30, 2017
Recipient Organization:	INFINIUM, Inc. (fka Metal Oxygen Separation Technologies, Inc.) 3 Huron Dr., Natick, MA 01760-1334
Partners:	Praxair Inc., Spartan Light Metal Products, Kingston Process Metallurgy, Trustees of Boston University, Magna International
Principal Investigator:	Adam C. Powell, IV, 781-898-3430, apowell@infiniummetals.com
Business Contact:	Denice Sakakeeny, 617-852-8892, dms@infiniummetals.com
DOE Project Officer:	Aaron Yocum, 304-285-4852, Aaron.Yocum@netl.doe.gov
DOE HQ Contact:	William Joost, 202-687-6020, william.joost@ee.doe.gov
DOE Contract Specialist:	Rochelle Hass, 720-356-1559, rochelle.hass@go.doe.gov

Acknowledgment: This material is based upon work supported by the Department of Energy under Award Number DE-EE0005547.

Executive Summary

Magnesium alloys, particularly those with rare earths, have higher strength-to-weight and much higher bending stiffness-to-weight than aluminum and steel alloys. For motor vehicles whose bodies are typically stiffness-limited, this can lead to considerable weight reduction. For example, the Ford-Magna Multi-Material Lightweight Vehicle (MMLV) project showed that an aluminum-intensive vehicle can achieve 25% weight savings vs. steel; a magnesium-intensive vehicle achieved 40-45% weight savings.[1]

INFINIUM led a project whose goal was at first to produce pure magnesium, and later magnesium-rare earth alloys, directly from oxides. The reduction technology is molten salt electrolysis with a fluoride salt bath, similar to the Hall-Héroult process for aluminum. The pure magnesium component of the project used novel oxygen-producing anodes with a zirconia solid electrolyte tube between the molten salt and anode. That component developed several novel methods for improving current density, current efficiency, and zirconia tube robustness including:

- Ability to hot-swap zirconia tubes in and out of the ≥1050°C bath, despite the low thermal shock resistance of zirconia;
- An integrated anode-cathode assembly to introduce Mg vapor-diluting argon at the cathode while facilitating hot-swap and contained any tube breakage;
- A liquid magnesium condenser with high yield despite 10:1 argon dilution;
- An anode current collector assembly which conducts high current from the liquid silver anode at ≥1050°C;
- A porous displacer to minimize liquid silver use in the anode;
- Up to 170 hours of continuous run time in a single zirconia tube;
- Up to 2448 hours of high-temperature electrolysis apparatus lifetime;
- 85-95% current efficiency (oxygen flow basis) over 90+ hours of continuous run time.

The project later shifted to direct production of magnesium-neodymium master alloy for Mg-rare earth alloys. These alloys are typically made by dissolution of rare earth metals into magnesium, and cost over six times the rare earth basis price of the master alloy. At the time of the experiments, Mg-30%Nd master alloy sold for $120/kg, i.e. $400/kg Nd basis, while pure Nd sold for $60. This project achieved continuous production of Mg master alloy with 45-50% Nd directly from mixed MgO and Nd_2O_3, resulting in very low raw material cost. Features of that process include:

- High current, up to 450 A, producing over 200 g/hour master alloy;
- Steel dam and ceramic liner for floating alloy product collection with 85-95% current efficiency (reduced metals basis);
- Automatic oxide feeding for reduced downtime and operator interaction;
- Low iron and other impurities when using a tungsten cathode.

The resulting process produced a total of over 30 kg of Mg-Nd master alloy, which was made into nearly 250 kg of AE42 (Mg-4%Al-2%Nd) alloy.

[1] Szszek et al, "Multi-Material Lightweight Vehicles," presented at DOE VTO Annual Merit Review 2015.

Table of Contents

Executive Summary....2
Table of Contents....3
Comparison of Accomplishments with Goals and Objectives....4
Project Objective....4
Background....4
Accomplishments....4
Magnesium Production with Reduced Operator Interaction....5
Anode Manufacturing....7
Make and Test Parts from Recipient Magnesium....9
Magnesium Life-cycle Cost, Energy, GHG and Other Emissions Modeling....9
Magnesium Production Plant....10
Summary of Project Activities....11
Magnesium Production with Reduced Operator Interaction....11
Magnesium Production....11
Mg-Nd Alloy Production....29
Anode Manufacturing....50
Make and Test Parts from the Recipient Magnesium....70
Model Lifecycle Costs, Energy Use and Emissions....72
Thermodynamic Modeling....72
Finite Element Analysis....72
Cost Model....75
Energy, GHG and Other Emissions....82
Project Products and Technology Transfer Activities....92
Publications & Presentations....92
Technologies/Techniques....94
Patents and Patent Applications....95
Computer Modeling....96
Model Description, Key Assumptions, Version, Source, Intended Use....96
Model Performance Criteria....96
Test Results....96
Model Theory....96
Mathematics Used....96
Hardware Requirements....97
Documentation....97
References....97

Comparison of Accomplishments with Goals and Objectives

Project Objective

The objective of this project is to develop of a low-cost molten salt electrolysis process to make high-purity magnesium directly from refractory-grade magnesium oxide which utilizes available raw materials from the United States, an energy conversion approach that is clean and efficient, and a form of the product that is sufficiently pure as to be readily inserted into a vehicle manufacturing value stream enabling a straightforward commercialization strategy into the vehicular market.

Background

Direct electrolysis of magnesium oxide has long been a grand challenge of the magnesium industry. Production begins with making magnesium oxide from brines or sea water by reacting dissolved $MgCl_2$ with NaOH to produce NaCl and insoluble $Mg(OH)_2$, which is removable by filtration. Heating the hydroxide then drives off its water to produce MgO. Today's chloride electrolysis plants must then use carbo-chlorination or chloride dehydration to produce pure $MgCl_2$, and electrolyze that to produce Mg metal and Cl_2 gas. Direct MgO electrolysis would save this carbo-chlorination step, which is energy- and capital-intensive and can produce harmful dioxin and furan emissions. MgO electrolysis would also eliminate the need to carefully contain chlorine that often escapes as a pollutant, and would potentially use less energy due to the lower enthalpy of formation of MgO vs. $MgCl_2$.

Many have tried MgO electrolysis in a Hall-Héroult cell equivalent, but current efficiency is very low, generally below 50, due to magnesium metal dissolution into the bath. In contrast, the INFINIUM magnesium-rare earth master alloy process runs at 85-95% current efficiency. It is continuous and highly automated, and could pave the way to efficient direct MgO electrolysis.

Master alloy, often called "hardener", is essential for production of magnesium alloys containing rare earth metals (typically 0.5-7 wt%). These alloys exhibit very high strength and low creep rate, including at high temperature, and are also more formable and less flammable than other Mg alloys. However, rare earth metal dissolution kinetics in liquid magnesium are very slow, much slower than other alloying elements such as aluminum, zinc and tin, resulting in high cycle time and low capital utilization for alloying furnaces. With fine structure, master alloy disintegrates quickly in liquid magnesium, and small rare earth precipitates dissolve in seconds rather than tens of minutes. For a die casting or sheet production operation, the much faster-dissolving master alloy can go straight into production equipment, lowering cost.

Accomplishments

INFINIUM produced over 30 kg Mg-Nd master alloy directly from oxides MgO and Nd_2O_3. A project partner blended this with other required elements to produce over 500 lbs of AE42 (4% Al 2% Nd, balance Mg) alloy. INFINIUM shipped most of that alloy to our automotive partner for testing in a die cast part to ensure fitness for motor vehicle use.

The project was comprised of five tasks:

- Magnesium (and master alloy) production with reduced operator interaction
- Anode manufacturing (zirconia-sheathed oxygen-producing anodes)
- Make and test parts from recipient magnesium
- Magnesium life-cycle cost, energy, GHG and other emissions modeling
- Magnesium production plant

Detailed accomplishments follow by task, and separated into three project phases.

Magnesium Production with Reduced Operator Interaction

Phase 1

- INFINIUM built and ran a large-scale (11-tube) pre-alpha system in the bell jar apparatus. (Q3)
- INFINIUM conducted an aggressive test to understand the ability of zirconia to operate in steep, transient, thermal gradients, which showed the zirconia capable of withstanding the harshest thermal ramp our system can produce. (Q3)
- INFINIUM conducted an experiment to understand the effect of high temperature steam (H_2O) on zirconia, finding zirconia to have a susceptibility to fracture in steam environments. (Q3)
- INFINIUM conducted the first tests of the alpha magnesium production prototype to integrate all subsystems, including raw material feeding, electrolysis with combined anode/cathode module, mechanical stirring, and condenser. (Q5)

Phase 2

- With continuous furnace operation, have developed better ways to resolve clogging and to hot swap anode assemblies. (Q6)
- Subcontractor Boston University (BU) completed analysis of current efficiency and electron transference number during a 30-hour electrolysis experiment. (Q6)
- Subcontractor Boston University (BU) developed a magnesium equivalent circuit to model current flow during electrolysis. Modeling led to the new concept of oxidizing dissolved metal in the flux to increase current efficiency and zirconia tube lifetime. (Q7)
- Furnace ran continuously from mid-July 2013 (2448 hours as of 1 0/25). (Q8)
- Operated a single anode continuously for 80 hrs to produce 52g H_2O and 26g recoverable Mg. (Q8)
- Fabricated and installed a mechanical tube loader. (Q8)
- Subcontractor Kingston Process Metallurgy (KPM) conducted a short-term magnesium oxide electrolysis experiment in a transparent crucible and furnace. The transparent crucible had a quartz sheath over part of the cathode, and exhibited magnesium vapor production without argon. (Q8)
- Upgraded Alpha 3.0 to a vacuum prototype. Built the vacuum furnace and installed metal gas lines/seals, pressure control system, replaceable salt crucible, and programmable logic controller. (Q9)

Phase 3

- Conducted electrolysis with Vendors A, B and C zirconia to establish a baseline of tube performance. (Q10)
- Designed experiments for Increased Immersion Electrolysis to begin in May 2014. (Q10)
- Alpha 4.0, a platform for uptime and anode assembly optimization, cooled down in May for a few minor alterations and gas line reconfiguration. It came back online the first week in June. (Q11)
- Conducted two successful electrolysis runs with oxygen-producing LSM current collectors and Vendor A zirconia tubes to determine anode assembly performance and design improvements. (Q11)
- Conducted first successful 'hot swap' of current collector, i.e., replacing the current collector within the same hot zirconia tube, eliminating the need to cool down and heat up the furnace. (Q11)
- As of September 30th, the longest single tube life in the Alpha 4.0 was 170 hours, an improvement from Alpha 4.0's previous benchmark of 135 hours. Recovered a total of 47g of Mg from the 4.0 prototype. (Q12)
- Successfully recovered approximately 25g of Mg metal from the Alpha 4.0 condenser following 65 amp-hours of electrolysis. Higher Mg yield may be a result of cooling of the system to prevent oxidation; metal solubility in the salt decreases along with temperature. (Q12)
- Developed process to produce Mg-Nd master alloy for distillation and alloying. (Q13)
- Conducted small scale Mg-Nd master alloy electrolysis with promising results. (Q13)
- Conducted 12 small-scale electrolysis experiments and produced 172g of Md-Nd alloy. (Q14)
- Commissioned a Gamma electrolysis cell for Nd production. (Q14)
- Identified Mg-Nd candidate flux composition, which still requires further optimization. (Q14)
- Refined the cathode and containment design to accommodate floating metal (as opposed to original concept of sinking metal). (Q14)
- Designed and developed first prototype of molten metal siphon. (Q14)
- Refined process to produce MgNd master alloy for distillation and alloying into AE42. (Q15)
- Conducted several small-scale electrolysis experiments, and produced 336g of MdNd alloy. Refined MgNd master alloy intermediate-scale cell design (Delta 1.0). (Q15)
- Continued design on Alpha 5.0, to have larger ports to accommodate up to 1.25" (3.2 cm) outer diameter tubes. (Q15)
- Gamma electrolysis cell came online and produced 2 kg of Nd. (Q15)
- Delta 1.0 scale-up production cell came online and ran first electrolysis, producing 390g of MgNd alloy over four days when a crucible failure ended the production run. (Q15)
- Produced a total of 3.5kg of MgNd alloy (approximately 50%Mg-50%Nd by

weight) at an average current efficiency of 60-70%. (Q16)
- Tested an MgO dam and a graphite dam for metal collection within the cell during electrolysis. (Q16)
- Conducted experiments which determine optimal feed to be 885.8g MgO + 542.4g Nd_2O_3 per kg metal which should also produce 53.5%-46.5% MgNd alloy. (Q16)
- Sent flux samples from most efficient electrolysis runs for GDMS analysis. (Q16)
- Continued design of molten metal siphon. (Q16)
- Produced 7 kg of MgNd Alloy (Approximately 50%Mg-50%Nd by weight) (Q17)
- Delta 2.0 brought online on December 17th, 2015 (Q17)
- Delta 2.0 produced 70-80g of MgNd per hour at a current yield of 90-95% (Q17)
- Identified a dam configuration allowing for collection of 5-10 times more metal during electrolysis (Q17)
- Conducted in house ICP-OES analysis of product metal composition in order to provide rapid feedback to production cell operators (Q17)
- Developed method for ICP-OES bath composition analysis (Q17)
- Produced 20 kg of MgNd Alloy (Approximately 50%Mg-50%Nd) (Q18)
- Began 2 shift operation of Delta 1.1, including weekends (Q18)
- Verified the use of steel as cheaper cathode material (Q18)
- Identified stable, low cost MgO supply chain. (Q18)
- Develop continuous oxide feeder (Q18)
- Commissioned Gamma 1.0 MgNd production cell (Q18)
- Minimized surface shorting (Q18)
- Produced 10 kg of MgNd Alloy (Approximately 50%Mg-50%Nd), bringing total production to **30kg (Q19)**
- Began production in 350A Gamma Cell (Q19)
- Further characterized properties of the electrolyte overtime (Q19)

Anode Manufacturing

Phase 1

No activity

Phase 2

- Produced 1 kg of INFINIUM 8YSZ powder and manufactured several pucks and one small tube, which sintered to 92.3% density. (Q6)
- Slip cast a total of 60 14” (35.6 cm) and 24” (61 cm) tubes from four different compositions; air and vacuum sintered all with 100% yield. (Q7)
- Commenced a three-phase tube optimization study: (1) corrosion, (2) current efficiency, and (3) cost. First phase corrosion study began with a 100 hr static test to determine yttria equilibrium for different zirconia compositions. (Q7)
- Filed a provisional patent application for a low-silver anode assembly that will minimize silver use, reducing it by a factor of ten for oxygen production. (Q7)
- Re-designed static soak test to minimize contamination and identified Brand C

as least corrosive out of four samples. Brand C tubes scheduled for manufacturing. (Q8)

- Designed and fabricated prototype for semi-static testing of seven different flux compositions simultaneously. Unable to reach required temperature in designated furnace, began installing a more powerful furnace. (Q8)
- Subcontractor Boston University (BU) and INFINIUM conducted initial experiments to oxidize metal in flux in order to reduce electronic conductivity with excellent results. The first demonstration at BU produced a 70x drop in electronic conductivity and measurable current efficiency improvement. A separately-funded INFINIUM test with dysprosium also improved electrical characteristics. We are planning magnesium tests at INFINIUM. (Q8)
- Fabricated multiple double walled cathodes to integrate and control argon stirring for the Beta prototype. Designed and manufactured single walled cathodes for the Alpha vacuum prototype. (Q9)

Phase 3

- Designed and began fabricating a static testing device that will test six different tube compositions simultaneously. Drafted SOP for static testing. (Q10)
- Repaired the semi-static testing device and ran two successful tests of tube and flux combinations to identify resistance changes before, during, and after 72-hour soaks. (Q10)
- Tested the stability of inert anode current collectors by suspending them in liquid silver at temperature for five days. Improved the design and began manufacturing. (Q10)
- Conducted two resistance tests on oxygen-producing LSM current collectors. Test results verified current collector resistance, determined usable life, qualified our manufacturing and assembly process, and provided data on failure modes to improve current collector lifetime. (Q11)
- Conducted two successful electrolysis runs with redesigned current collectors. During the first run, the current collector failed after 30 minutes, likely because we inserted it too far into the silver. We revised the insertion procedure accordingly. (Q11)
- Conducted our first successful ‘hot swap’ of the current collector and maintained a current efficiency of 65-75% over the first 40 hours. (Q11)
- Made a slight modification to current collector geometry in hopes of further lowering the resistance and facilitate higher current capabilities. Fabricated this new version and are conducting the silver bath resistance test. Initial results indicated resistance at approximately 0.08Ω per current collector. (Q11)
- Ran electrolysis with graphite current collector in salt anode liquid for 48 hours. Initial results promising with regard to zirconia membrane corrosion. Conducted literature and phase diagram review to identify alternative current collector materials. Have identified two candidate electrode materials and procured samples for testing. (Q11)
- Ran electrolysis to test three cathode cage designs: perforated cathode, offset purge cathode, slotted cathode. Results indicate tube degradation corresponding to purge areas on the cathode cage are the result of

concentrated gas bubbling, not electric field. (Q12)
- Conducted additional static test to determine correct Y_2O_3 concentration to prevent yttria enrichment or leaching of the YSZ membrane. Lowered the Y_2O_3 concentration from 1.25% to 0.5% then soaked samples at 1150 °C for 72 hours with promising results. Boston University is conducting a separate analysis to confirm validity of our measurement technique and achieve higher resolution. (Q12)
- Conducted electrolysis with Vendor C tubes fired at a higher temperature with outstanding results in current efficiency. (Q13)
- Successfully fired 1" (2.5 cm) and 1.25" (3.2 cm) tubes for testing. (Q15)
- Designed and manufactured by sintering porous thimbles made from fused alumina particles to minimize the amount of silver required for electrolysis. (Q14)
- Conducted thimble experiment to test silver infiltration into sintered alumina compacts using powders with three different particle sizes, and identified optimal material for this application. (Q15)

Make and Test Parts from Recipient Magnesium

Phase 1

No activity

Phase 2

No activity

Phase 3

- Conducted two electrolysis runs. (Q11)
- Conducted nine electrolysis runs and recovered 41g of Mg metal, 25g in a single run. (Q12)
- Finalized plans for producing AE42 die casting alloy, including nearly all vendors. (Q14)
- Shipped 30 lbs (13.6 kg) of 50-50 MgNd master alloy to MagPro. (Q18)
- Shipped 50 lbs (22.7 kg) of 50-50 MgNd master alloy to MagPro. (Q19)
- Cast 590lbs (267.6 kg) of AE42 in two separate lots utilizing a large casting partner company. (Q20)
- Shipped 507lbs (229.9 kg) of AE42 alloy to Vehma. (Q20)

Magnesium Life-cycle Cost, Energy, GHG and Other Emissions Modeling

Phase 1

- INFINIUM developed a new axisymmetric finite element model of the anode assembly, including the current collector, liquid metal anode, and zirconia solid electrolyte, with temperature-dependent material properties throughout. (Q5)

Phase 2

- Conducted an energy and emissions impact model of this technology. (Q6)
- Completed a ground-up preliminary plant cost model, which starts with a heat

balance on electrolysis cells, and proceeds to cell house scale and a complete plant (Q9)

Phase 3

- Built a new Finite Element Analysis (FEA) model of our full 300 A industrial tube design, which is axisymmetric and very fast, and includes temperature-dependent properties of all materials. (Q12)

Magnesium Production Plant

Phase 1

No activity

Phase 2

- Completed a detailed plant design narrative to refine capital and balance of plant cost estimates. The electrolysis cell house reaches good returns to scale in modules of about 3500-4000 tons/year, indicating ability to scale down to “minimills” at mines or customer sites. (Q8)
- Completed a new preliminary plant design in tandem with the plant cost model of Task 5. (Q9)

Summary of Project Activities

As with Accomplishments, these are listed by major task and phase of the project.

Magnesium Production with Reduced Operator Interaction

Magnesium Production

Work in Phase I consisted of multiple experiments designed to gather data for design of subsystems, and design and construction of an "Alpha" prototype system for long-term operation and integrated testing of materials and components and small scale.

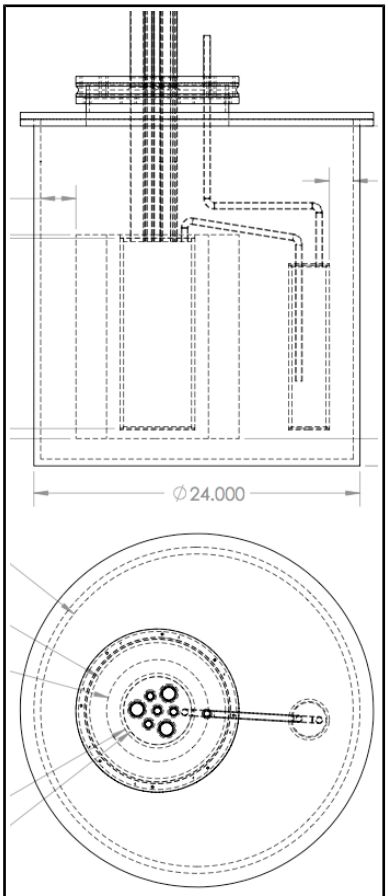

Figure 1: design of the first three-tube

Figure 2: Bell jar with advanced one-tube experiment apparatus.

INFINIUM conducted the first magnesium oxide electrolysis experiment in a side-by-side crucible-condenser configuration. This used three zirconia anode tubes and three stainless steel cathodes. The crucible and condenser apparatus were made of welded stainless steel, with the crucible heated by a Kanthal heating element, and heating tape on the condenser and crucible-condenser tube. The entire apparatus was in a sealed inverted bell jar back-filled with argon.

Figure 1 shows the design of the bell jar, lid, heating element, crucible and condenser. This was the first magnesium electrolysis experiment not conducted in a tube furnace, and the new side-by-side arrangement buildt our understanding for later designs. The experiment produced a few grams of magnesium before the crucible-condenser tube clogged due to failure of its heating tape.

Following that experiment the team conducted a second experiment in the bell jar. Figure 2 shows the bell jar, heating element, and stainless steel crucible-condenser apparatus. This experiment employed just one zirconia anode, and added mechanical stirring and MgO feeding. It also demonstrated the first "hot swap" on-line zirconia anode tube replacement out of and into a hot crucible with molten salt, which is very challenging because zirconia's low thermal conductivity and high CTE make it very susceptible to fracture by thermal shock.

Zirconia Robustness to Thermal Gradient INFINIUM conducted a test to understand the ability of zirconia to operate in steep, transient, thermal gradients, which showed the zirconia capable of withstanding the harshest thermal ramp our

system can produce. An apparatus was constructed with a ½" steel heated section surrounding a zirconia tube with the regions above and below the tube insulated (Figure 2). This testing aggressively mimicked the transient thermal profile during heat-up. At the normal rate of heat-up, as well as twice the normal rate of heat-up, no damage was noted. In fact, at maximum furnace heat-up (i.e., 2.3 to 4 times normal rate) no damage was noted.

Magnesium Condenser An experiment was conducted to demonstrate the ability to successfully condense magnesium vapor within a controlled condenser unit. 300 grams of magnesium was condensed, which was greater than 97% of the available material.

Initial Design.

INFINIUM completed the initial design and engineering of a long-run continuous kilogram-scale magnesium production system, this exercise was used to determine the potential failure points of the process. The goal was to develop a unit work well for the desired 4000-8000 hour lifetime of the process. The largest process risks for this project as a whole is long-term durability of the apparatus, because of the high temperature, chemically aggressive molten salt, and high electrical current. The goal of this apparatus is to reduce this risk at small scale by running electrolysis experiments. Two prototype families were built, Alpha and Beta. The process was to iterate on the two process so that problems found in Alpha unit would be applied to the beta units, The beta units more closely resembled the final operating unit based on the initial design, for as long as possible. Subsequent changes due the challenges in alpha and beta operation led to development of the delta and gamma furnaces, these were designed for Mg-Nd alloy production.

Figure 3: Furnace rendering for long-run kilogram-scale experiments.

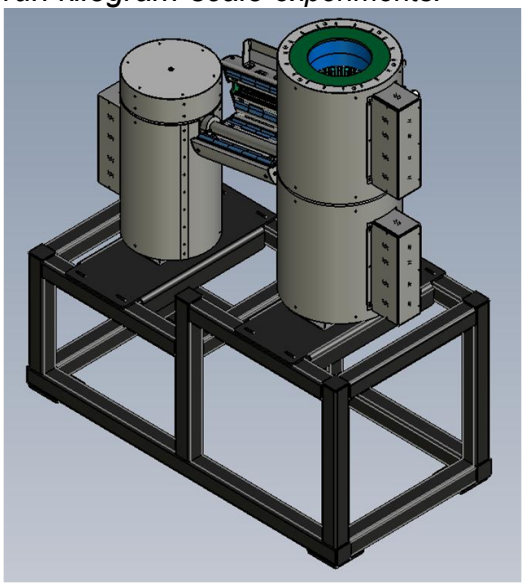

Figure 3 shows a rendering of the four-component furnace which will house these experiments. On the right are the two components holding the crucible with zirconia tubes leading up to the top manifold. These two components have a total of four independent temperature-controlled heating zones to carefully manage the thermal gradients around the zirconia tubes. The bridge component holds the tube bringing magnesium and argon vapors to the condenser, which transitions from the 1150° C crucible to the 650° C condenser. The condenser itself is in the furnace component on the left.

Alpha Prototype

This apparatus will used one zirconia tube at 20-60 A current, and 80 hours. The furnace operated 2448 hours continuously. Continuous furnace life-time was found to a limiting factor, the goal of 5000 hour operation was not achieved. Operation started late in 2012 Q1, and continued for 2400 hours. A schematic of this apparatus is shown below in Figure 4.

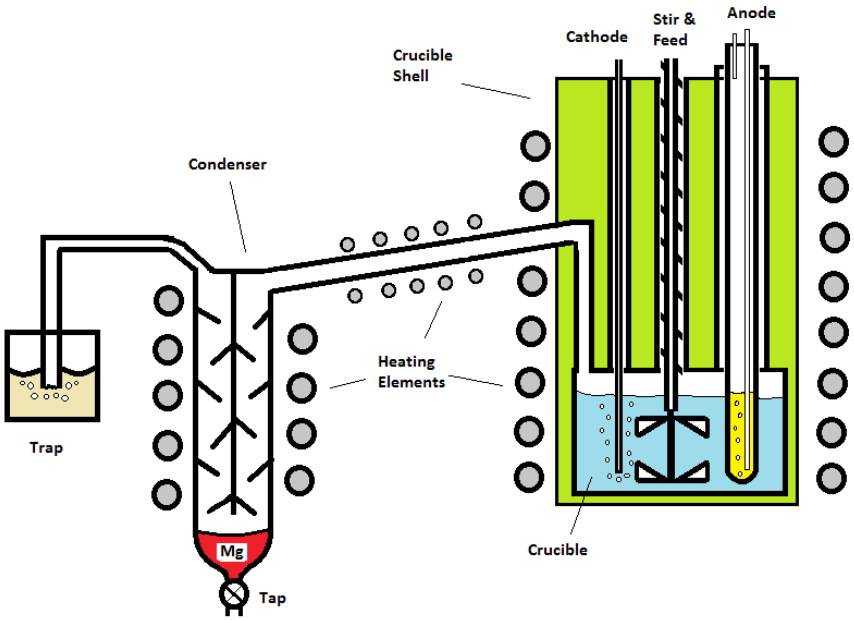

Figure 4 Schematic diagram of a long-term MgO reduction testing apparatus.

.

INFINIUM designed and acquired hardware and software for our prototype control system for the kilo-scale experimental apparatus. This control system is based on the National Instruments Compact Real-time I/O (cRIO®) platform, which is a scalable platform which both leverages INFINIUM's extensive experience with existing LabView control systems which have run our experiments for two years, and also allows for future growth to the alpha and beta prototypes and even plant operations. The control system includes the following components:

- Multiple thermocouple inputs to monitor process temperatures;
- Analog inputs to monitor pressures, flow rates, oxygen concentrations and other analog signals;
- Digital inputs such as switches and user interface components;
- Analog outputs for flow controllers and some motor controllers;
- Digital outputs for relay-controlled motors and other devices.

Figure 5: Long-run kilogram-scale 6-zone magnesium furnaces.

Figure 6: Controller and power supply for kilo-scale furnace system.

There are two of these cRIO® systems now at INFINIUM: one controls the new long-run experimental apparatus described above, and with the second was used for software (PLC ladder logic) development in parallel with the experiment. The control system architecture is complete, and there is a working software module for interfacing with the six Eurotherm controllers which comprise the long-run experiment furnace temperature controls.

The kilo-scale furnace array was received, assembled and installed (Figures 5 and 6). The furnaces were located within an isolated area of the laboratory and hardwired to 208V power supply. All thermocouples were installed and test. The unit was vented out of the building, and each zone was baked out sequentially.

Sub-systems for the furnaces are completed. In order to replace tubes that may fracture, a precision mechanism was designed and built to slowly insert and remove tubes within the heated crucible. The tube removal stepper motor was attached to appropriate gearing and mounting brackets. One four-button controller was programmed and the entire system was tested.

For proper mixing of the MgO into the fluoride salt, a molybdenum stirrer was designed. The stirrer motor was wired and tested. The molybdenum stirrer was used successfully.

Given the need to precisely dispense both MgO and fluoride salt into the heated crucible, a commercial auger (Teqweigh) system was purchased. The system has two different auger blades quills – one for fluoride salts and one for MgO. Each one is designed to precisely dispense the powders at different rates. A sealed hopper for holding the powders is mounted to the top of the unit.

The condenser and pour box design was modeled, finalized, and fabricated. (Figure 7).

The pour box is a sealed chamber located between the crucible and the condenser. A tube is submerged in the molten magnesium at the bottom of the condenser, and it runs back through the center tube section and down into the pour box. When a vacuum is applied to the pour box, molten magnesium will travel from the condenser into a mold within the pour chamber.

This tapping (and condensing) approach was be tested with a crucible pre-loaded with magnesium. The operation worked, however it was subject to clogging, the clogging issue was never solved to INFINIUM's satisfaction. Attaching the electrolysis crucible to the tapping system was attempted, the combination of these two process made the operation very difficult to manage.

Figure 7: Rendered cross-section of crucible (left), condenser (right), and pour box (center) of alpha system.

Argon Sampling Effluent gas samples were taken from an electrolysis set-up to determine the potential impurities present in the argon that may affect recyclability (Figure 8). This activity is being supported by our subcontractor, Praxair. Four cylinders were filled and sent to Praxair for analysis, and two cylinders were filled and sent to an independent testing facility. The results from these analyses will determine the design needs of the argon recycling system.

Figure 8: Experiment to collect exit gas from condenser for analysis.

Flux Preparation INFINIUM has begun large-scale preparation of MgF_2-CaF_2-MgO-additive flux for magnesium oxide electrolysis. This system uses a 48" (122 cm) heated length vertical tube furnace with four large crucibles to prepare several kilograms of flux in each batch. This will satisfy the needs of the alpha prototype.

Argon Sampling At the end of the previous quarter, INFINIUM conducted an electrolysis experiment lasting 160 hours with exit argon sampling, as mentioned in the Q3 Progress Report. This experiment's goal was to begin to estimate argon recycling costs by identifying gases which accumulate in the system and must be removed. It also tested thermodynamic software predictions of gas equilibria.

Both INFINIUM and subcontractor analyses showed that there were two gas impurities present in the argon. It is very likely that nitrogen entered via diffusion into a long polyethylene argon line, so we replaced that line with one with much lower gas diffusivity. The subcontractor indicated that separating the other hydrogen impurity from argon is not difficult, and INFINIUM filed a provisional patent application on a chemical separation mechanism.

Alpha Prototype INFINIUM built an alpha prototype designed to run for as long as possible. The goal of this prototype is to run for long periods of time and identify and

ameliorate as many failure modes as possible at a small scale, and apply those lessons to future magnesium production machines. Figure 9 shows the first iteration of this prototype on a large scale.

This prototype has multiple new features, including: continuous MgO raw material feeding using an augur, molten salt stirring, the INFINIUM integrated anode/cathode module, baffled magnesium condenser/holding tank with level sensor, two-exit second-stage solid magnesium condenser, and direct thermal/mechanical vertical tapping of liquid magnesium into a separate mold.

As of the end of September, INFINIUM demonstrated successful production of liquid magnesium in the condenser, and identified a potential safety issue with a weld. Electrolysis tests began in late October 2012.

Figure 9*: "Infinite Magnesium" pre-alpha prototype in fume hood (right) with gas panel (upper left) and furnace power supply (lower left).*

INFNIUM began full operation of the alpha prototype magnesium production system, and soon made changes to remove the bridge furnace between the electrolysis and condenser chambers. Figure 10 shows the “Alpha 2” version of this prototype.

Two subsystems experienced difficulty. First, the MgO raw material augur feed subsystem required substantial redesign to avoid clogging. Testing validated the new design concept, and the new feed augur was completed at the end of the quarter. Second, the crucible heating element needed a minor. With these issues resolved, the alpha prototype was back on-line by the end of January 2013.

Figure 10: INFINIUM alpha magnesium production prototype in fume hood (right) with gas panel (upper left) and furnace power supply (lower left). New this quarter are the raw material augur and hopper system (to right of crucible), anode gas treatment system (upper right in fume hood), and new gravity cast mold (below crucible).

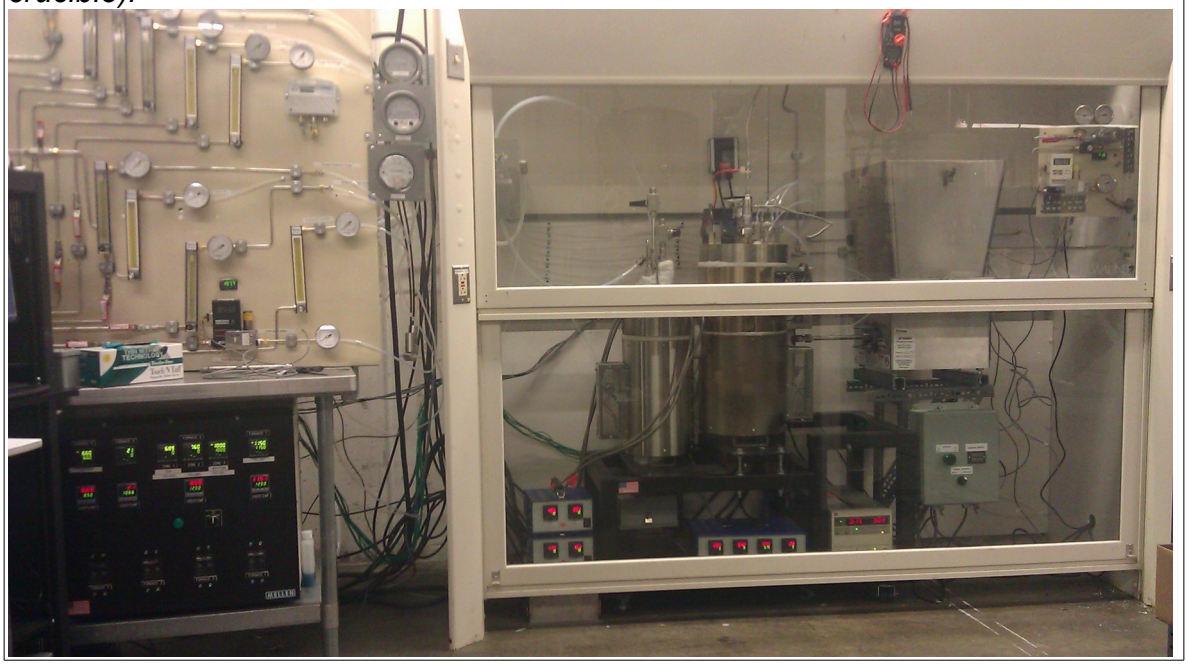

After a furnace failure and crucible breach in the alpha prototype, we repaired and upgraded the system with an integrated anode/cathode, two electrolysis sites, second-stage condenser, and expanded gas panel. INFINIUM recommenced full operation of the alpha prototype after moving to a new facility (Figure 11), and ran continuously. Failure modes encountered include clogging in the MgO feed tube, exhaust and condenser lines plugs. The feed tube clogging was resolved by replacing the auger feed with a manual plunger feed. Exhaust line clogs in the second-stage condenser lines and other condenser clogs were mitigated by enhancing the heaters in those section. Moreover, INFINIUM developed a method for hot swapping the anode assembly.

To address the issue of silver splashing in the anode assembly, the tube was packed with ceramic chips into the zirconia tube. Initial results were promising and require further experiments.

Subsequent “Alpha 3” design improvements included: controlled atmosphere in the annulus between the elements and the crucible to prevent scaling; three ports on the lid for various electrode configurations, such as port for a reference electrode; argon stirring integrated into the cathode design; a porous alumina bushing inside the zirconia membrane tube to prevent the silver (anode/conductor) from splashing; and more accurate oxygen production measurement with flow meter. This shown in figure 12.

The Alpha 3 ran continuously for 500 hours, scaling of the crucible shorted the furnace heating elements, causing the furnace to fail. Six zirconia tubes were removed and replaced at operating temperature of 1100 °C. A total of 3.86 kAmp-hrs of current was

passed during the experiment. The new design maintained clear condenser exit duct, a dual design was used. Liquid magnesium metal was tapped from the condenser.

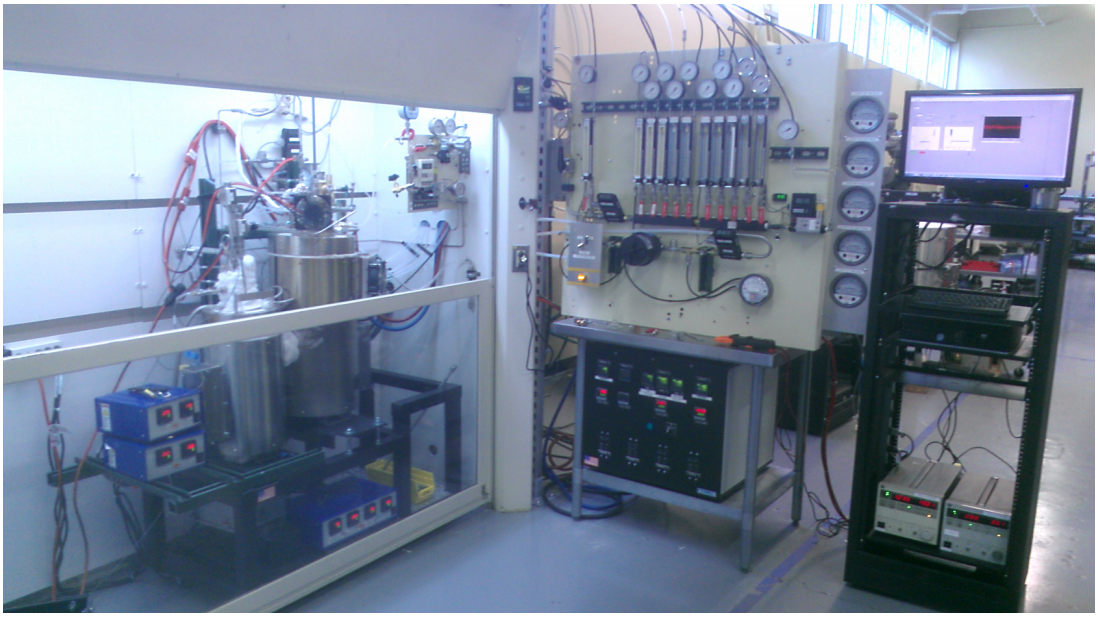

Figure 11: INFINIUM alpha magnesium production prototype in fume hood with gas panel and furnace power supply.

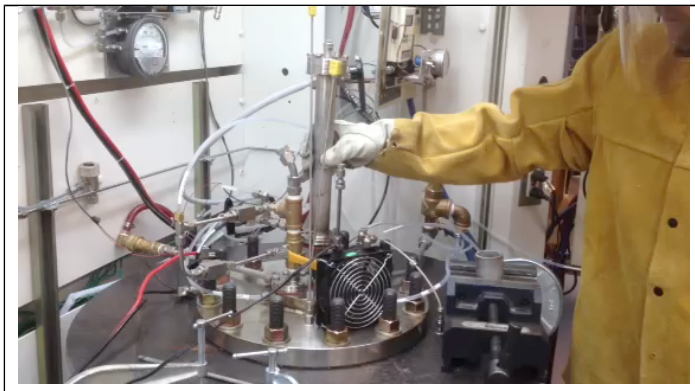

Figure 12. INFINIUM Alpha 3.0 magnesium production prototype with modular condenser being removed

Alpha 3 began operation on July 10, 2013, and the furnace stayed hot continuously for the remainder of the quarter, running numerous experiments in this period. The cell was operated a single anode continuously for 80 hrs to produce 52g H_2O and 26g recoverable Mg. The redesigned condenser cartridge included a cold finger to improve magnesium retrieval. Conducted electrolysis with an 8" (versus 24") tube sealed within the crucible with frozen flux. With our new cathode design, INFINIUM commenced establishing a baseline with commercial zirconia tube (Brand A).

After the heating elements in the Alpha 3 experiment failed, the Alpha 4 was constructed, the new design had metal/glass seals for a pressure. High purity salt to replace the previous flux. Reusable condenser was used to minimize salt evaporation due to the vacuum pump pull.

Alpha 4 (Figure 13) was commenced on low-pressure electrolysis in February 2014 to establish a baseline with Vendor A 6YSZ tubes. Figure 14 shows the Alpha 4 cell.

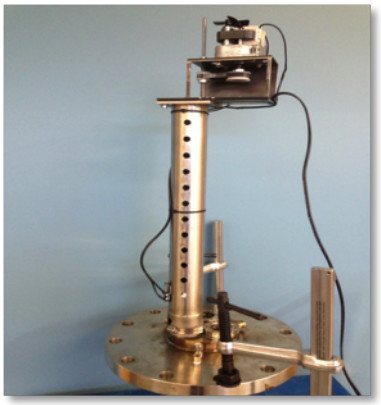

Figure 13 Mechanical tube loader.

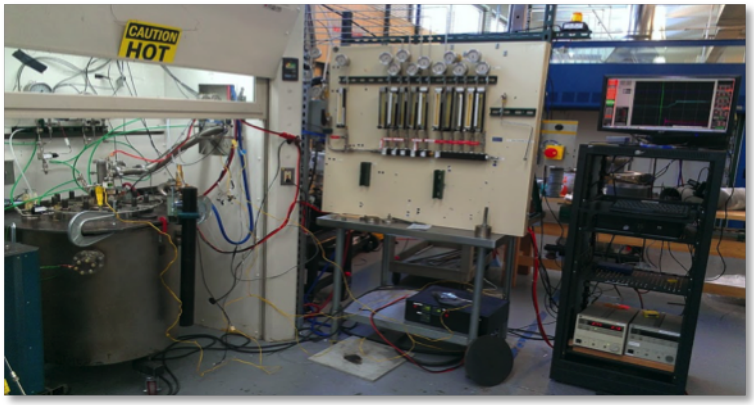

Figure 14 Alpha 4.0 with Programmable Logic Controller

After heating up and testing the system, INFINIUM conducted electrolysis with Vendors A, B and C zirconia and successfully established a baseline of tube performance at both vacuum and atmospheric pressure.

As of March 31st 2014, the longest single tube life in the Alpha 4, was 135 hours, a significant improvement from Alpha 3's 95 hours.

The Alpha 4 design completed the development of the Alpha Cell. For the remainder The Alpha 4 will use it for anode optimization experiments and initial magnesium production. Table 1 depicts our Alpha dashboard as of March 31st 2014. Table 1 shows the performance improvements in the Alpha designs.

As of September 30 2014 the longest single tube like the Alpha 4 was 170 hours. An improvement over the 95 hours tube life in the Alpha 3. In the Alpha 4 25 gram of Mg metal was recovered form one electrolysis run.

Table 1. Alpha Dashboard

	Alpha 1.0	Alpha 2.0	Alpha 3.0	Alpha 4.0
Longest Continuous Uptime Hours		672	2280	1968
# Tubes Used	4	7	14	22
Total Amp-Hours			1200	1266
Longest Single Tube Lifetime Hours			95	170
Mg Recovered		>65g	*	47

INFINIUM successfully recovered approximately 25g of Mg metal from the Alpha 4 condenser following 65 amp-hours of electrolysis. In order to prevent oxidation from high temperature metal removal, we cooled the prototype down before recovering the Mg. We hypothesize that the higher Mg yield may be a result of this cooling since Mg metal solubility in the salt decreases as 5temperature decreases. Figure 15 shows Mg produced.

Figure 15 Mg recovered from Alpha 4.0 condenser

Our next electrolysis run ended after 160 amp-hrs when the zirconia tube failed. SEM analysis confirmed that salt had penetrated through cracks in the YSZ membrane near the cathode holes. See Figures 16 and 17. As a result, we lost electrical conductivity when the salt attacked the LSM (lanthanum strontium manganese oxide) current collector.

Electrolysis lasted for 92.6 Amp-Hours and produced 157 ml of O_2. The anode and cathode were periodically shorted when the current decreased. The current increased drastically after shorting for a few hours; however, it remains unclear if the increase was due to shorting or time off for mass transport. See Figure 18.

Figure 16 Cathode cage holes correspond to YSZ membrane degradation.

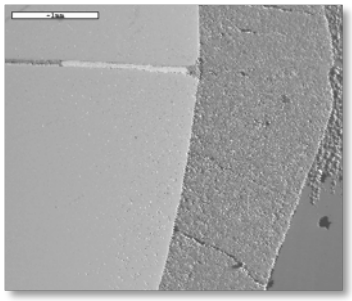

Figure 17 Cross section of YSZ membrane with crack near cathode hole area.

In the next experiment the gasket failed separating the cathode cage and the tube manifold flange, causing the cathode cage argon purge to malfunction. Without this gasket the argon purge exited out between the two flanges rather than through the cathode purge holes as intended. Upon removing the tube there was no evidence of degradation around the cathode holes, leading to the conclusion that the tube degradation observed in other runs was a result of bubble formation rather than electric field.

We experimented with a new zirconia powder composition, Vendor C, and an increased firing temperature of 1575 °C, the highest capability of our furnace. (Previously, we fired Vendor B tubes at 1500 °C.) We also produced tubes with slightly thinner walls, 0.112” (2.85 mm) versus the standard 0.125” (3.17mm).

In order to remove any dissolved magnesium metal in the Alpha 4.0 flux, we bubbled argon through the system for several days. We then conducted electrolysis at 2.5V for 66.5 amp-hrs to generate 208.4 ml of oxygen. The current was remarkably stable throughout the run, unlike in all previous runs, and we achieved an oxygen-basis current efficiency of 85-95%, the highest to date. See Figures 19a and 19b.

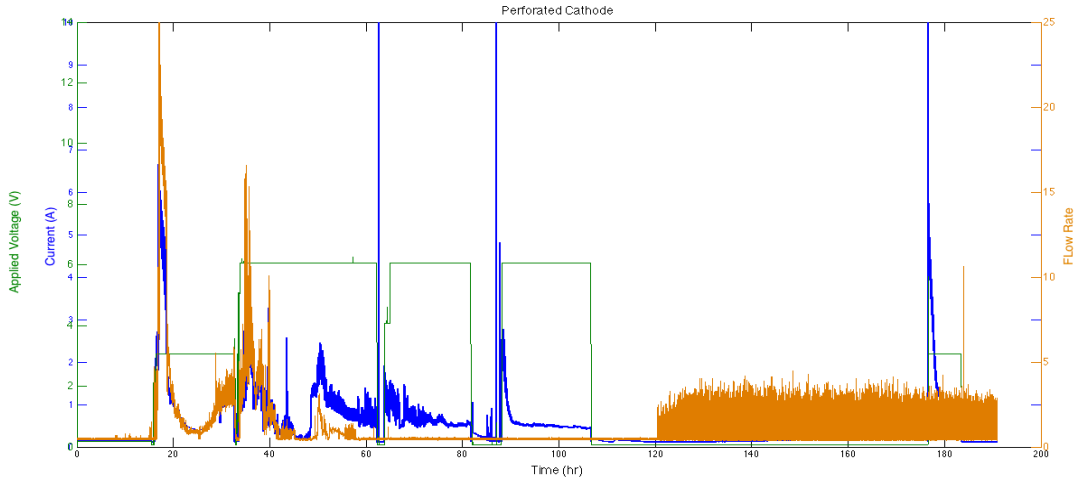

Figure 18. Current Effects with Shorting

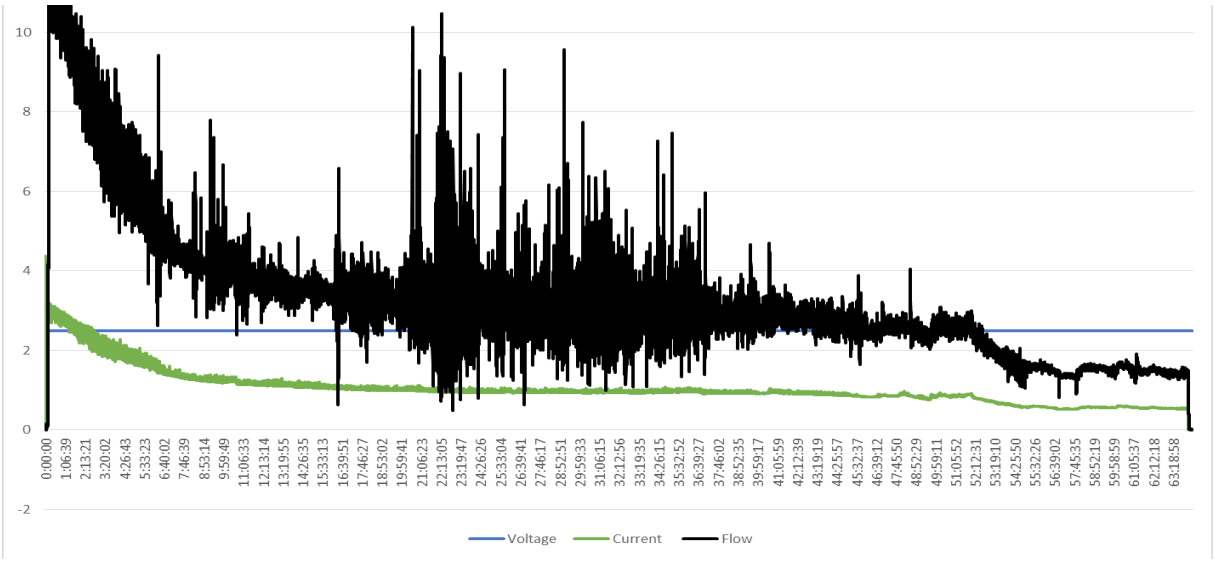

Figure 19a. Alpha 4.0 Current

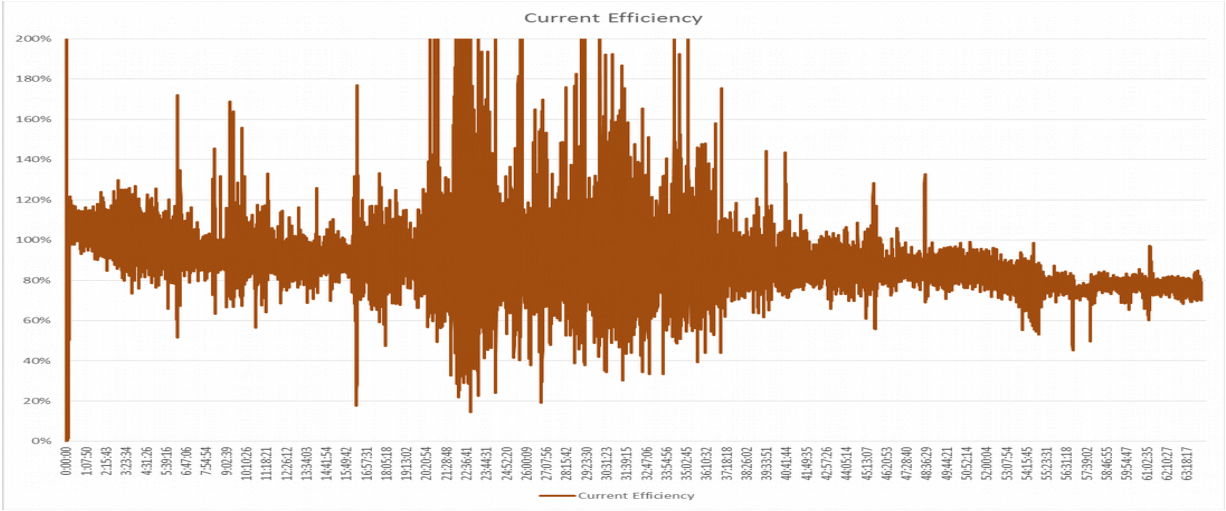

Figure 19b. Alpha 4.0 Current Efficiency

INFINIUM repeated this experiment and also run electrolysis with Vendor B tubes fired at the higher temperature. Our hypothesis is that, in addition to the increased tube firing temperature, the system purge was a major factor in the improved performance.

INFIINUM continued to design the Alpha 5.0 prototype with larger ports to accommodate up to 1.25” (3.2 cm) tubes. Larger tubes will provide space for new current collector designs and more oxygen flow, and the increase in surface area should also improve maximum current. We are considering furnace options since the Alpha 4.0 furnace is still offline with a damaged heating element.

Beta Prototype INFINIUM designed the beta prototype MagGen™ magnesium production system and fabrication is in progress. Figure 20 shows the furnace heater and insulation design, consisting of two 12” (30.5 cm) inner diameter (ID) 12” (30.5 cm) tall cylindrical furnaces for the crucible and condenser, with a “bridge” furnace to carry the argon-magnesium mixture from crucible to condenser. Since the head space requirement might change the furnace was designed to be modular. The head space above the molten salt is adjustable. Figure 20 also shows several 12” (30.5 cm) ID heater components which can stack to adjust those dimensions.

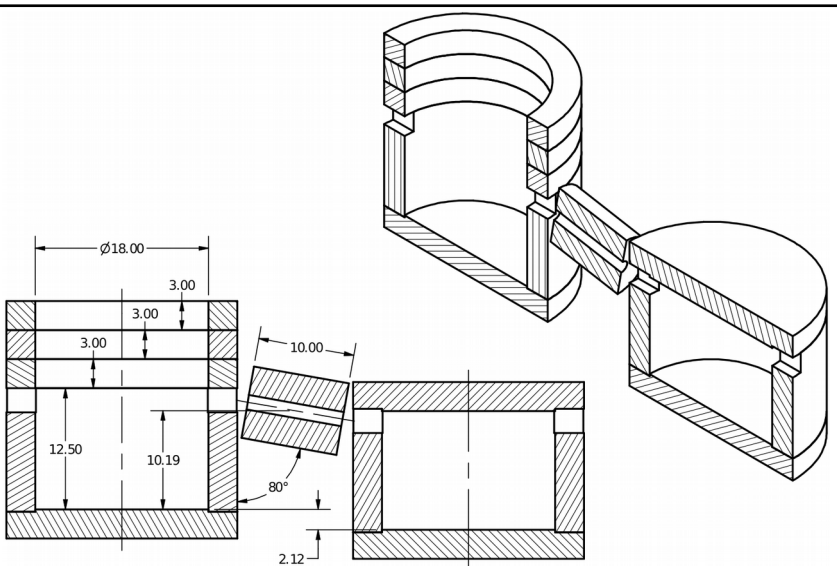

Figure 20: INFINIUM MagGen™ magnesium production system alpha prototype modular furnace concept.

The beta prototype would accommodate up to 20 zirconia tubes in integrated anode/cathode modules, like the one in alpha “Infinite Magnesium”, each of which will hold between one and seven zirconia tubes with anodes. It was expected to run at up to 2000-3000 A current, *i.e.* 2-3 lbs/hour (0.9-1.4 kg/hr).

INFINIUM ordered and received the modular furnace for the beta magnesium production prototype. Figure 21 shows the newly-arrived furnace heater and insulation, consisting of two 12” (30.5 cm) inner diameter (ID) cylindrical furnaces for the crucible and condenser, with a “bridge” furnace to carry the argon-magnesium mixture from crucible to condenser.

The furnace design was modular, with the ability to reconfigure in each experiment the head space above and molten salt depth below the bridge furnace, as well as the condenser height. Figure 21 also shows the 12” (30.5 cm) ID heater components

which can stack to adjust those dimensions.

INFINIUM completed fabrication and beginning component tests during spring 2013, and ran the first electrolysis tests in August 2013. The first electrolysis tests were scheduled for in August, it was difficult to operate this system, the process scale back to work on tube life issues in the Alpha system.

Figure 21: Modular furnace for INFNIUM beta magnesium production prototype cell, with two main 12" (30.5 cm) ID chambers for the crucible and condenser, and power supply on

INFINIUM installed a ventilation hood, upgraded power, and baked out the furnace. We then loaded flux and tested instrumentation and controls. It was planned to commence electrolysis in three sites with Brand A tubes in early November with the goal of producing 1 kg of magnesium and achieving 100 A and 100 hours by the end of December. This was postponed due to tube life issues.

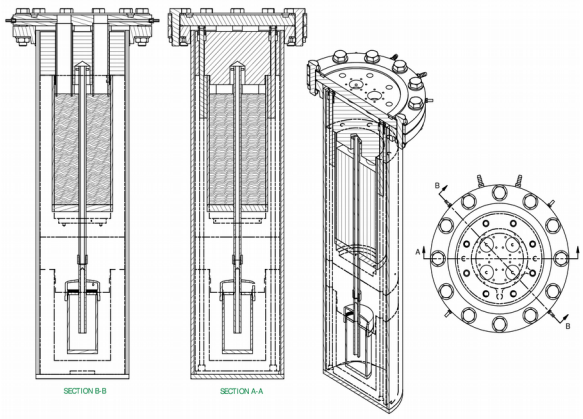

Figure 22. INFINIUM Beta 1.1 magnesium production prototype design

In November INFINIUM finished assembling the Beta 1.0 prototype, loaded flux, and tested instrumentation and controls. During the condenser test, flux adhered to the graphite crucible, causing it to crack. We believe the adhesion was due to magnesium metal in the salt. The design was then upgraded to include a steel crucible with liner and a replaceable condenser. Figure 22 shows the Beta 1.1 magnesium production prototype furnace design with steel crucible and improved condenser. The new design was operated in May 2014, this is shown in figure 23.

INFINIUM began increased immersion electrolysis in May 2014. The plan was to

conduct baseline electrolysis at 3” (7.6 cm) immersion followed by 6” (15.2 cm) immersion at reduced current, then increased current at 6” (15.2 cm) immersion, then proceed to 12” (30.5 cm) immersion.

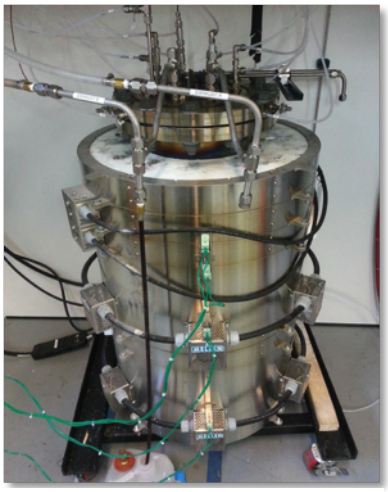

Figure 23 Beta 1.1 furnace.

During baseline electrolysis, salt condensed in cathode port, preventing insertion of the cathode cage. Additionally, the outer casing buckled and cracked from excessive load at temperature. See Figure 24.

Consequently, INFINIUM designed an alternative deep-immersion setup in a smaller furnace and are reconsidering material creep strength.

This new Beta 2.0 prototype was then fabricated. The change in the SOPO to Mg-Nd production resulted in the development of the Delta and Gamma cell based on Beta 2 work. This work is shown later in the report.

The process was moved away from collection of magnesium to the production of Mg-Nd alloy, since the recovery process appeared to be less of an engineering challenge, and the production of Mg-Nd alloys would also achieve the overall goal of vehicle light-weighting, where high-strength Mg-rare earth alloys could be used in the replacement of steel and aluminum parts in automobiles.

As part of the magnesium process work, several ancillary studies were conducted. These were used to visualize the cell (transparent crucible), determine methods of salt recovery (salt recycling) and reuse and physical modeling of the electrolytic process.

Transparent Crucible Direct observation of electrolysis in this system would answer many questions behind the physical chemistry of the molten salt electrolysis cell. Toward this end, INFINIUM subcontractor KPM ran many experiments to characterize the application to our electrolysis process of their transparent high-temperature furnace, shown in Figure 25a.

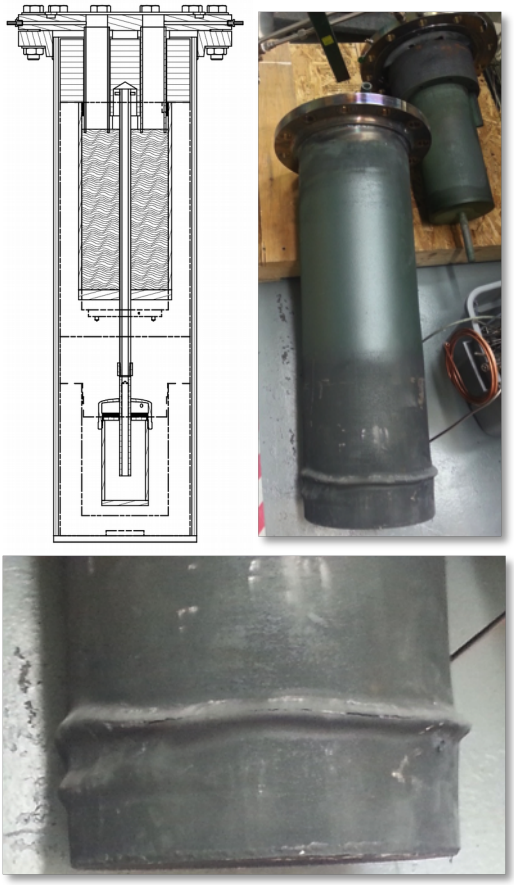

Figure 24. Beta 1.1 Damaged Casing

Figures 25b and 25c show the first challenge: thermal radiation at the very high process temperature (1050 °C) made visualization very difficult. KPM overcame this challenge by using a stainless steel shield with Thurmalox black silicone ceramic coating shown in Figures 26a and 26b, to prevent direct radiation emitted by furnace heating elements from interfering with visualization.

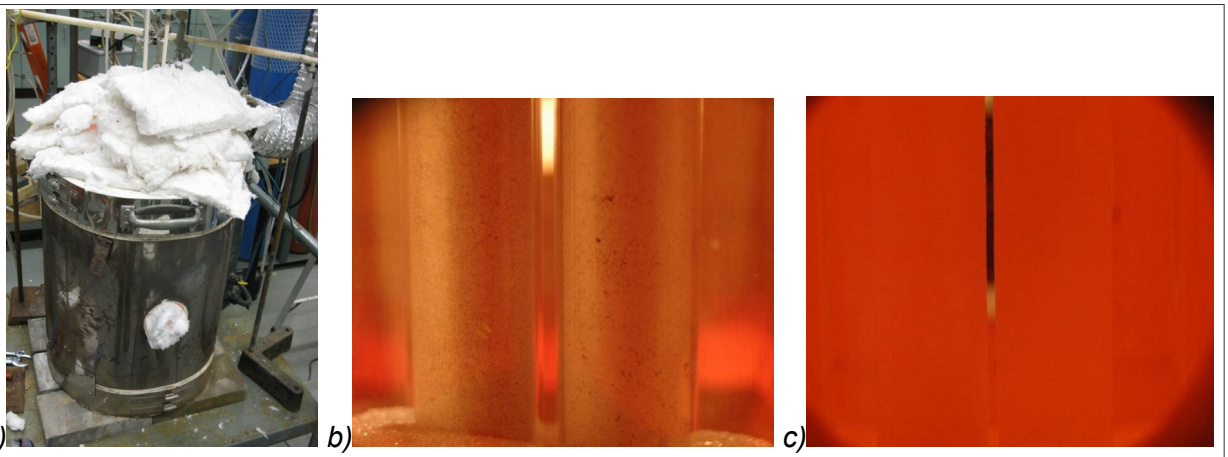

Figure 25: a) High-temperature furnace at KPM with transparent section for direct experimental observation; b) two quartz crucibles in the furnace at 700° C; c) the same crucibles at 1050° C.

The next challenge is molten salt opacity: MgF_2-CaF_2 is substantially opaque at the process temperature, with additions of MgO the opacity increased. However, it is possible to directly observe features in liquid sodium cryolite Na_3AlF_6 at this temperature (1050 °C), as shown in Figure 25c.

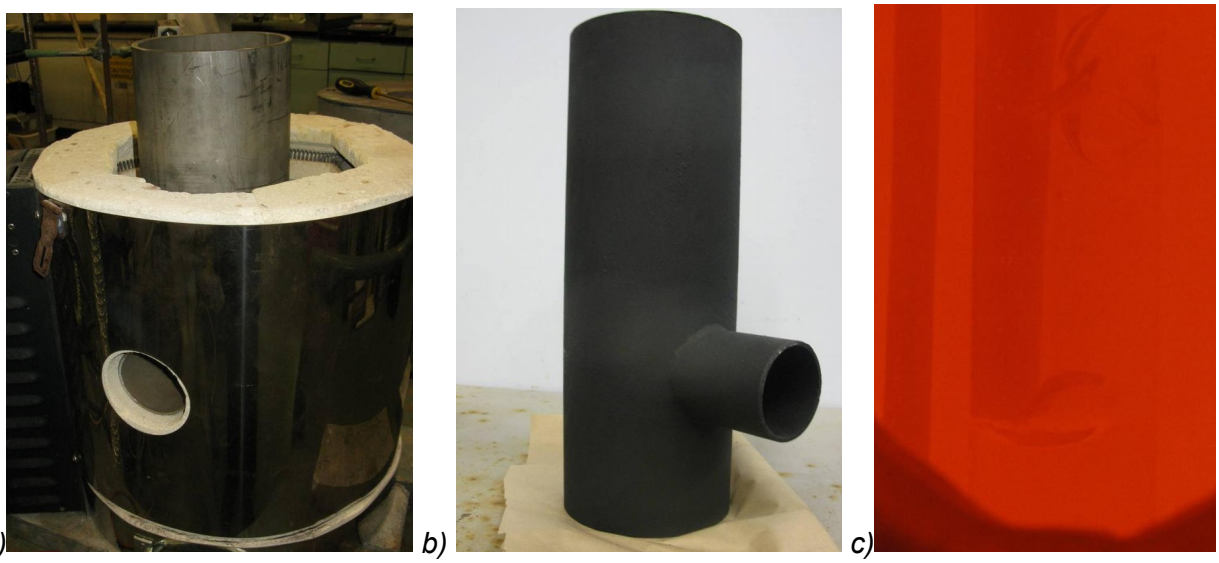

Figure 26: a) Furnace with stainless steel radiation shield; b) stainless steel radiation shield with Thurmalox silicone ceramic coating; c) molten sodium cryolite at 1100° C with argon bubbles.

KPM ran numerous experiments to characterize the application to the electrolysis process in KPM transparent high-temperature furnace, shown in Figure 27a. KPM identified a surrogate molten salt electrolyte composition suitable for MgO electrolysis experiments in a transparent crucible and furnace, which was MgF_2-NaF-MgO. This salt composition overcomes the problem of molten salt opacity identified in the previous quarter and is compatible with the quartz crucible material. Figure 27b shows the transparent furnace and the view through its port of the new surrogate molten salt.

a)  b) 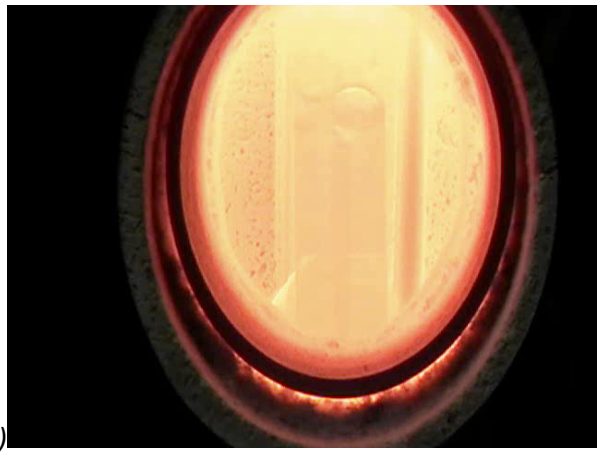

Figures 27: a) High-temperature furnace at KPM with transparent section for direct experimental observation; b) quartz crucible shown through the furnace viewport with surrogate molten salt and argon bubbles

The surrogate salt also has oxygen anion concentration and magnesium cation concentrations similar to those of the standard INFINIUM salt, such that anode and cathode mass transfer characteristics should be very similar to standard electrolysis cells. It degrades the zirconia tube more quickly than the INFINIUM salt, but this will not be a problem due to the short experiment duration. KPM used the transparent high-temperature furnace, shown in Figure 28a, to run two MgO electrolysis experiments using INFINIUM SOM anodes. Figure 28b shows the view through the furnace port of an electrolysis experiment.

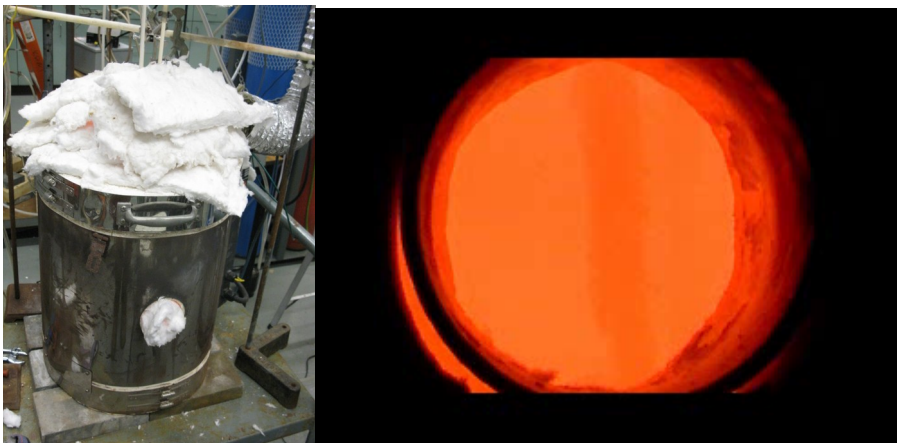

Figures 28: a) High-temperature furnace at KPM with transparent section for direct experimental observation; b) quartz crucible with electrolysis experiment shown through the furnace viewport with cathode coated by a dendritic deposit.

The first experiment did not succeed: the salt dissolved through part of the crucible and spilled out, damaging the furnace. The second experiment at 1050° C succeeded in running an electrolysis current, and produced a deposit of unknown composition on the cathode, which fell off the cathode to the crucible bottom when tapped. Based on this behavior, the deposit is likely denser than the salt, and not magnesium. This program needs more development than time allowed for and was stopped.

Salt Recycling INFINIUM and subcontractor KPM developed three concepts for

separating MgF_2 from CaF_2 in used molten salt and recovering fluorine. Molten salt separations are based on the reciprocal phase diagram for this system. Figure 29 shows such a diagram for the CaF_2-MgF_2-MgO-CaO reciprocal system. This is a cross-section through the four-component Ca-Mg-F-O quaternary system, which assumes all species are ionized (Ca^{2+}, Mg^{2+}, F^-, O^{2-}) and charge is neutral. Figure 29 shows the liquidus contours of this system based on a commercial database which in turn is built on the four pseudo-binary phase diagrams CaF_2-MgF_2, MgF_2-MgO, etc. Unfortunately the liquidus shown here is incorrect: it shows only ~1 mol% solubility of oxide in the MgF_2-CaF_2 eutectic salt, whereas differential thermal analysis (DTA) experiments by Uday Pal et al. at Boston University have shown approximately 10 wt % solubility.

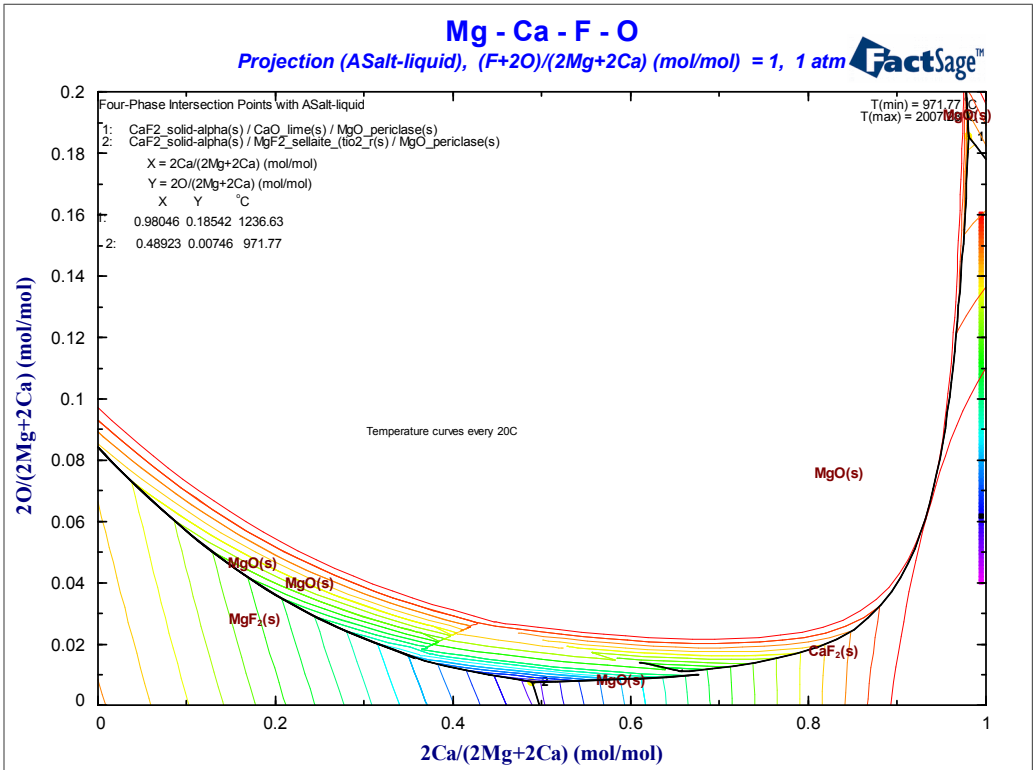

Figure 29: Reciprocal phase diagram liquidus surface contours in the CaF_2-MgF_2-MgO-CaO system, as calculated.

INFINIUM and subcontractor KPM developed three concepts for separating MgF_2 from CaF_2 in used molten salt and recovering fluoride. KPM investigated the thermodynamics of one of those concepts using a “cold finger” experiment in the apparatus shown in Figure 30a. The cold fingers themselves, shown in Figure 30b, are air-cooled stainless steel tubes with thermocouples inserted into a crucible with molten salt. The fingers are withdrawn from with frozen salt for analysis.

Composition analysis indicated that frozen salt compositions were highly enriched in CaF_2, indicating that MgF_2-CaF_2 separation is indeed possible using selective freezing. More broadly, this proved the concept of managing CaO impurities in the raw material, which shift the Mg/Ca balance in the molten salt, by selective freezing out of CaF_2. Comparing the compositions of the frozen salt and that which remained in the crucible also provided valuable insights into the ability to separate out other

cations using this method.

a) 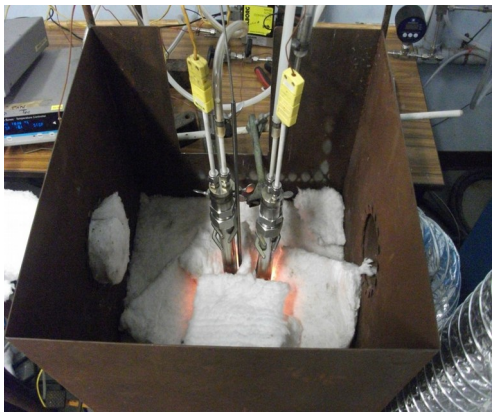 b) 

Figures 30: a) KPM furnace with cold fingers protruding from the top. b) Cold finger details.

Based on these initial results, in July 2013 KPM performed two additional selective crystallization trials. The first trial consisted of 35-second cycles (with no hold) around the eutectic temperature. The second trial had the same cycles with a one-minute hold at higher temperature. The first trial showed a slight increase in Ca concentration on cold-finger relative to melt of about 1%, and the second trial showed no Ca concentration increase. Given these initial results, KPM suggested an alternative to salt recycling that may prove even more economical. The need for salt recycling is due to feedstock impurity, i.e., calcium oxide, which gradually accumulates as solid suspension in the molten salt, increasing salt viscosity and decreasing ionic conductivity.

INFINIUM and subcontractor KPM concluded the KPM work on selective crystallization as a method of salt recycling. The calcium oxide impurity in MgO raw material shifts the cell salt balance to the calcium-rich side. The goal of this set of experiments was to test the ability to drop below the calcium fluoride liquidus temperature to selectively freeze that salt, shifting the balance back toward magnesium chloride. Unfortunately experiments did not show appreciable enrichment of calcium fluoride in the deposit, even when cycling the temperature above and below the liquidus line to promote equilibrium partitioning. Therefore this approach to salt recycling is not likely to work.

Other approaches to salt recycling remain promising, such as grinding and density separation. That said, cost modeling has shown that having no salt recycling in the system at all only adds about 3% to total manufacturing cost, and will likely not have a large effect on process viability.

Physical Modeling. As mentioned above, direct observation of electrolysis is difficult; furthermore, the integrated anode-cathode assembly uses a large metal sheath as a cathode, making direct observation impossible. Simplified mathematical models of bubble-driven flow, such as the slip-velocity model, are imprecise, for these reasons, INFINIUM built a water model of the integrated anode-cathode assembly using the same three-nozzle argon injector. Water/argon mixtures have good similitude with salt/gas systems. See Figure 31.

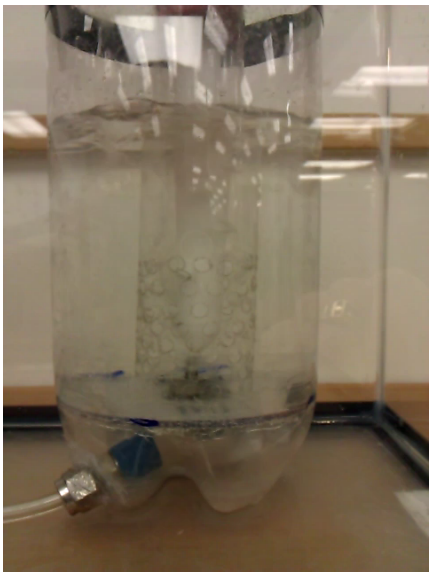

Figure 31: Physical model of argon bubbling between cathode (perforated tube) and zirconia (white tube).

The physical model shows that bubble distribution is not very sensitive to zirconia tube position. That is, if the nozzle is as much as 2-4 mm off center relative to the zirconia, bubbles are still uniformly distributed around the tube, on a subjective basis.

Mg-Nd Alloy Production

Producing Mg-Nd alloy instead of pure magnesium metal is a significant change which requires a shift in prototype functions. See Figure 32 for the original versus new process.

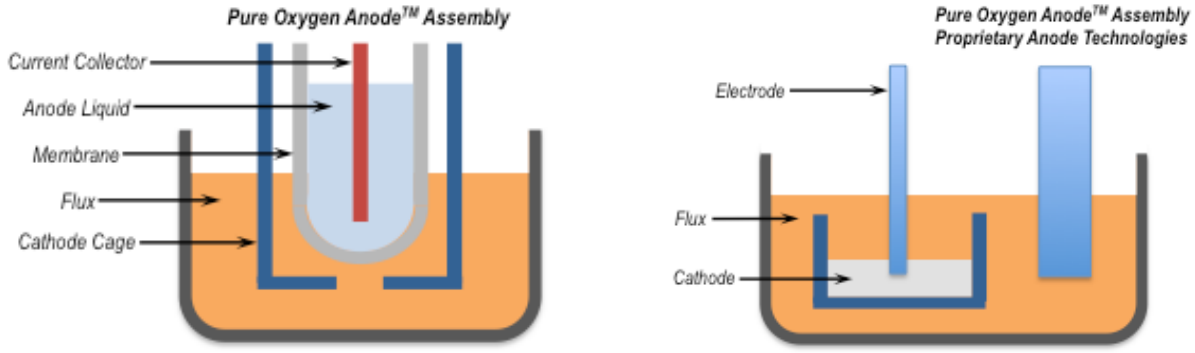

Figure 32. Mg versus Mg-Nd Production

To produce Mg-Nd alloy via electrolysis, INFINIUM used liquid pool Mg-Nd as the cathode. A cup holds the liquid Mg-Nd and an electrode within the flux. INFINIUM used a proprietary anode for production while optimizing the Pure Oxygen Anode™ assembly for the new electrolyte. During electrolysis liquid Mg-Nd collects in the cup, thereby eliminating the need for a condenser, while this removed the operation challenges of the condenser, it presented several new ones.

Figure 33 shows the INFINIUM process to produce WE43 or other alloys via liquid alloy electrolysis. INFINIUM electrowon the neodymium into the magnesium, and can directly produce neodymium by electrolysis. Flux will contain MgO which is electrowon in parallel with neodymium to produce a 50% Mg-Nd alloy. MagPro or similar manufactures could distill some of the magnesium from the master alloy and return it, or use it to make alloy.

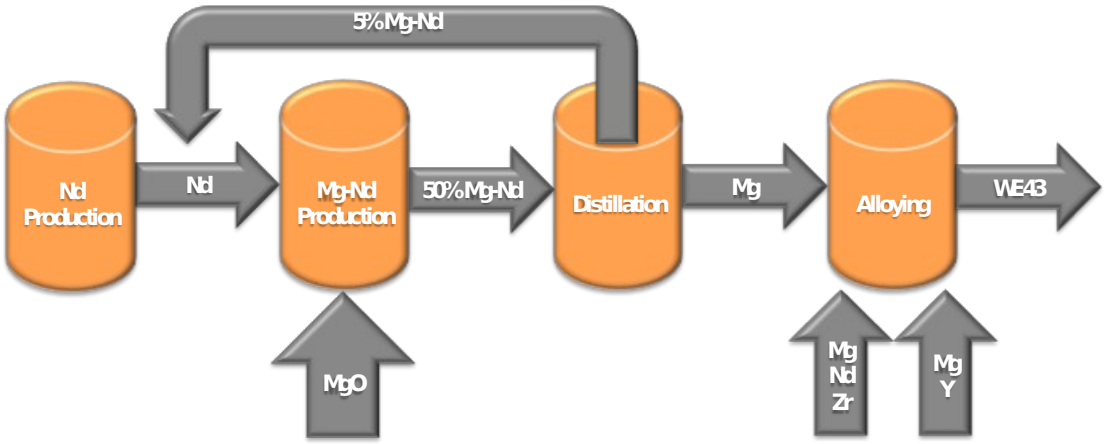

Figure 33. INFINIUM Liquid Alloy Process

Given this process change, INFINIUM changed the primary focus of the Alpha prototype to anode optimization, and reconfigured the Beta into a Mg-Nd production cell. Our electrolysis prototypes and their functions are:

- Alpha: Anode Optimization
- Beta: Reconfigured to Delta
- Gamma: Nd production
- Delta: Mg-Nd production

Beta and Gamma 1.0

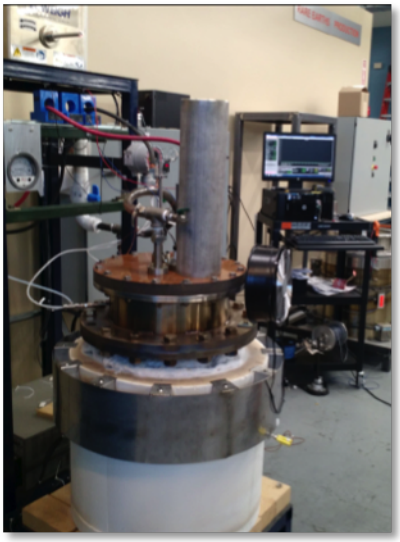

Figure 34. Gamma 1.0 Nd Cell

INFINIUM built a Gamma electrolysis cell for neodymium production shown in Figure 34. As mentioned, we reconfigured the Beta from magnesium production scale-up cell to a Mg-Nd alloy production cell and renamed it (Delta).

Delta 1.0: Mg-Nd Alloy Production

INFINIUM designed and built Delta 1.0 after preliminary process development. Design work started with flux composition determination which must satisfy several additional criteria beyond our usual molten salt requirements, floating Mg-Nd product and large enough solubility of MgO and Nd_2O_3

Alloy compatibility and MgO solubility testing began with first results in Table 2.

Table 2. Mg-Nd Flux Tests

MgF_2-LiF	NdF_3-LiF-MgF_2
• All Nd metal reacted with MgF_2 to form NdF_3 and Mg metal	• Only small amount of NdF_3 formed; added MgO • Nd metal reacted with MgO to form Nd_2O_3 • No Mg recovered

Following these tests, we decided to omit MgF_2 from the flux in order to reduce reactivity with Nd metal (and its expense) and to omit NdF_3 in order to reduce its density. The latter was motivated by calculations leading to Figure 35a, which assume zero volume change of mixing in both the flux and metal. Calculations show that with 100 wt% NdF_3, metal floats if it contains more than just 10.5 wt% Mg, and with 100 wt % MgF_2, metal with over 47 wt% Mg floats. This is shown in Figures 35a and 35b.

Figures 35a and 35b. Bath Density Thresholds

INFINIUM selected LiF for low density and stability, with CaF_2 in order to reduce volatility. For that flux system, the metal can have up to 43% Mg for pure CaF_2, and up to 82 wt% Mg for pure LiF.

To this CaF_2-LiF fluoride flux, MgO was added as the magnesium cation source. Neodymium compatibility was tested by melting flux, lowering into the CaF_2-LiF-MgO flux a small molybdenum charged with 28g Nd metal, removing the cup, cooling the furnace, and measuring the weight of remaining Nd metal. We used the same flux for four separate tests, and reloaded some Nd into the cup each time, with the following results: two hour soak, 17% loss, four hour soak, 10% loss, 8 hour soak, 12% loss. No increase in loss was seen with longer soak times.

At this point Nd appeared to approach an equilibrium between the alloy in the cup and the flux outside it. This bath it satisfies our Nd stability requirement.

Next we ran electrolysis using this CaF_2-LiF-MgO flux with a Nd metal cathode.

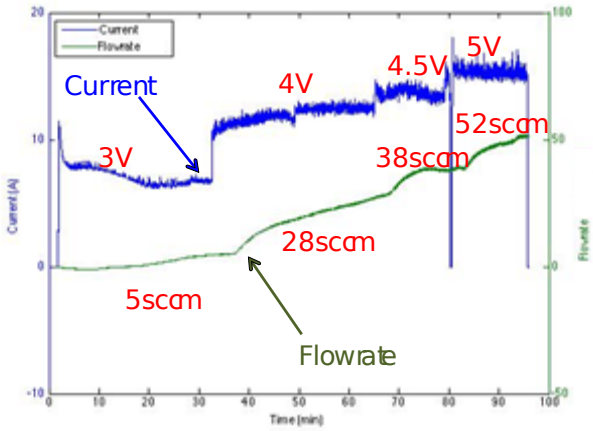

Figure 36. CaF-LiF Electrolysis

Figure 36 shows the current-time relationship, as well as gas flow rate indicating gas production. Voltage increased in increments from 3V up to 5V.

With each increase in voltage, current jumped, and flow rate increased, indicating successful electrolysis. The experiment passed 16.8 A-hr charge, leading to theoretical production of 7.6 g Mg. A total of 1.6 g oxygen was produced, indicating 2.4 g Mg, and ~30-40% current efficiency.

Figure 37 shows the cathode cup after the experiment, which contained an Nd-Mg alloy. Due to difficulty mounting the metal, we verified this by cutting the metal product and analyzing the swarf, which was mostly MgO.

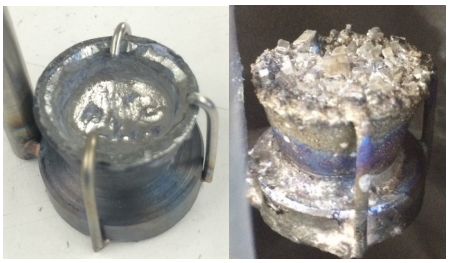

Figure 37. CaF_2-LiF Test Results

However, four electrolysis experiments with CaF_2-LiF failed to produce any alloy. The reason was due to Mg having a higher solubility in a CaF_2 melt, particularly at the high temperature of those experiments. We then chose NdF_3-LiF-MgF_2, which successfully produced 172g of Mg-Nd in the eight consecutive runs. The alloy produced in the process floats and ranges in composition from 45 to 55% Nd.

We first conducted 12 small-scale electrolysis experiments and produced 172g of Md-Nd alloy. Experiments have refined our production cell design. See Figure 38 for a comparison of the original and final designs.

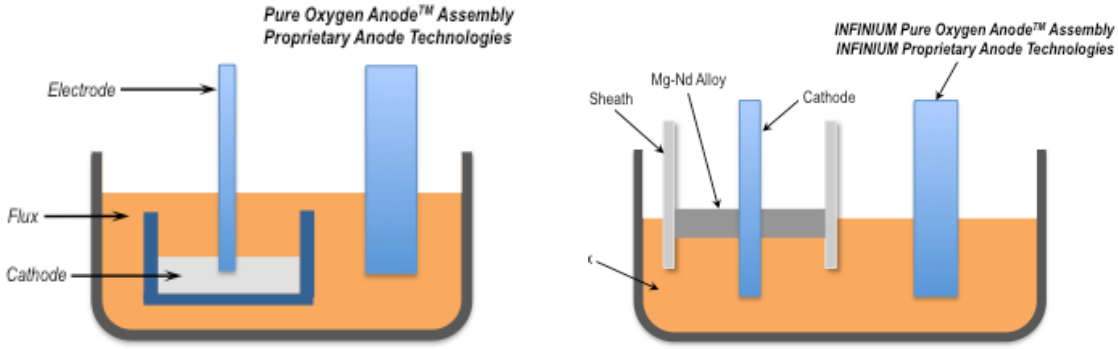

Figure 38. Original Mg-Nd Production Cell vs. second generation

Instead of using a cup of liquid Mg-Nd as the cathode, the design was changed to a 0.25" tungsten rod that is sheathed with a ceramic tube. The ceramic insulation contains the floating Mg-Nd alloy and keeps it from electrically shorting to the anode or crucible. It also facilitates metal removal.

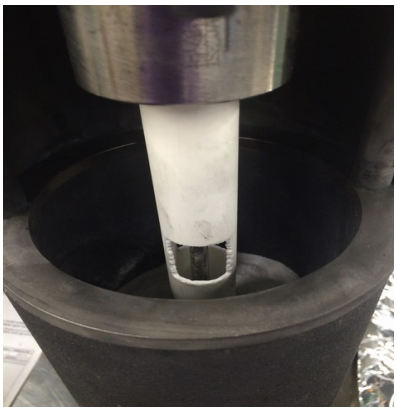

Figure 39. Ceramic cut out

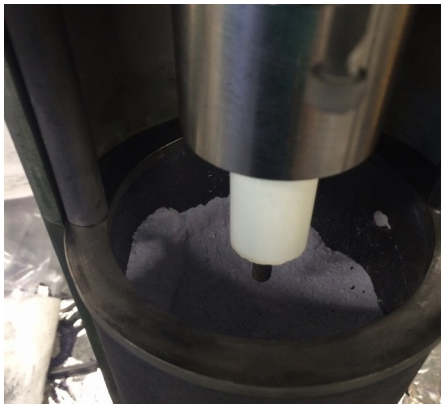

Figure 40. Open ended cathode sheath.

In all but two of the twelve runs the Mg-Nd alloy floated. This resulted in adding a cathode sheath with a window to allow the flux the transport Mg and Nd, as shown in Figure 39. In the 13th experiment the test was with an opened ended sheath. Figure 40 shows this design. The result of this change was poor a result subsequent designs used a dam to separate metal product from the anode to avoid recombination.

Gamma 1.0: Nd Production

INFINIUM commissioned a Gamma electrolysis cell for Nd production in February 2016 and upgraded our facility for its safe operation. This cell successfully produced about 2 kg of Nd-alloy. However, process changes in Mg-Nd alloy production reduced the need for Nd production as we shifted away from a liquid Nd cathode to a tungsten cathode with neodymium oxide in the bath. The geometry involved with using a liquid cathode proved quite constraining by limiting our electrode size on the development scale, causing our cells to run slower. In turn, it was difficult to measure any mass increase or composition change.

Delta 1.0: Mg-Nd Alloy Production

After 12 small-scale electrolysis runs which produced 336g of MdNd alloy, we identified a candidate Delta 1.0 flux composition [NdF_2-LiF-MgF_2]-[Nd_2O_3-MgO] and refined our production cell design. See Table 3 for a summary of these experiments.

Table 3 Mg-Nd production.

Exp. No.	Date	Cathode	Voltage (V)	Flux	Feed wt% (Nd2O3/MgO)	Temp. (°C)	Amp*Hours	Yield (g)	Composition (Mg/Nd wt%) [ICP-OES]	Notes
#1	02.26.15	Mg-Nd alloy	2.7-3.5	(a)	60/40	850	28	10	60/40	Liquid Cathode
#2	03.02.15	Tungsten	2.7-5	(a)	60/40	850	30	8	60/40	Cup collection
#3	03.09.15	Tungsten	2.7-5	(a)	60/40	850	300	100		Cup collection
#4	04.03.15	Tungsten	3.4-3.8	(a)	60/40	850	32	26	50/50 [32/68]	YSZ tube collection
#5	04.08.15	Tungsten	3.8	(a)	60/40	850	50	20	50/50	YSZ tube collection
#6	04.10.15	Tungsten	3.8	(a)	60/40	850	50	50	50/50	YSZ tube collection
#7	04.16.15	Tungsten	3.8	(a)	60/40	850	50	45	50/50	YSZ tube collection
#8	04.27.15	1018 Steel	3.8	(a)	60/40	850	50	45	60/40	YSZ tube collection
#9	04.30.15	Tungsten	3.8	(a)	20/80	850	36	18	65/35 [45/55]	YSZ tube collection
#10	05.12.15	1018 Steel	3.8	(a)	20/80	850	40	22	60/40 [45/55]	YSZ tube collection
#11	06.03.15	1018 Steel	3.8	(a)	60/40	850	36	12	60/40	No sheath, contained Fe
#12	06.05.15	Tungsten	3.8	(a)	60/40	850	32	0	-	No sheath

(a) 65%NdF_3-28.4%LiF-6.6%MgF_2
Alloy composition based on SEM/EDS analysis. 3rd party analysis by ICP-OES yields consistently lower Mg%

Tungsten was chosen as cathode material because it was successful in producing Nd in the gamma cell and was not reactive with Mg. INFINIUM also experimented with a steel rod cathode. We chose 1018 mild steel because it has a high manganese content, which should suppress the solubility of iron in Mg. Experiments 10 and 11 were both successful in producing MgNd alloy. However, the higher the Nd content in the product alloy, the higher the content of iron was as well, making this unsuitable for die cast magnesium alloys.

For experiments 11 and 12, INFINIUM tested a new electrolysis cage with a viewport into the electrolysis cell. The cathode sheath was removed in order to observe the cathode during electrolysis. Experiment 11 used a steel cathode and experiment 12 a tungsten cathode. Experiment 11 produced metal at a 40-50% current efficiency, but experiment 12 failed to produce any recoverable metal. Magnesium in the alloy was evaporating and/or reacting with anode product gas faster than we could make it on that scale.

The Delta 1.0 cell has four equally spaced ports on the top plate, all capable of supporting a 2" diameter anode or cathode flange. The top of the furnace is water cooled and sealed with an o-ring. The crucible is divided in half by a dam (Figure 41 a & b) with two ports on each side of it. On one side are a 0.5"(12.7 mm) diameter cathode and a viewport (Figure 42). The other side has a 2" (5.1 cm) diameter anode with a light and shutter. The salt bath in the cell is approximately 42kg and 12" (30.5 cm) deep. The dam operated for four days before it began to fail.

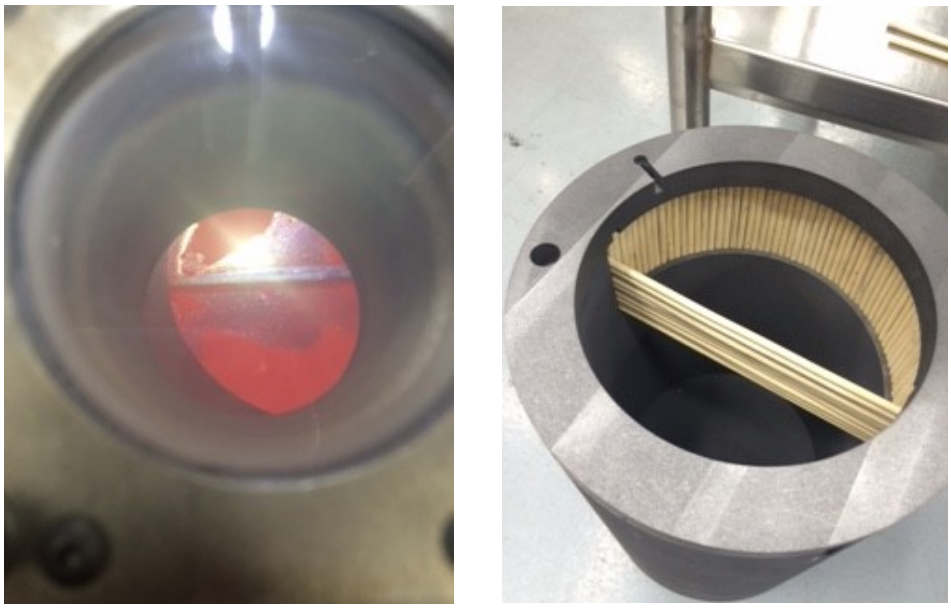

Figure 41 a & b, Ceramic Dam in Mg-Nd Electrowinning cell.

The dam and “picket fence” together are a new alloy containment method replacing the sheath. We changed the design for reasons of both cost and material compatibility.

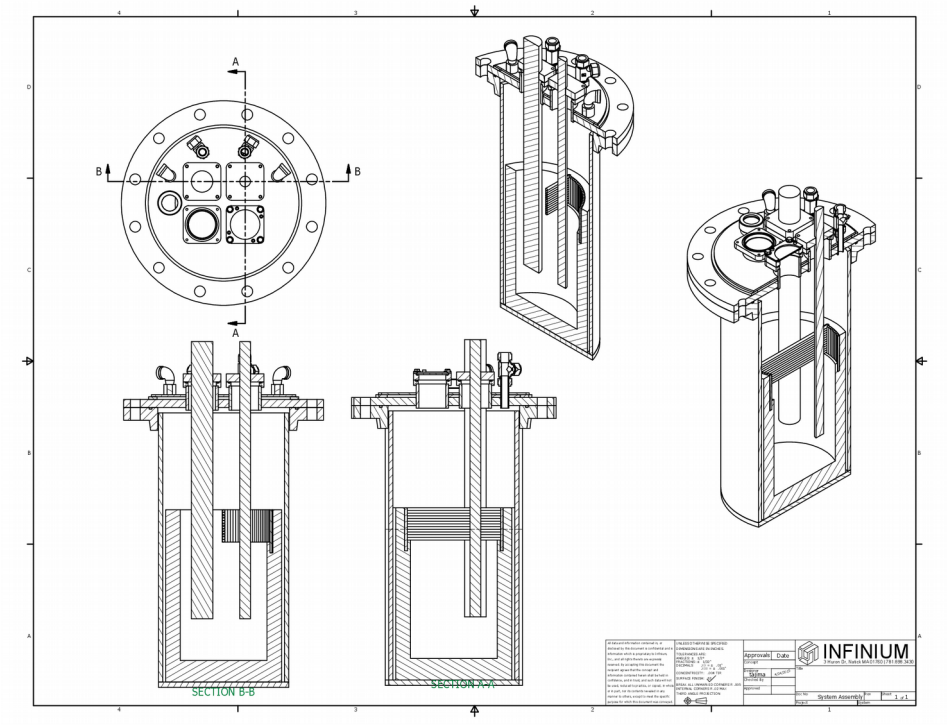

Figure 42. Drawing of Delta Mg-Nd cell.

The results of the small scale work are shown in table 4 below.

Table 4. Small scale work results.

	MgNd (g)	Metal Composition (Mg-Nd)	Oxide Added	Efficiency*	Notes
Monday	190	-	116g MgO 80g Nd_2O_3	50%	Metal Was produced on 7/17. The cell was cooled and metal harvest as a solid
Tuesday	50	-	0	52%	Cell was cooled to 770C to solidify the metal. The metal was then harvested with a ladle
Wednesday	N/A	-	350g MgO 350g Nd_2O_3	N/A	Oxide was added to feed the bath for overnight operation. Stirring also provided instant increase in current.
Thursday	~150	-	350g MgO 350g Nd_2O_3	~13%	This metal was harvested using a hand held small siphon. Test 1 was successful, needs further modification to prevent salt siphoning.
Friday	N/A	-	Offline	N/A	Flux height dropped significantly during operation, suspected broken crucible. Cell was cooled down over the weekend to assess damage.

Despite dam degradation, our first production run was promising; we produced about 390g of MgNd and harvested it with both a ladle after cooling and a small siphon while hot. See Figures 43 and 44. The siphon requires modification to prevent removing salt along with metal.

Figure 43. 180g of metal adhered to cathode

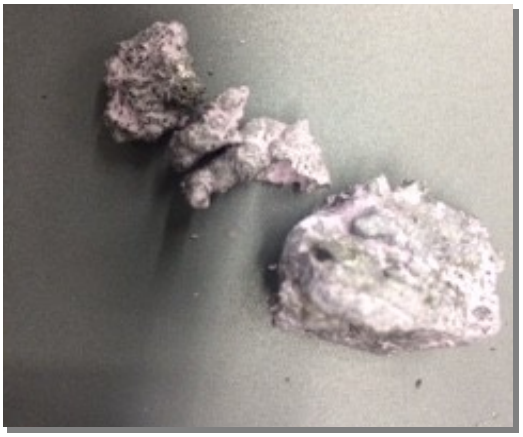

Figure 44. 50g of metal harvested by cooling the bath to solidify the metal and keep the salt molten

The next campaign operated for two weeks with the dam before the crucible broke just below the bottom of the dam. After dismantling the cell, it was observed that the rods swelled to approximately twice their original size. The swollen rods caused the crucible fracture. The long rods that spanned across the center of the crucible were almost entirely dissolved, likely due to electrolysis.

During electrolysis the metal produced formed a large ball around the cathode instead of floating in a pool as expected. This alloy never contacted the dam; the dam was essentially a barrier between the metal and the anode. We changed the design to a graphite dam since graphite is more mechanically and chemically stable in the salt.

See Figure 45. And unlike, if the alloy pool touches the graphite dam, the dam becomes cathodic which may result in metal plating on the side of the dam that faces the anode.

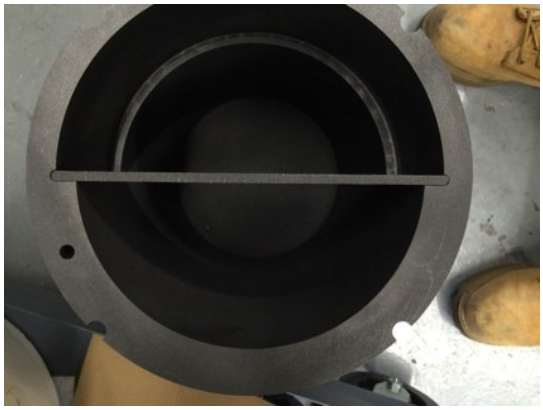

Figure 45. Graphite Dam

This second configuration operated for one week before the crucible broke. During the week long run, we produced floating metal the first two days, a mix of floating and sinking metal on the third day, and sinking metal on the fourth day.

After dismantling the cell, we determined that the alumina spacers used to center and isolate the graphite crucible from the shell caused the crucible break. We replaced the spacers with stiff, moldable insulation that does not swell as the alumina spacers did and used this design for our oxide feed experiments. The metal harvested bridged from the cathode to the dam.

From our small-scale experiments in the PPC, we have produced 3.5kg of MgNd alloy (approximately 50%Mg-50%Nd) at an average current efficiency of 60-70%. A large portion of the loss in efficiency was caused by the oxide film that formed on the surface of the metal. Hypothetically, if we were to produce more metal before harvesting, the proportion of oxide film to MgNd alloy would decrease, thereby improving current efficiency.

Molten Metal Siphon

The molten metal siphon was developed to remove electrowon alloy from the cell. This technology is current used on a much larger scale in the production of magnesium and aluminum. The research goals were to design a siphon that could remove Mg-Nd alloy and other alloys from molten salt cells. It also could be used to remove bath from a cell for maintenance work on the cell. Figure 46 shows the first prototype, the three legs are adjustable to meet uneven surfaces on tops of cells.

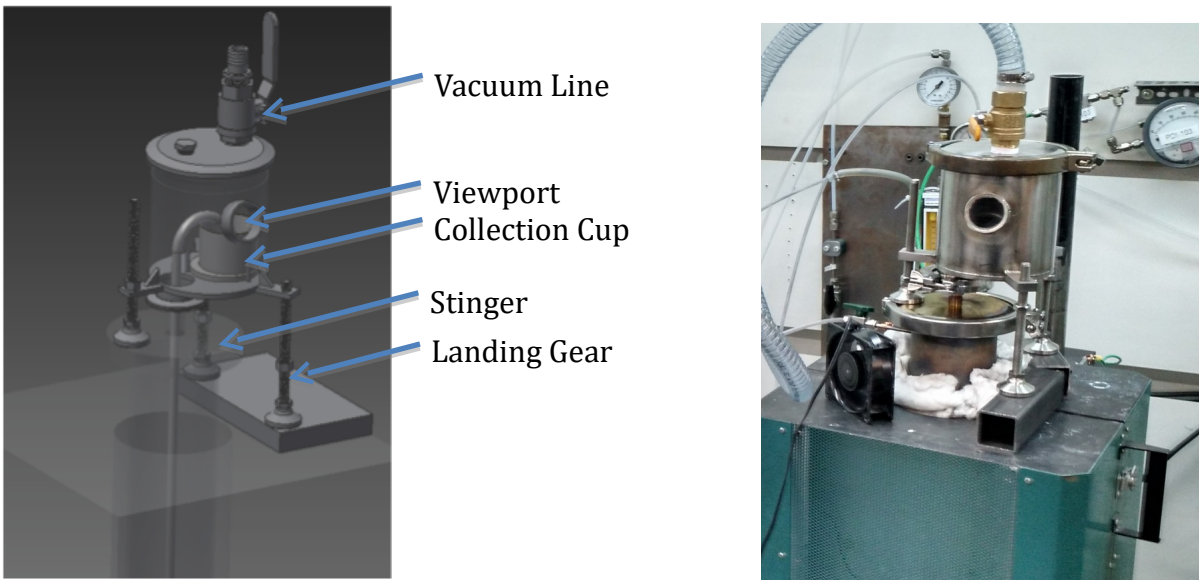

Figure 46. Molten Metal Siphon, aka the Lunar Landing Module

Initial testing had some promising results. The Lunar Landing Module did siphon molten Cu and Nd into the collection cup without heating in separate runs, and one could easily observe what was happening through the viewport. It was difficult to control the flow rate, which was quite fast, approximately 1.44kg/sec. Also, we were not able to reuse the stinger.

To begin optimizing the siphon system, trials were conducted with molten copper. A needle valve was installed to control the vacuum and slow the siphon. Additionally, a three-way valve was installed to allow the chamber to return to atmospheric pressure and stop flow. We also used ¾" (19 mm) tubing to prevent clogging, but this was unsuccessful. See Figure 47.

Figure 47. Copper Siphon Result- Plug

Neodymium siphon trials were attempted from a molten pool of metal (not electrowon). The molten Nd was contained in a molybdenum cup at melting point and 100g of Nd siphoned before the stinger clogged. We ran this trial a second time with the same result. There appears not to be enough superheat in the metal to stop it freezing before it is all collect. Typical industrial practice it to use the stinger about ten times before it is worn or plugged. The large cylinder on the right side of the figure is the vacuum storage chamber, since vacuum pumps take too long to spool up for use.

Figure 48 shows the siphon prototype, which we referred to as the "Lunar Landing Module," seated atop the furnace on the right. No solution was found to long term use

of the stinger, the small scale of operation makes freezing in the tube very likely.

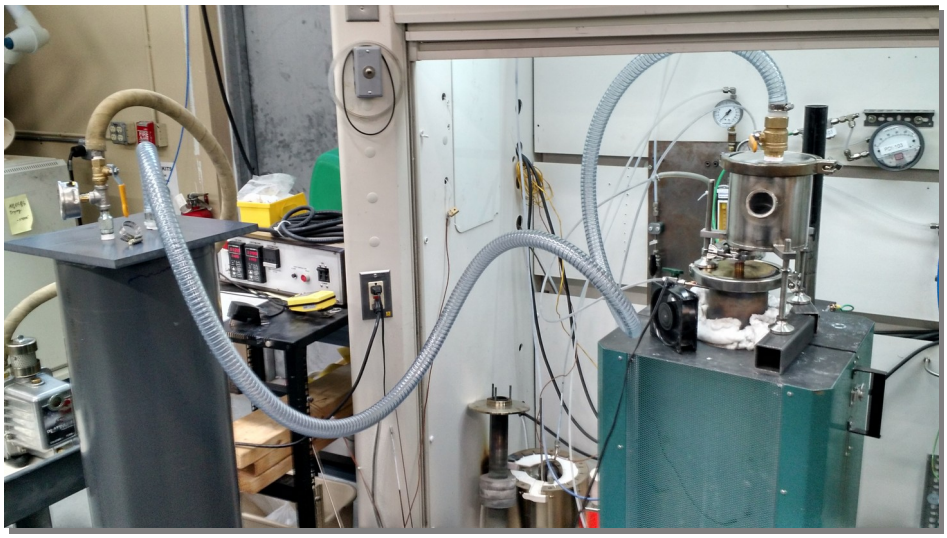

Figure 48. Molten Metal Siphon, aka the Lunar Landing Module

Master Alloy Melting

INFINIUM developed a new method for master alloy surface finish improvement, which is remelting 2 kg ingots and casting using a tilt furnace. It was found that casting of magnesium alloys was possible if the metal was melted under argon. Tests with small additions of a R134A Freon to create a passive film worked. Operating in a glove box to control the atmosphere was difficult, heat removal from the chamber required the use of an air to air heat exchanger, for which we used an automotive heat exchanger.

Oxide Feed

In order to maximize the magnesium content in our MgNd alloy, we experimented with various oxide feed compositions to determine the optimal ratio. Our original oxide feed produced 45%Mg-55%Nd (by weight) alloy.

We then experimented with feeding only MgO into the bath. The first day of production produced the same composition alloy, 45%Mg-55%Nd. After collecting metal each day, we continued to feed only MgO into the bath. One week later the metal composition shifted to 51%Mg-49%Nd, an improvement. The second week the metal composition improved even more to 53.5%Mg-46.5%Nd. We attribute this shift to the following reaction:

$$MgO+NdF_3 \rightarrow MgF_2+Nd_2O_3$$

This equation shows that by adding only MgO, the ratio of NdF_3 to MgF_2 decreased, resulting in the Mg^{2+} in the salt increasing and the Nd^{3+} decreasing. Figure 49 plots the weight percent of each component of the salt as a function of time.

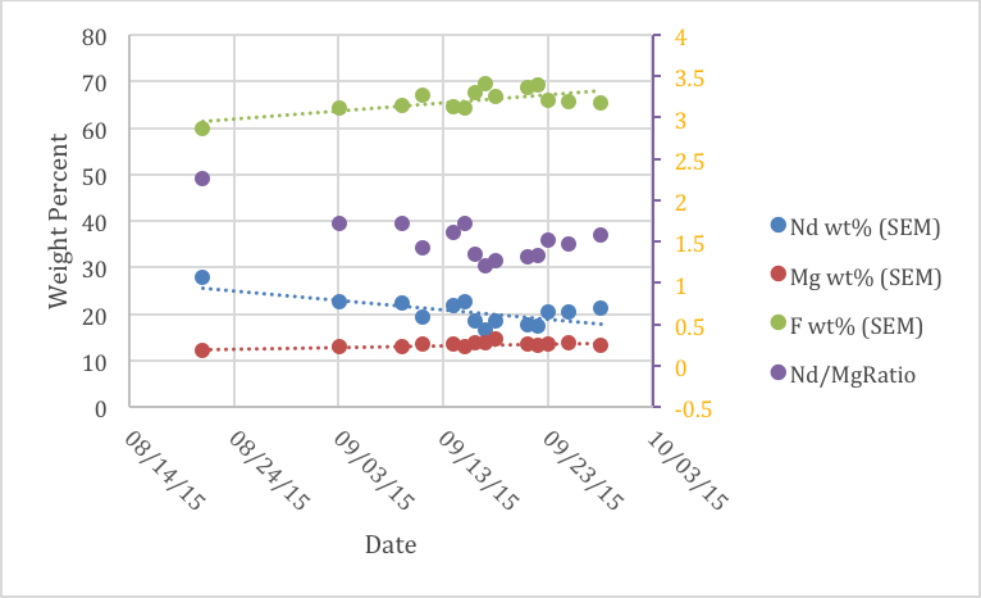

Figure 49. Compositional Drift of MgNd Flux

This shift in composition ceased to produce a coalesced product between 9/16/15 and 9/18/15. The Nd content of the metal deposit over those three days was lower than on any other day during the production run. Therefore, a critical concentration of Nd^{3+} in the salt, and Nd in the metal, is necessary to coalesce the metal. Based on this, we added two kilograms of NdF_3 to the salt on 9/22, and metal production continued. An optimal feed ratio should also produce 53.5%-46.5% Mg-Nd alloy.

Flux Investigation

The oxide feed experiments affected flux composition and yielded some insights. In order for the optimal flux to be highly productive, it should be dense to ensure alloy floats to the top. We have sent flux samples from our most efficient runs for composition analysis via GDMS

Production Rate

To reach the desired production totals, the overall production rate of the Delta cell platform needed to increase. Delta 1.0 would product approximately 0.132lb (.0599 kg) of metal over an entire shift. This equated to approximately 0.0175lb/hr (0.0079 kg/hr).

Based on previous small scale experiments and overall results from the Delta 1.0, the anode surface area was established as the limiting factor in the resultant current. Therefore, the anode area was drastically increased in the Delta 2.0. The larger anodes resulted linear increase in overall current proportional to the increase in surface area between the models. The current density on the Delta 1.0 anode was approximately 0.43A/cm^2 and the average current density on the anodes in Delta 2.0 was approximately 0.41A/cm^2. The slight discrepancy can be attributed to the change in location and configuration of the anode in the cell.

Previously, the Delta 1.0 cell produced approximately 9 lb (4.1 kg) of MgNd alloy (approximately 50%Mg-50%Nd) at an average current yield of 60%. Delta 2.0 addressed the source of inefficiency in Delta 1.0 by relocating the metal collection in a

central tube equipped with an argon purge. The combination of the centralized metal collect and new geometry resulted in an **increase from 0.0175lb/hr (0.0079 kg/hr) to 0.175lb/hr (0.0794 kg/hr) and a current yield from 60-70% to 90-95% on average.**

Unlike the resultant current, the metal production rate was not linear between the two Delta configurations. The change in production rate is function of anode area and electrode configuration. The efficiency drastically changed between the two cells. The increase in current efficiency combined with the increase in overall current resulted in a drastically increase production rate, illustrated in figure 50.

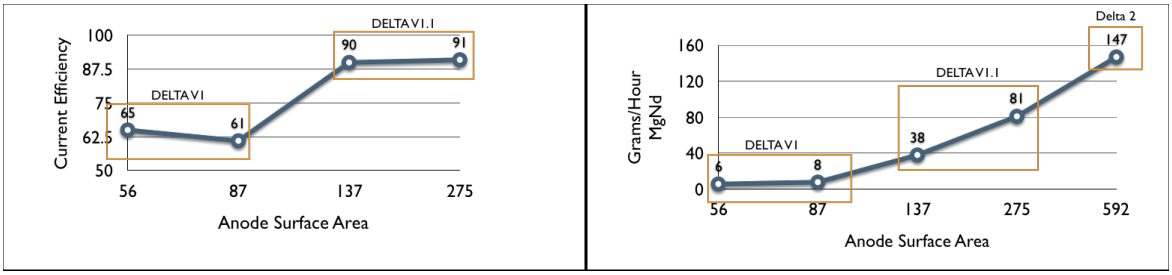

Figure 50 Current Efficiency (left) and Production Rate (right) as a function of cell configuration

The sharp increase can be attributed to both the collection assembly and the geometric orientation of the cell. It is also important to note that the production rate in each configuration is linear with respect to anode surface area, shown by the similar current efficiency between the anode's sizes used in each configuration.

In Delta 2.0, the cathode was located at the center of the cell and the product metal is separated from any potential oxidizing environment by central collection tube that extends out of the cell and is blanketed by argon.

Metal Collection

INFINIUM tested a new cathode spacing design (either tungsten or steel) is located at the center of the cell surrounded by a 1018 steel dam assembly. Moving radially outward are two anodes located opposite each other. See Figure 51. Also included in the design but not shown in the illustration is an auger feeder assembly that allows for the feeding of oxide during electrolysis. The oxide feed allows for a more sustained production rate. This cell is also equipped with a viewport to monitor the condition of the cell without exposing to the air.

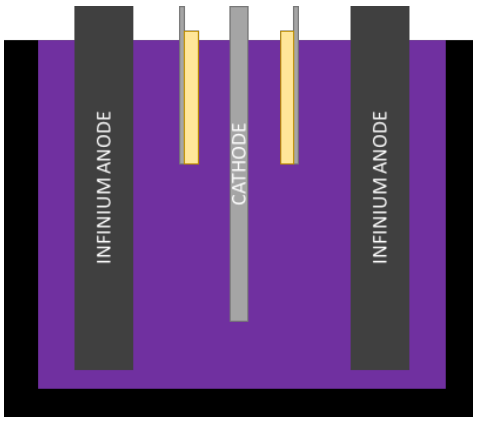

Figure 51 Delta 2.0 Illustration

In between the cathode and 1018 steel dam is a ceramic tube (illustrated in yellow above). Unlike the rods that were isolated for the dam in Delta 1.0, these tubes are widely available and inexpensive. This insulator allows the metal to pool in the center of the cell without shorting to the dam. The insulator can contain upward to 1kg of metal before harvesting in necessary. Figure 51 illustrates the insulating dam configuration, and Figure 52 shows a photograph of the dam assembly with the tube.

Figure 52 Ceramic dam assembly

The four small steel tabs on the bottom of the collection tube are designed to hold the tube in place and minimize the contact area for a potential electrical short to the steel tube.

Without the insulator, electrolysis runs were stopped after approximately 100-150g of metal were produced. The metal would bridge the cathode to the dam cause the dam to become cathodic allowing metal to be plated outside the collection. Using the ceramic, over 200g of metal was produced before electrolysis was stopped early to verify the effectiveness of the dam. This early success has prompted the investigation of eight hour electrolysis runs which could produce upward to 1.65lb (0.75 kg) of metal in a single shift in the smaller Delta 2.0 PPC.

Cathode Material

In the Delta 2.0, we investigated the possibility of using a cheaper cathode material. Originally, Delta 1.0 utilized a tungsten cathode and any attempts with steel were proven to be ineffective despite the success of steel on the smaller scale. In the Delta 2.0, steel was used as a successful cathode material, matching the performance of tungsten in almost every metric. The only discrepancy between the two materials is the iron content in the product metal. Using in house ICP-OES, the iron content in the metal produced with tungsten was 0.2% by weight and with a 1018 steel cathode the iron content was approximately 1.0% iron by weight. The iron impurity is of little concern because it will be removed in the distillation process. (Q17)

Continuous Production

A central focus for INFINIUM's production campaign was centered on maintaining a level of continuous production in the renovated Delta V2 MgNd electrolysis cell. Continuous and predictable production allowed INFINIUM to expand total operating hours from a single shift operation to a two shift, seven days a week production schedule. Expanding shifts required the training of several operators to run the cell to ensure there was coverage through any absences. The major difficultly for continuous operation revolved around electrolyte composition drift which resulted in sporadic performance.

Because the electrolyte used is a mixed fluoride bath, each component evaporates at a different rate. Lithium fluoride has the highest vapor pressure of the electrolyte components and needs to be replaced accordingly. When the concentration of LiF is too low, the viscosity of the electrolyte increases, significantly hindering the production of MgNd. The increase in viscosity significantly decreases the resultant current and

subsequently the production rate. The slower production rate is coupled with lower oxide solubility which in turn decreases overall production rate as well. Lastly, a low concentration of LiF effects how the metal coalesces on the cathode. The metal forms tiny droplets which are difficult to remove and post-process. If LiF concentration is too high, product MgNd sinks because LiF significantly decreases the density of the electrolyte. Early testing relieved that LiF needed to be added every day maintain a proper ratio of fluorides in the electrolyte to maintain consistent electrolysis of approximately 100A.

Production rate remained inconsistent in the Delta until agitation was applied. Agitating the electrolyte helps increase both the limiting current of the system and also increase the dissolution rate of the oxide into the bath. Increasing the dissolution rate can increase the overall oxide concentration present in the electrolyte which will result in a higher overall current. The addition of two bubbling tubes into the electrolyte effectively increased the current response of the system from 100A to 120A which is the equivalent of increasing the overall production rate from 68g/hr to 82g/hr, approximately a 20 percent increase in production rate.

Automated Feeding

Adding oxide into the electrolyte to sustain production was the most time intensive process associated for a cell operator. Over the course of a run an operator was opening the cell to added oxide up to six times to sustain a relatively constant production rate. However, each time the cell is exposed to air the internal components experience an elevated rate of corrosion reducing the cell life time. Periodically adding oxide allows the resultant current to drift from 120A initially to 90A between oxide feeds.

To reduce the operator involvement, INFINIUM developed an automated feeder that continuously added a runs worth of oxide during electrolysis. The feeder shown in Figure 53 consists of three major sections; the removable cover with drive assembly, the hopper, and the auger shaft.

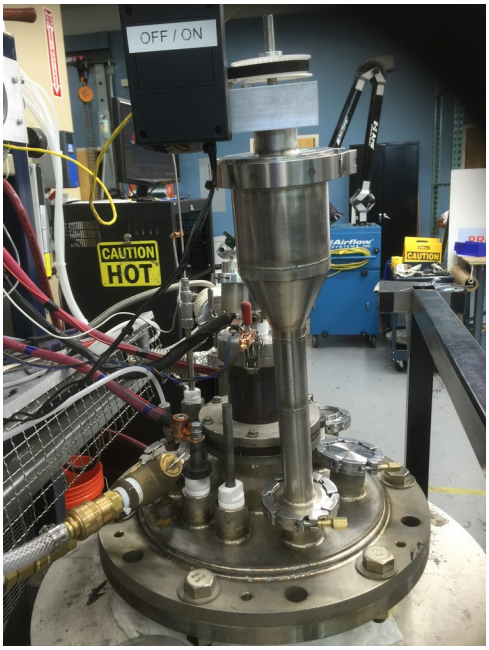

Figure 53 INFINIUM semi-continuous feeder

The top of the feeder is a removable flange, utilizing an O-ring seal to ensure that the feedstock loaded remains dry. Wet feedstock significantly affects the overall efficiency of the process in two ways. First, it produces HF vapors when coming into contact with the electrolyte and the oxide fails to dissolve in the electrolyte forming a sludge layer on the bottom of the cell. Second, wet oxide is stickier than its dry counterpart and does not flow through the auger assembly easily. Oxide sticking to the walls of the feeder can lead to a clog in the feeder which is difficult to clear.

A high torque NEMA 17 stepper motor is mounted on top of the flange. The motor runs at a constant speed controlled by an Arduino controller and motor shield. The controller is located inside a plastic casing to product

the controller from the dust and other matter in the lab. The power to the unit is controlled by a simple toggle switch. This allows the stepper motor to be powered down before removing the lid to fill the hopper with the desired oxide mixture. The feeder is calibrated to feed an average 1.8g/min of oxide mixture into the cell to support a resulting current of 120A.

The hopper is a cylinder with a conical bottom to funnel the flow of powder down to the auger shaft. The hopper can hold enough feed stock to produce upwards of one pound of MgNd alloy. If the cell operated at 100 percent current efficiency, it would take approximately 6 hours to produce one pound of metal.

Over long periods of time, the contact between oxide and respective fluoride vapors can produce a cement like substance that clogs the end of the feeder and lock the auger in place. The Delta V1.1 continuous feeder is equipped with a high velocity argon purge that is flows 1.5 SLPM of argon at five PSI (0.034 MPa). The argon flow is sufficient that the fluoride vapors will not enter the end of the feeder, preventing the formation of the oxide cement.

The addition of the automated feeder significantly reduced operator intervention during electrolysis. The operator now is only required to load the hopper, periodically check the cell, and extract metal at the end of the run. In addition to reduced involvement, the feeder has allowed the system to run at a constant current of 120A which fixes the kinetics of the system and creates a more consistent product.

Overnight Electrolysis

INFINIUM successfully conducted several unattended overnight runs to produce MgNd in the Delta V1.1 cell. This is a result of two major improvements in the process. The graphite crucible containing the electrolyte had begun to degrade under electrolysis, which covered the surface of the electrolyte in graphite powder. This graphite powder would short the anodes to the dam and the crucible wall. The shorting of the system reverted any product metal back into oxide. To solve the issue, a stainless steel liner was placed inside the graphite to serve as new crucible. Immediately following the addition of the liner the graphite dust was no longer observed on the surface and no shorting was observed over extended periods of electrolysis.

After resolving the surface shorting in the cell, the cathode dam was coated in a thick film of MgO each morning after the overnight runs and no metal was recovered. The Mg evaporated from the metal alloy shifting the composition to a denser, Nd rich alloy that sinks in the given electrolyte. A small, controlled air leak was introduced into the dam which oxidized the surface of the metal, limiting the overall evaporation of the Mg. Following the controlled introduction of air overnight runs because successful, producing upwards to 0.5 lb (0.22 kg) of MgNd overnight.

Commissioning of Gamma MgNd Cell

INFINIUM began the commission of the Gamma MgNd (PC1) cell. The unit featured four anodes of similar size to the two in the Delta V1.1. Anode surface is the limiting factor in the overall production rate, therefore doubling the anode surface area should result in at least a 1.5X increase in overall production rate.

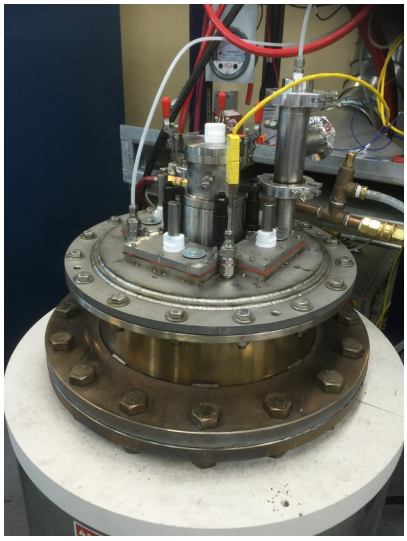

Figure 54 Gamma MgNd PC1

The Gamma unit features the same dam configuration as Delta V1.1. The two units use the same ceramic liner which has a lifetime of approximately four weeks before slight shorting to the dam is observed. The dam configuration can contain up to two pounds of material before any harvest is required, which is the expended production of 1.5 runs in the unit. The feeder assembly will also remain very similar to that of the Delta V1.1 to capitalize on both the use of standard parts and previous successes. Figure 54 shows the cell top.

Two major improvements over the Delta configuration revolve around total bath size and the anodes. Currently the Delta V1.1 cell contains approximately 35kg of total electrolyte which has a maximum oxide solubility of 700g. The Gamma cell will contain approximately 70kg of total electrolyte which can dissolve upward to 1.4kg of oxide. The higher capacity for oxide should help increase the overall consistency of production. The second major improvement is the ability to remove and replace the INFINIUM propriety anodes within one hour. This is significantly faster than the 12 hour time require to replace anodes in the Delta V1.1 which will allows for the potential to produce upwards of two pounds of metal in the time saved.

Gamma 1.0 ran uninterrupted for one month during the second phase of commissioning. The cell reached a peak current of 250A, and a production rate equivalent to 1 metric ton/year. The high costs and time requirement to keep Delta V1.1 in production lead INFINIUM to decommission the unit. The electrolyte from Delta V1.1 was repurposed to continue production in the more efficient Gamma V1.0 cell.

Production Cell Material Selection

Over the life of the Delta V1.0 and V1.1 pilot production cell, several roadblocks were encountered that effected both production rate and metal purity. After approximately four months of continuous production in the Delta V1.1 cell, the internals of the cell began to show significant signs of wear, mainly the heat shield baffles located under the top plate and the electrolyte. The degradation of the baffles ultimately led to a decrease in overall product purity while the change in electrolyte lead to low production rate. After approximately one month of subpar and inconsistent production, INFINIUM decided to decommission the Delta cell and reuse the internals in the more efficient Gamma production cell.

The original baffles were constructed from 304 grade stainless steel, which is a relatively low cost stainless steel that offers good corrosion and oxidation resistance at elevated temperatures. Originally, it was believed the use of Argon would protect the baffles but routine exposure to air during tapping and maintenance combined with the highly corrosive salt vapors resulted in severe corrosion of the baffles, as shown in Figure 55. The baffles began to form thick layers of scale that eventually fell into the electrolyte below. The addition of the stainless steel scale to the electrolyte became a major source of a nickel impurity in the produced MgNd.

Aside from the effect on product purity, the baffles also served as an insulating material by reflecting radiation to keep the top plate cool. As the baffles degraded, more heat was absorbed by the top plate. This increased the load on the water cooling. This also increased the temperature of the top plate making it far more difficult to operate.

Figure 55: 304 baffles after 1 month of electrolysis

The material of construction for the baffles was changed from 304SS to 310SS in an effort to reduce and or eliminate the baffle corrosion. 310 stainless steel is stable up to 1200°C unlike 304SS which is only stable until approximately 700°C. The difference in oxidation resistance is attributed to the higher nickel content of 310SS. However, it appeared that the fluoride vapors from the salt disrupted the oxide scale film, allowing the 310SS baffles to corrode and scale similar to the 304SS baffles. The 310SS baffles lasted upwards to 2.5 months while the 304SS baffles only lasted one month. Moving forward the baffles should be replaced with a different material that is more oxidation-resistant, thus reducing the downtime necessary to replace the baffles as they corrode.

Longevity of Electrolyte

Maintaining the composition of the electrolyte over time is critical in maintaining consistent levels of production in any electrolytic process. Initial investigation of the electrolyte was focused on the evaporation of the most volatile salt component, LiF. However, there was a slower, more influential drift in salt composition observed over the life of the Delta 2.0. This shift ultimately led to a production halt while the electrolyte was corrected.

An analytical method for ICP-OES was developed in house to analyze the Delta 2.0 electrolyte. This method involved fusing the fluoride electrolyte to convert it into a water soluble form. The water soluble fused electrolyte was then digested in acid and analyzed. Since this method was developed for the ICP-OES, analysis was limited to the total cation concentration and not the fluoride/oxide anion concentration. For quantification of the composition drift, the electrolyte sample was assumed to be 100% fluoride so an overall composition could be established. The oxide concertation was neglected because overall oxide solubility was below 1.5 percent. Analysis of several samples from the lifetime of the cell revealed that the overall Mg content increased from 6.6 weight percent to 16.1 weight percent, while the Nd content decreased from 64 weight percent to 10 weight percent.

Our hypothesis was that composition drift was caused by a shift reaction. Thermodynamically speaking, MgO will react with NdF_3 as shown below:

$$MgO + NdF_3 \rightarrow MgF_2 + Nd_2O_3$$

Therefore, as MgO was added into the cell, a small amount of MgO was reacting with electrolyte slowly changing the composition. This shift reaction of MgO was further supported by consistently lower material yields compared to that of Nd_2O_3, 97% and 98.7% respectively.

While the MgF_2 will stay in solution or form a two phase liquid with LiF and NdF_3, Nd_2O_3 has a limited solubility in the electrolyte dependent on the NdF_3 concentration. As a result, the newly converted Nd_2O_3 precipitates out of solution and forms a sludge layer at the bottom of the cell. The decrease in NdF_3 then causes some of the previously dissolved Nd_2O_3 to precipitate as well. The loss of NdF_3 and the precipitation of dissolved Nd_2O_3 cause the significant decrease in the overall Nd^{3+} concentration. As mentioned in previous reports, the ratio of Mg^{2+} to Nd^{3+} in the electrolyte is critical to producing MgNd alloy. The final alloy ingot bar of AE42 cast by Magpro are shown in figure 51.

The restoration of the bath took place in two parts. First the oxide sludge layer was removed from the cell entirely, leaving a single phase solution behind. That single phase solution was then analyzed using the aforementioned ICP-OES method. The necessary amount of electrolyte was then removed before the addition of NdF_3 took place. After the addition of NdF_3, the salt was analyzed again to verify the addition brought the composition back within the working range.

Product Purity

All metal produced at INFINIUM was analyzed using ICP-OES to track both the Mg content and the impurities within the produced metal. The MgNd produced during the commissioning of both the Gamma and Delta was approximately 45% Mg by weight. The composition of the metal was dialed in at 50-55% Mg by weight as proper current densities and aspect ratio of electrodes were developed. The major impurities found in the hardener were Fe, Ni, and Li. ICP-OES analytical results for one lot can be seen below in table 5.

Table 5: Sample analysis for MgNd

Sample	Cr	Fe	Li	Mg	Nd	Ni
MgNd - 02	0.00	0.18	0.15	55.30	44.06	0.04

In addition to these three impurities, there may have been other impurities unaccounted for because detection via ICP was not feasible.

INFINIUM did not subsequently implement any material changes because the AE42 produced using the hardener, shown in Figure 56, was in specification for all major impurities. We determined the sources of each impurity. The 0.15% Li was present from the electrolyte. The ingots poured from the production furnaces were approximately 80g in size. Each ingot poured was covered in electrolyte, and it appeared that the top few millimeters of the ingot contained the electrolyte. This layer formed on top of each ingot poured, regardless of size or aspect ratio. Therefore, if the pours were to increase in size, the electrolyte impurity should

decrease.

Figure 56 270lbs of AE42 produced using INFINIUM hardener

While a process change would be sufficient to reduce the Li impurity, material changes are required to reduce the overall impurities. As mentioned above, the stainless steel baffles were corroding in the molten salt environment. This allowed pieces of baffle to fall into the electrolyte where the Ni could be leached from the baffles. Once leached, Ni was plated into the product metal during electrolysis. This impurity can be removed by moving to a graphite based insulation material or refectory metal baffles. The Fe impurity was traced to cathodes used during electrolysis. Over one month of electrolysis the cathode diameter reduced from 1" (25.4 mm) to 0.85" (21.6 mm). This is because Nd will alloy with both Fe and Mg. Once the Mg content is the alloy is high enough, the Mg will leach the Nd from the iron and prevent any further alloying. Changing the cathode material from 1018 steel to tungsten would significantly reduce the Fe content in the metal.

Overall Production Rate

Following commission of Gamma 1.0, load was increased to 350 A by pre-treating the steel cathodes. A new steel cathode can support a current of 100A. Anything above that results in a grey deposit and sinking metal, which is difficult to recover. However, after one run at 100A the cathodes can support currents up to 350A, more than tripling the production rate. Running the production cell at 350A, INFINIUM can produce upwards to 750g per shift utilizing a batch process where the oxide is added in between runs after the metal harvest.

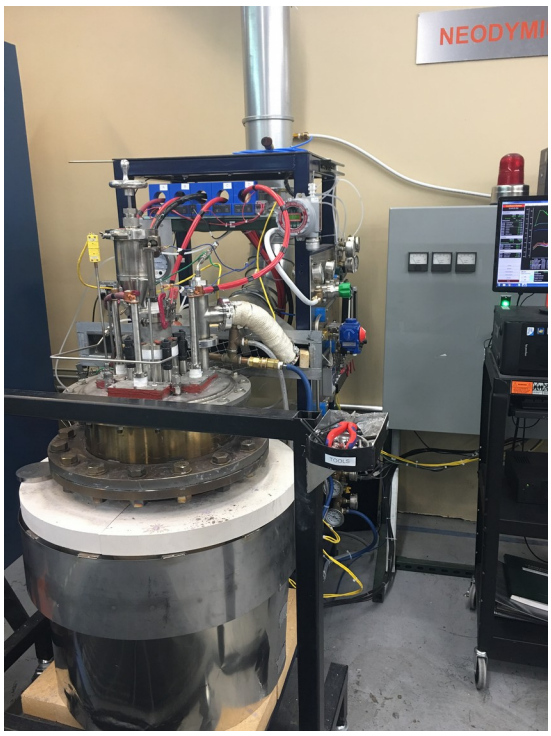

Figure 57 Gamma 1.0 Production Cell with Manual Feeder

While the batch process if effective, it allows for several hours of downtime during each shift. The operator must add the oxide into the cathode port and wait until the oxide has dissolved before the cathode can be reloaded. This process equates to approximately one hour of downtime after each run. Given that the operators can fit three runs into a shift, the cell is down for three hours. The addition of a manual feeder (Figure 57) reduced the cell downtime to 30 minutes per shift which would increase the production time by 50%. If the same efficiencies are assumed, the production rate

would increase to 1.125kg/shift, which is the equivalent to a 1MT/year electrolytic cell.

The second phase of feeder development was centered on reduction of operator involvement. Previously, INFINIUM developed an Ardunio controlled feeder to feed oxide in a slow, continuous manner. This reduces the need for an operator to tend the cell several times during the shift. Instead the operator loads the cell has they would normally and simply checks the cell throughout the day. This frees the operator's time, allowing them to tend to more cells in the same amount of time.

Anode Manufacturing

Over the course of the project, INFINIUM received zirconia tubes for sheathing our anodes from five different vendors, including tubes with very different composition from one vendor. INFINIUM tested these tubes early on, and made a preliminary vendor selection for initial long-run and alpha prototype experiments.

Two thermal gradient tests demonstrated the ability of the selected vendor's zirconia tubes to withstand the relatively steep gradient of 90°C/cm. Each test inserted a zirconia tube through two chambers with zone set points 500° C different and an insulated zone break around the tube. A stainless steel-sheathed profile probe measured temperatures at several points along the tube center line to estimate the temperature gradient in the zirconia.

INFINIUM also ordered equipment and materials to manufacture our own zirconia tubes. We will first make simple samples to test chemical interactions with the molten salt and density measurements. Following this, INFINIUM began to slip cast tubes for electrolysis testing in order to determine the effects of zirconia manufacturing process parameters and microstructure on performance in a magnesia electrolysis process environment. To our knowledge, this is the first effort to optimize zirconia for long-term service in a molten salt environment, and the use of new zirconia powders and process parameters may prove advantageous for this unique application.

INFINIUM engaged the services of a ceramics consultant who began working with us in January. Vimal Pujari is a leading expert in both R&D and industrial production of zirconia and other oxide and non-oxide ceramics, including high-precision forming of complex shapes. He is helping us to optimize zirconia tubes for this very new application, and to begin fabricating zirconia tubes for testing and later use in alpha and beta prototype experiments.

Figure 58: Candidate low-cost anode material diffusion through zirconia.

INFINIUM began tests of a new anode material as a low-cost replacement for silver. The material was placed in the zirconia tube and heated to its melting point. Results showed the material readily diffused through the zirconia (Figure 58). Its orange hue clearly permeated the tube well up its length. This result eliminates this material from contention. Further candidate materials will be tested in future experiments.

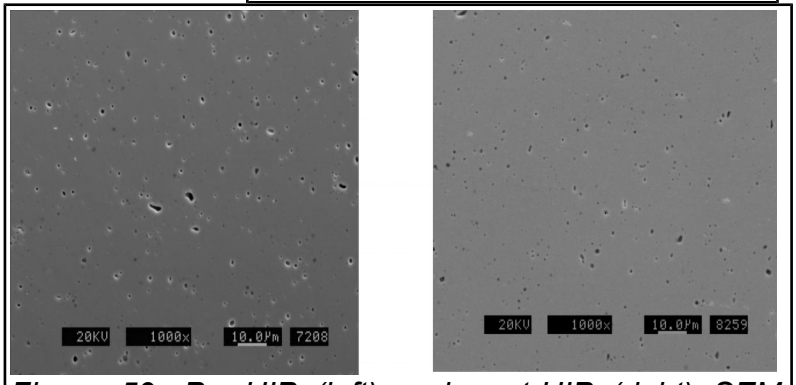

Figure 59: Pre-HIP (left) and post-HIP (right) SEM images of zirconia.

INFINIUM's baseline 6YSZ commercially-procured zirconia

tubes were hot isostatically-pressed to evaluate potential increases in density. Micrographs of the before and after images, clearly show a decrease in the porosity of the zirconia (Figure 59). Measurements showed an increase in density from 5.92 g/cc to 5.97 g/cc. The grain size was found to remain constant at 4-6 μm.

High-purity 8YSZ zirconia tubes were slip cast and sintered by INFINIUM. After expected shrinkage, the tube was 5" (12.7 cm) long with a 1" (25.4 mm) OD and 0.75" (19 mm) ID. The density measurement of the tube was 5.94 g/cc, which is higher than that of the 6YSZ commercial tubes, and very close to the 5.95 g/cc 8YSZ theoretical density.

INFINIUM made several advances in zirconia tube and material production and testing. And Boston University and INFINIUM developed a new oxygen-generating low-resistance current collector assembly, and filed a non-provisional patent application on the design.

Zirconia Disc Corrosion in Molten Salt INFINIUM made several zirconia discs using high-purity zirconia powder and a Carver press, and sintered them.

Accurate Zirconia Corrosion Measurement INFINIUM began developing methods for masking parts of a zirconia sample surface for high-precision measurement of corrosion. Without masking, salt wetting covers the sample surface such that it has not been possible to compare the as-received and corroded surfaces. INFINIUM tested nickel and platinum paints for masking: nickel flaked off during firing, platinum adhered well. A fifteen-hour corrosion test in molten salt showed no difference between masked and exposed surfaces, *i.e.* no measurable corrosion, so INFINIUM will run longer salt exposure tests with platinum masking, and also investigate other masking methods.

Zirconia Tube Slip Casting INFINIUM conducted tube slip casting development including elimination of more defect types and casting longer tubes. INFINIUM's first slip cast and sintered tubes achieved 99.5% theoretical density, vs. 98.3% density measured for the commodity off-the-shelf tubes which perform best in electrolysis. INFINIUM achieved this by using high-purity powder and optimizing firing conditions to dramatically reduce the number and size of microscopic defects.

INFINIUM used various controls to eliminate bubbles which cause macroscopic defects. Figure 60 shows the (post-sintering) macroscopic defect structures which formed in tubes cast using simple pouring of slip, as well as defect-free structures produced under more controlled mold filling conditions. This improvement did not make a noticeable difference in density.

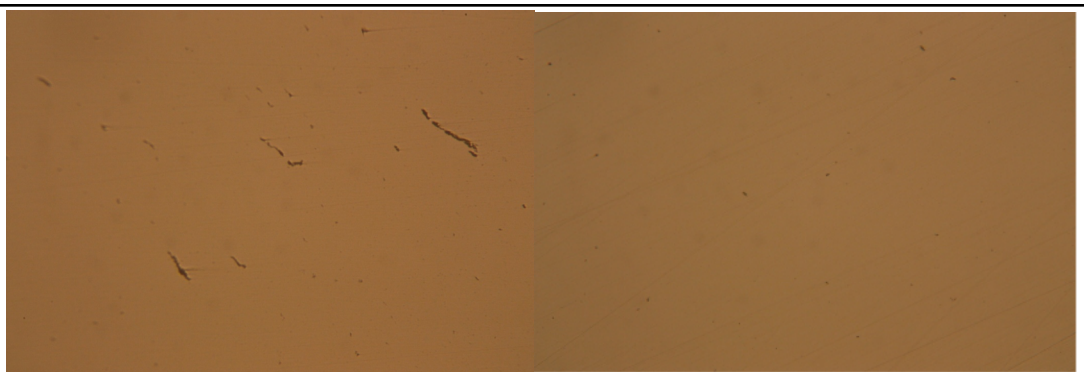

Figure 60*: Zirconia tube structures: (left) produced by simple slip pouring into themold, showing macroscopic defects; (right) made by more controlled slip pouring without such defects.*

INFINIUM also made a new 16” (40.6 cm) long mandrel for producing molds for 16” (40.6 cm) pre-sintered length tubes, which sinter to about 12”(30.5 cm) length, and made our first zirconia tubes using this new tooling. Tubes of this size are suitable for full magnesium electrolysis testing under industrial process operating conditions.

Zirconia Testing under Electrolysis Conditions INFINIUM fabricated parts for eleven long-term zirconia tube electrolysis test setups, and assembled four complete setups, shown in Figure 61. Zirconia corrosion by molten salts is easy to measure in simple disc salt exposure experiments, but additional corrosion mechanisms operate during electrolysis. These new test setups will allow INFINIUM to perform multiple controlled magnesium electrolysis experiments inexpensively. Zirconia corrosion rate in electrolysis is the best metric for determining tube lifetime and assessing cost. These setups will allow INFINIUM to determine the effects of zirconia tube chemistry and structure on performance in service.

New Current Collector Subcontractor Boston University and INFINIUM developed a

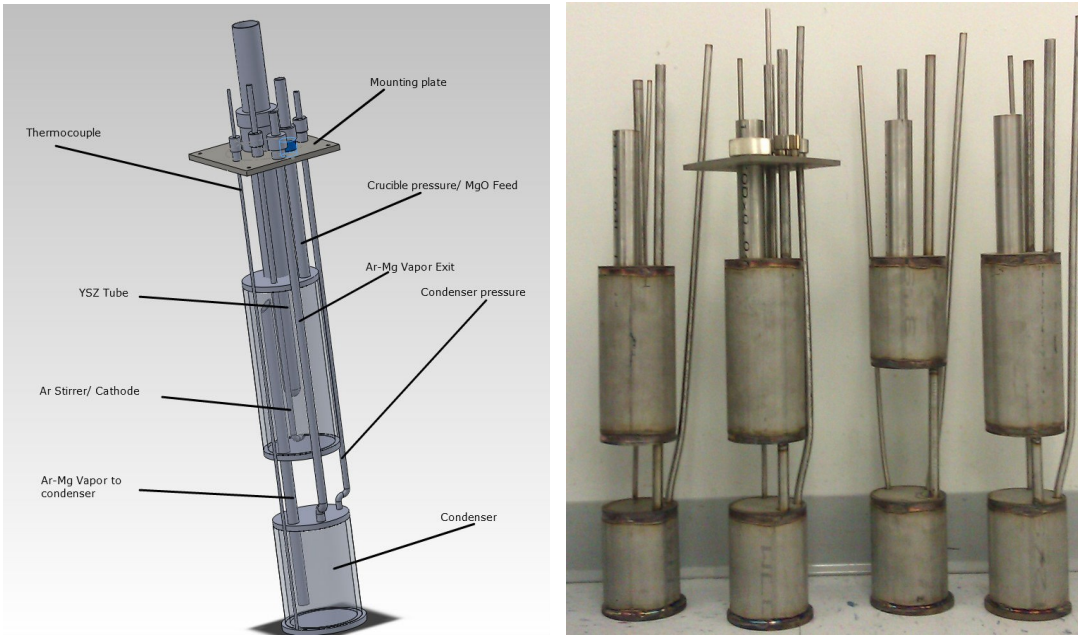

Figure 61: Electrolysis test apparatus design (left) and four assembled units (right).

new low-resistance moderate-cost current collector assembly for an oxygen-generating liquid silver anode. The current collector must have low electronic conductivity and be stable in pure oxygen at high temperature, and not corrode in the liquid metal anode. Iridium works but is prohibitively expensive; platinum dissolves in silver; electronically-conductive oxides such as strontium-doped lanthanum manganite (LSM) work well at high temperature but are expensive and do not conduct well at low temperature.

The solution reached by INFNIUM and BU involves using LSM sparingly where it is most needed, and excellent conductors with low cost such as nickel and copper where possible, and sheathing and sealing the device to prevent nickel and copper oxidation. The result shown in Figure 62 has multiple components: the liquid silver anode, an alumina tube sleeve protecting the nickel conductor, an LSM bar connecting the silver anode to the inside of the sleeve, alumina and LSM sealing the LSM bar to the alumina tube sleeve, and another small amount of silver electrically connecting the LSM to the nickel rod.

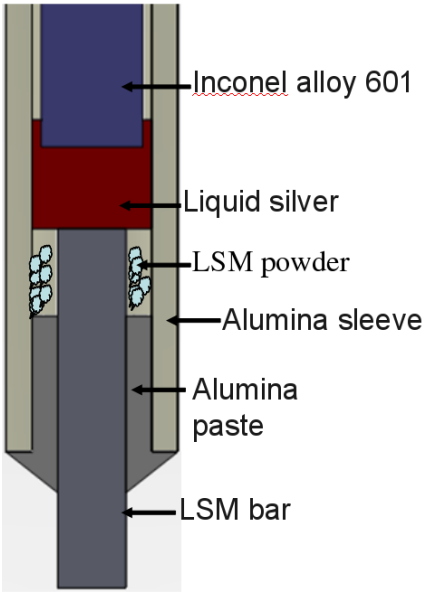

Figure 62: BU/INFINIUM low-resistance current collector assembly connects anode lead to liquid silver anode below (not shown).

This device as shown has approximately 0.1 Ω resistance at the 1150° C operating temperature, and is stable with no measurable increase in resistance for at least twelve hours. This is far lower and more stable resistance than any other current collector tested for this application.

Electrolysis Corrosion Study INFINIUM designed and constructed an initial experimental electrolysis setup with a dedicated data acquisition system, power supply rack, and gas panel. (Figures 63a and 63b) In December we ran two electrolysis experiments on commercial off-the-shelf YSZ tubes and developed a tube-screening protocol. We determined that platinum does not protect YSZ immersed in molten salt and are developing alternative methods to measure corrosion accurately. Additionally, we sampled the molten salt after each experiment to monitor its composition, with a focus on measuring dissolved metal content (see apparatus in Figure 64).

Figure 63 a & b: Gen I zirconia electrolysis setup.

After observing more corrosion on one side of the YSZ tube after electrolysis, we designed a setup upgrade to incorporate the cathode cage concept from our alpha prototype design. INFINIUM also designed more robust and flexible instrumentation. These Gen II upgrades should allow for more repeatable experiments and better representation of the alpha prototype, as shown in Figure 65.

Figure 64: Apparatus for testing magnesium metal content of process salt.

Zirconia Tube Slip Casting After establishing a protocol for conducting corrosion studies on commercial off-the-shelf tubes, we will test in-house tubes made of Vendor C powder along with a few in-house powders. We will also use our in-house Vendor C tubes to conduct uptime experiments on the alpha prototype.

Zirconia Powder Synthesis In order to trace tube components back to the manufacturing step, we have begun manufacturing our own zirconia powder compositions, beginning with an 8YSZ composition. Our initial batches of 8YSZ powder has better structure than commercial off-the-shelf powder; we slipcast this composition into 1" x 0.5" (25 mm x 12 mm) pucks for static salt exposure testing. We anticipate these pucks will require a lower sintering temperature. All in all we will

develop several different compositions of fully stabilized zirconia and conduct static salt exposure tests on each during Phase II.

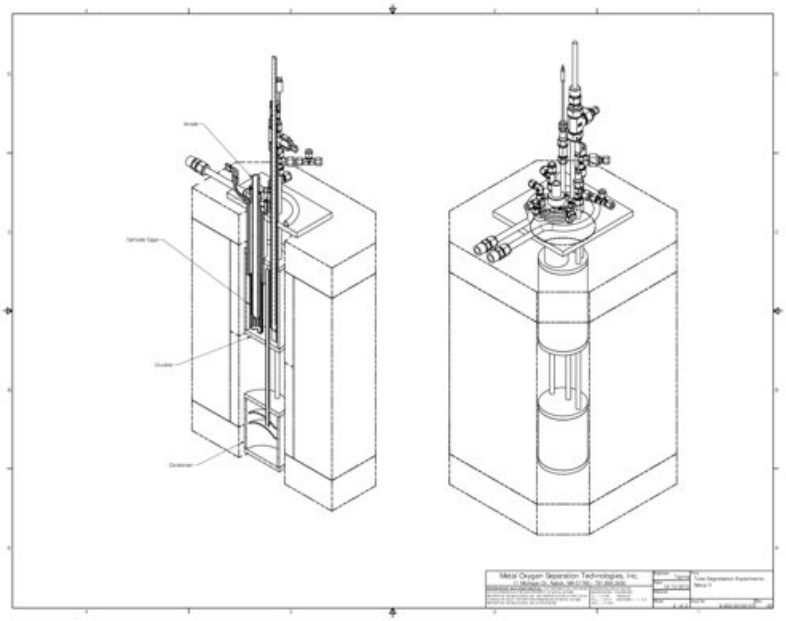

Figure 65: Gen II zirconia electrolysis testing apparatus design.

When scaling zirconia powder synthesis by traditional co-precipitation up to the kilogram level, increased volume expansion during pyrolysis poses a challenge. We are addressing this by designing a flame pyrolysis setup. The flame pyrolysis approach will not only address the problem of significant volume expansion but also simplify the overall process and reduce energy consumption.

Ceramics Laboratory We have constructed a new lab setup for preparing and testing ceramic slurries and acquired new equipment for testing viscosity and moisture content (Figure 66).

Figure 66: New INFINIUM ceramics laboratory setup.

Current Collector Subcontractor Boston University conducted further experiments using the inert oxygen-evolving current collector described in the prior report. The electrolysis cell with this current collector has an ohmic impedance of 0.368 Ω, which is very close to the 0.30 Ω impedance with a straight metal collector. The difference

is nearly exactly equal to the calculated resistance of the LSM bar, which is 0.066 Ω.

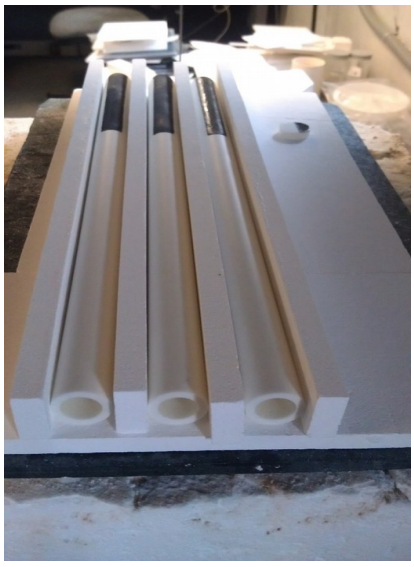

Figure 67 INFINUM custom zirconia tubes.

The objective is to maximize zirconia membrane performance in an economically viable manner.

Custom Tube Production. After moving to a new facility in mid-March, we set up a new ceramics lab and slip casting room. In-house production of 24”(61 cm) and 14” (35.6 cm) 8YSZ Vendor C tubes is well underway; we have standardized mold composition, improved slip casting technique, and manufactured custom firing trays. Additionally, we have established a tube defect testing procedure using dye penetrant and infrared light. We are currently at 10 green tubes/week capacity. Figure 67 shows our custom tubes.

Figure 68 INFINIUM tube sintering furnace.

INFINIUM has a total of 60 14” (35.6 cm) and 24” (61 cm) tubes from four different zirconia compositions. We air and vacuum sintered these tubes with 100% yield and densities of 99.5% and higher. This quarter INFINIUM also purchased a 10ft^3 (0.3 m^3) sintering furnace that is awaiting electrical service; 42 tubes can be sintered a one time. See Figure 68. This inventory, along with 10 green tube/week production capacity, meets our prototyping needs. INFINIUM have continued to maintain an inventory of 14” (35.6 cm) and 24” (61 cm) long 3/4” (19 mm) outer diameter tubes from four different zirconia compositions with three different mole percents. INFINIUM also received a supply of 6” (15.2 cm) long tubes for corrosion studies. This quarter we acquired a custom transformer for our 10ft^3 (0.3 m^3) sintering furnace; we anticipate it coming online in February and being able to fire 42 tubes every other day. See Figure 69. This inventory, along with the 10 green tube/week production capacity, meets our prototyping needs.

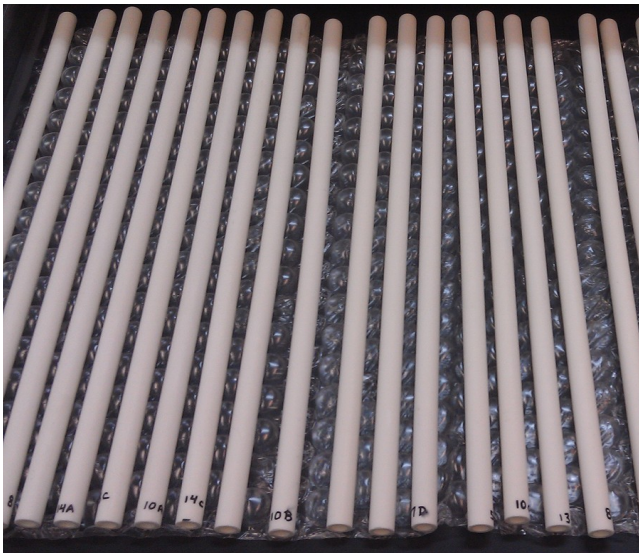

Figure 69 INFINIUM custom zirconia tube inventory.

Anode-Cathode Assembly

INFINUM optimized each component beginning at the inside with the current collector and anode liquid and working outwards through the membrane toward the cathode cage and flux composition. See Figure 70.

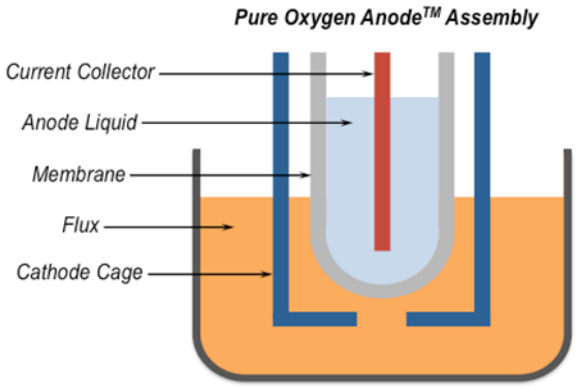

Figure 70 Integrated anode-cathode assembly schematic.

Custom Powder Synthesis. INFINIUM produced 1kg of INFINIUM 8YSZ powder by co-precipitation and from it manufactured several pucks and one small tube, which sintered to 92.3% density. INFINIUM conducted particle size analysis and modify powder synthesis to match Vendor C particle size distribution.

In addition to co-precipitation, we are exploring flame pyrolysis. When scaling zirconia powder synthesis by traditional co-precipitation up to the kilogram level, increased volume expansion during pyrolysis poses a challenge. The flame pyrolysis approach addressed the problem of significant volume expansion, but also simplify the overall process and reduce energy consumption.

In order to have more control over the electrochemistry of our production cell, INFINIUM produced 1kg custom zirconia powder, then slip cast and fired one tube to good density, though somewhat less than our custom tubes from COTS powder. We then compared the particle size of our custom powder to the COTS and milled ours down to match.

Water Corrosion Study. For hydrogen-fueled or natural gas-fueled anodes, which have an H_2O by-product, INFINIUM conducted water exposure tests on 6YSZ COTS tubes; the zirconia failed at a much lower temperature than expected, above the electrolysis zone. We will experiment with sheathing the failure zone of the tube to extend its lifetime. Figure 71 shows results of the water exposure test.

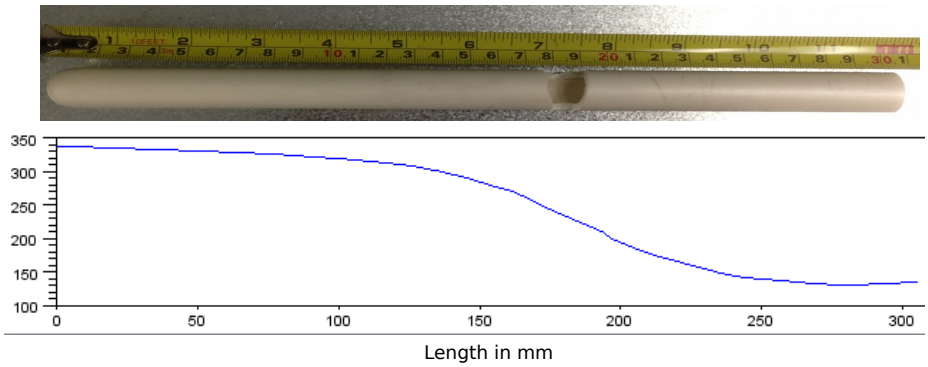

Figure 71: Zirconia Water Exposure Test Results, showing temperature distribution. Failure occurred in the 199-240°C zone after 24 hrs.

Temperature in °C

Electrolysis Corrosion Study

In January 2013, INFINIUM designed and fabricated a second generation experimental electrolysis setup with the same integrated anode-cathode assembly as the alpha prototype, as well as more robust and flexible instrumentation. (Figures 72a and 72b) INFNIUM ran electrolysis on COTS 6YSZ tubes and sampled the molten salt to monitor dissolved metal content. We will run electrolysis on various zirconia compositions, both COTS and custom.

Figure 72a: Integrated anode/cathode assembly

Figure 672: Gen II corrosion electrolysis setup

Current Efficiency. Subcontractor Boston University (BU) analyzed the current efficiency in the oxygen-generating experiment described in the previous report, as measured by flow rate of anode product oxygen. Over the course of the 30-hour experiment, current efficiency fell from just over 90% to around 50%. Electrochemical measurements showed that electron transference number of the molten salt increased from below 5% to over 50%. Figure 73 below shows both of these trends.

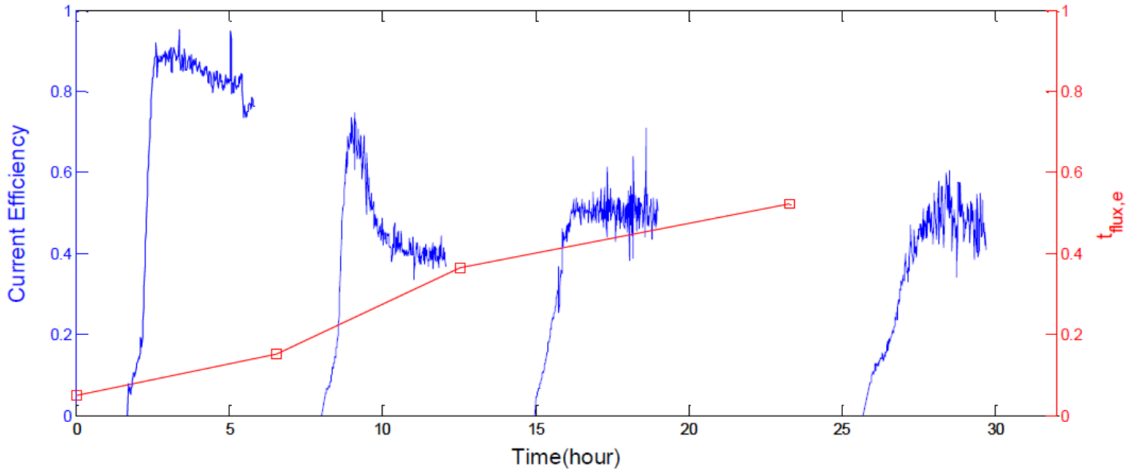

Figure 73: Current efficiency (left) and electron transference number (right) during December 2012 electrolysis experiment.

BU also created an equivalent circuit model of the electrolysis cell.

Subcontractor Boston University (BU) and INFINIUM invented a new method for

oxidizing dissolved magnesium in the molten salt, and thereby reducing its electronic conductivity and improving current efficiency. This new method does not require any modifications to the electrolysis cell, distinguishing it from all four of the methods described in a joint patent application (WIPO Publication WO/2013/052753, US PTO Publication 2013/0152734).

Custom Powder Synthesis. In order to have more control over the electrochemistry of the production cell, INFINIUM produced 1kg custom zirconia powder, then slip cast and fired one tube to good density, though somewhat less than our custom tubes from COTS powder. We then compared the particle size of our custom powder to the COTS and milled ours down to match. The density results from our milled down powder remained unchanged. Infinium planned to conduct a sintering study next quarter to determine how to increase density.

Static Exposure. INFINIUM prepared three new zirconia samples and soaked them in the appropriate fluxes at 1150 °C for 96 hours. Figure 74 shows details of each sample post soak.

(1) Vendor A 6YSZ (2) Vendor B 6YSZ (3) Vendor C 8YSZ

Figure 74. Static Exposure results for Vendors A, B, C

Porosity shown in Sample 1 was inherent in the material before salt exposure, so porosity remained largely unchanged and there was minimal surface degradation. Salt appears to have penetrated throughout Sample 2 as revealed in significant grain boundary attack, and INFINIUM did not continue with that material. Salt does not appear to have penetrated Sample 3. An interesting phenomenon of this sample is the band of slight inter-granular porosity with increased grain size near the interface. See figure 74.

Zirconia Composition Selection

INFINIUM has standardized the process for identifying the top performing zirconia composition. See Figure 75 below.

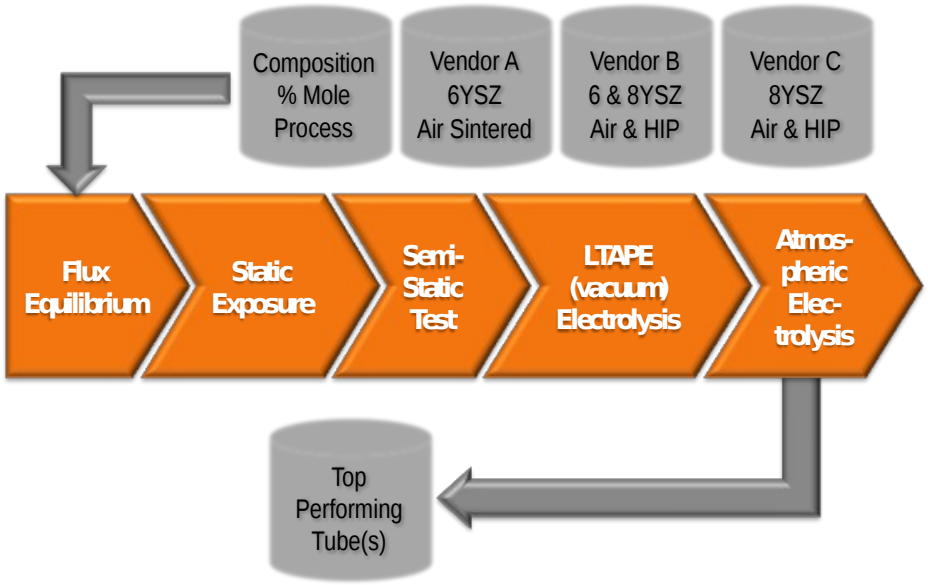

Figure 75. Process for Zirconia Composition Selection

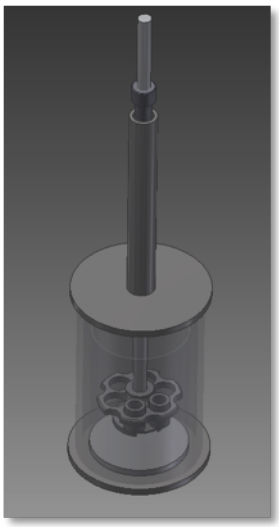

Figure 76 "Revolver" six-sample static test device.

Factors for zirconia membrane optimization include vendor composition, percent mole, processing procedures such as sintering methods and hot isostatic pressing (HIP). INFINIUM narrowed candidates by conducting improved, standardized static tests in a six-sample prototype called the "Revolver." See Figure 76.

After determining the best performing membrane candidates in these soak tests, INFINIUM conduct "semi-static" testing, then compare their performance in the Alpha 4.0 to the baselines then proceed to Increased Immersion Electrolysis in the Beta 1.1.

Semi-Static Testing. INFINIUM designed, fabricated, and assembled a prototype to test zirconia behavior in seven different flux compositions simultaneously, as shown in Figures 77 and 78. The procedure conducts electrochemical tests before, during, and after a 72 hour soak at temperature. INFINIUM monitored changes in salt composition to determine tube performance. After failing to reach temperature in the original furnace, INFINIUM installed a more powerful furnace and prepared the flux. The tube seals leaked, new sealant had to be obtained.

Once INFINIUM had identified the top performing samples from these tests, those zirconia compositions underwent low-pressure electrolysis in the Alpha and then atmospheric pressure electrolysis in the Beta.

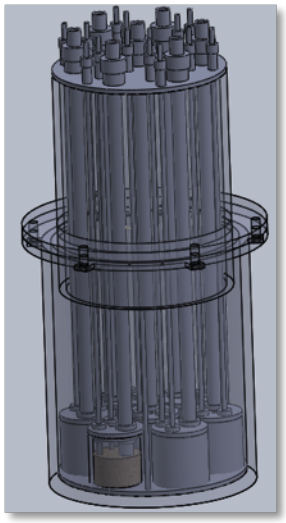

Figure 77. Semi-Static prototype design

Figure 78. Fabricated Semi-Static prototype

Current Collectors

In order to refine our inert anode current collector design, INFINIUM tested the stability of the hybrid LSM-nickel current collector in air by suspending two of them in a liquid silver bath and measuring resistance change over time by driving a current between them. Decoupling the current collector testing from electrolysis in this manner produced more reliable data and improved post-test analysis.

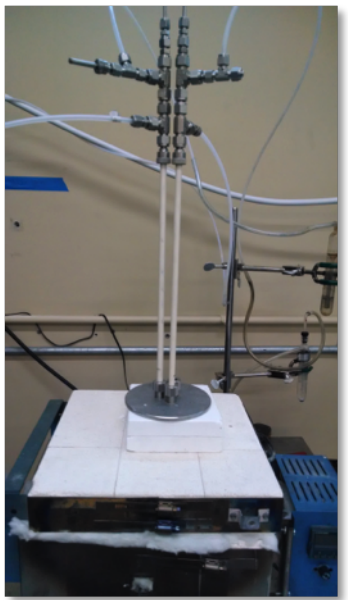

Figure 79 Current collector test apparatus.

In order to refine the inert anode current collector design, INFINIUM conducted two resistance tests on the hybrid LSM-nickel current collectors. For the first run, INFINIUM tested two current collectors in a silver bath at 1000ºC and applied a 0.4V potential between the two for 100 hours. See Figure 79. During the run INFINIUM recorded voltage/current and calculated resistance as a function of time: 115.5 A·h, 0.1Ω over the first 35 hours. After cooling & removal, one current collector remained functional with resistance at room temperature. Inconel rod oxidation and/or insufficient silver in the current collector caused failure of the other. The alumina paste joints functioned properly with no degradation to the LSM current collector.

For the second resistance test, we used a new furnace and power supply to allow testing at 1150ºC. The current was controlled at six amps throughout the run. Similar to the first test, resistance started at ~0.23Ω for system. Assuming equal resistance of each current collector, it was calculated a 0.115Ω resistance per current collector. After several hours, resistance increased to ~0.2Ω per current collector then stabilized. The test ran for 162 hours @ 6 amps, and we stopped it before current collector failure. The total cell resistance was 0.25Ω (0.125Ω per current collector), the experiment was

concluded. The new setup appears to be stable for at least one week.

Test results verified current collector resistance, determined usable life, qualified the manufacturing and assembly process, and provided data on failure modes to improve current collector lifetime.

During two electrolysis runs this period, the LSM current collector failed quickly after starting electrolysis. INFINIUM replaced the current collector during the first run, but the replacement also failed quickly. Upon inspection a yellowish was discovered film on the LSM surface which was confirmed to be non-conductive. The film was removed to re-expose the conductive LSM bulk material.

INFINIUM analyzed the yellowish film with SEM and EDS and discovered it contained phosphorous. The most likely source of phosphorus would be a cleanser. It is suspected that Vendor A uses a phosphorus cleaning agent which may not have been rinsed properly. Consequently, all Vendor A tubes were thoroughly washed.

Electrolysis Run 1

During the first electrolysis run, the redesigned current collector failed after approximately 30 minutes. Failure analysis revealed an alumina paste joint failure that likely caused silver to leak, and the LSM rod moved ¼" (6 mm) lower than originally manufactured. It was determined that the current collector was inserted too far into the silver, procedure was revised.

Electrolysis Run 2

INFINIUM constructed a simplified argon input manifold to reduce congestion, weight, head room, and Inconell tube length. The argon outlet was insufficient and caused the current collector to pressurize to 5psi (0.034 MPa), causing the alumina paste joint between the alumina tube and LSM rod to fail. A small hole was drilled in the fitting to allow the argon purge gas to exit. The failed current collector from the zirconia tube was removed and replaced without cooling down the furnace. With the new current collector, current efficiency averaged 70% over the first 40 hours. The calculated current efficiency based on instantaneous current /oxygen flow relationship averaged over time is shown in Table 5.

Table 5: Time and Current Efficiency, Alpha 5 electrolysis run 2.

Time Interval (Hours)	Current Efficiency
0-2	88%
0-10	82%
10-20	77%
20-30	66%
30-40	57%
40-50	53%
50-60	35%
0-40	70%

Low Resistance Current Collector

INFINIUM made slight modifications of the current collector geometry to lower the resistance, facilitating higher current capabilities. This new design was fabricated and tests silver bath resistance were made.

Initial results were promising with the resistance at approximately 0.08Ω per current collector.

Molten Salt Anode Liquid

With silver anode liquid, oxygen ions convert to O_2 at Ag-ZrO_2 interface, which can lead to reducing conditions and corrode the membrane. With salt anode liquid,

oxygen ions remain in ionic form until they reach the current collector, where they convert to O_2. And if the zirconia tube breaks, the flux will remain intact rather than contaminated by silver. The current collector for salt anode liquid must be stable in molten salt and O_2 at operating temperature and have good electrical conductivity.

INFINIUM ran electrolysis with a graphite current collector in salt anode liquid for 48 hours. Initial results were promising with regard to zirconia membrane corrosion. A literature and phase diagram review was conducted. Two candidate materials were found and procured for testing.

Static Soak Data

Results suggest a correlation between firing temperature and penetration depth, i.e., the higher the firing temperature, the less the penetration. INFINIUM designed further static tests to determine the effect of firing temperature on membrane corrosion. Table 6 details each sample's performed in the static soak tests and Figure 80 shows Vendor A and C samples post soak.

Table 6: Vendor and soak time.

Sample	Powder Supplier	Stabilization	Manufactured	Firing Temp.	Apparent Penetration Distance (μm)	Interior Porosity Band? Distance from Edge (μm)
1	Vendor B	8Y	Praxair	1450	32	75
2	Vendor C	8Y	Praxair	1450	25	105
3	Vendor B	8Y	Infinium	1500	21	-
4	Vendor C	8Y	Infinium	1500	21	-
5	Vendor B	10Y	Infinium	1500	16	95
6	Vendor A	6Y	Vendor A	1700	8	-

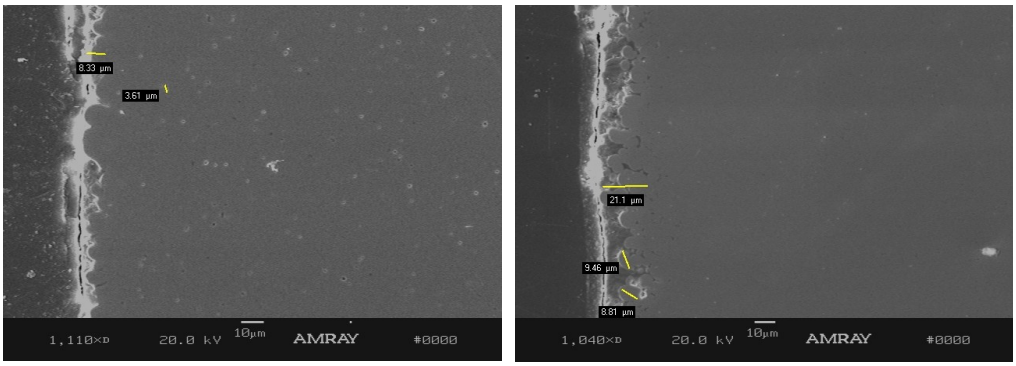

Figure 80. Vendor A (left) and C (right) static results.

Factors for zirconia membrane optimization include vendor composition, percent mole, processing procedures such as sintering methods and hot isostatic pressing (HIP). We are narrowing candidates by conducting improved, standardized static tests in a six-sample prototype we call the "Revolver."

After testing zirconia samples in the Revolver, we discovered that there are often, but not always, three layers within the membrane:

- A dissolution layer in which the grains appear to be dissolving and then eventually dislodge;
- A dense region typically starting at approximately 100um from the surface;
- A porous region (not evident in three of the six samples) See figure 81.

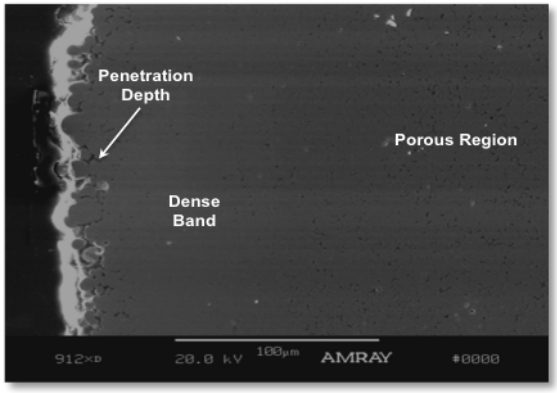

Figure 81 Changes within zirconia membrane after static exposure testing.

Results suggest a correlation between firing temperature and penetration depth, i.e., the higher the firing temperature, the less the penetration. INFINIUM conducted an additional static test to determine the correct Y_2O_3 concentration to prevent yttria enrichment or leaching of the YSZ membrane. The Y_2O_3 concentration was lowered from 1.25% to 0.5 %, the sample were then soak at 1150 °C for 12 hours with promising results.. See Figure 82.

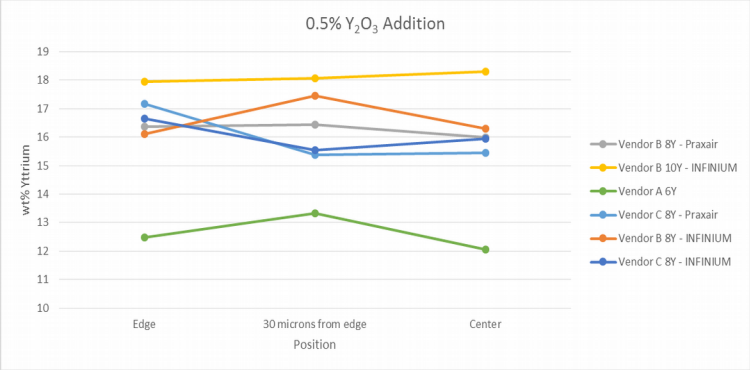

Figure 82 Static Test Results at 0.5% Y_2O_3 Concentration

INFINIUM electrolysis with a graphite current collector in salt anode liquid for 48 hours and conducted literature and phase diagram reviews to identify alternative current collector materials. No suitable candidates were found that met the following performance criteria:

- Stable in oxygen atmosphere @ 1150ºC
- Stable in molten salt @1150ºC
- Electrical conductivity in necessary range.
- Reasonable cost, i.e. not platinum or iridium

Per the design timeline, *anode liquid conduct is fixed as silver.*

Anode Assembly

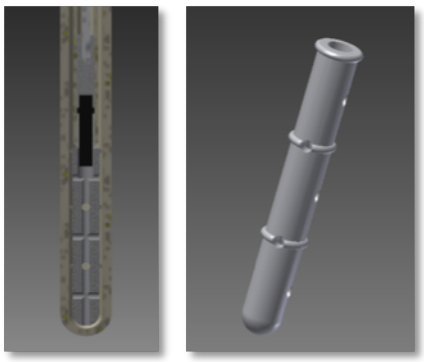

Figure 83 Low Silver Anode Assembly, version 1

In order to reduce the amount of silver used in the anode assembly, for both cost savings and splash reduction purposes, we designed a low silver version that uses a porous displacer inside the zirconia membrane. See Figure 83. The displacer must have the following characteristics:

- Chemical compatibility (high alumina)
- Open porosity
- Stable porosity up to 1200 °C

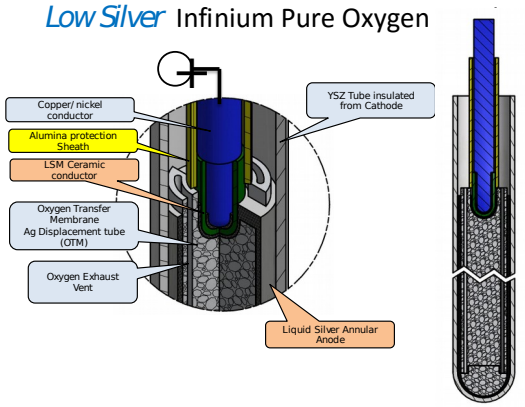

Figure 84 Low Silver Anode Assembly, version 2

After the initial design review, we changed the design of the silver displacer hoping to reduce cost and enhance oxygen gas removal rate. Figure 84 shows the new design, which includes a porous extrusion with a bottom cap and green-machined silver well at the top. We will contact a ceramic extrusion manufacturer to assess the manufacturability and to provide input to a final design.

Cathode Cage

After 96 hours of electrolysis during run 2, the zirconia tube displayed previously unobserved changes. There was an enlarged area above the liquid salt level that was encrusted with salt. Additionally, there was significant tube corrosion that corresponded directly to the location of the cathode cage holes. Measurement of the tube diameter revealed very little erosion outside of the cathode hole locations. See Figure 85. The cathode change was redesigned to reduce tube corrosion. Additionally, MgO was added to the salt bath. Samples of the current Alpha 4 salt were submitted to the LECO combustion Analyzer to confirm oxide content.

Figure 85 Cathode cage and zirconia tube post electrolysis

Low Silver Assembly

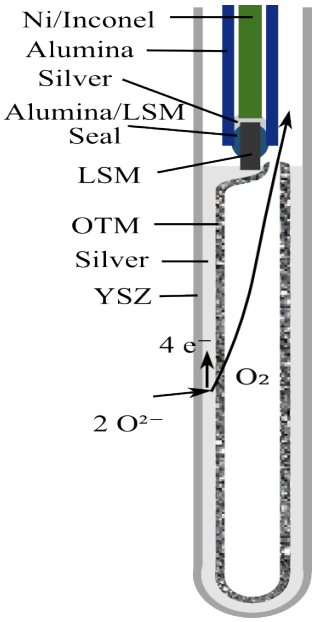

Figure 86. Low Silver Anode Assembly

In order to reduce the amount of silver used in the anode assembly, porous displacer was added inside the zirconia membrane. The displacer must have the following characteristics: A) Chemical compatibility (high alumina), B) Open porosity, C) Stable up to 1200 °C

INFINIUM ordered a small part to test its gas permeability and silver wetting. Results of this experimentation were very encouraging. Silver did not wet into the pores of any of the porous sintered alumina samples, despite 55 vol% density, i.e. 45% porosity. That said, test pieces made from the coarsest alumina were very fragile, so we have chosen the second-coarsest particles to produce the first batch of prototype silver displacers See figure 86.

Perforated Cathode Cage

After observing the zirconia tube degradation near the cathode cage holes, INFINIUM fabricated a cathode cage with a stainless steel perforated tube welded to the bottom.. See Figure 87. Electrolysis with this new design resulted in tube failure above the salt level at around 120 hours. See Figure 88. There was no sign of localized erosion on the YSZ membrane. The lower section of the zirconia tube was roughly the same diameter as the original. The tube appears to have split open from the inside outward; the split, near the solid/perforated joint section, appears to be a result of pressure build-up with silver splashing then freezing, blocking the oxygen exit path.

Figure 87. New Cathode Cage

Offset Purge Cathode Cage

As another version was fabricated with cathode cage with the cathode-membrane annulus purge

hole raised up out of the area of electrolysis. The hole was ¼" below the salt surface level, with 2" above the top of the anode silver level. The objective of this design was to remove the hole pattern from the active electrolysis area while still maintaining its purge function.

Unfortunately an instrument power failure over a weekend caused data loss after approximately 20 hours of operation. Electrolysis was running well at the time of instrument power failure; therefore, 54 amp-hours produced and 109 ml O_2 up to the failure.

Upon inspection, it was found that the zirconia tube degradation near the cathode holes appears to be a result of bubble formation rather than electric field effect, further confirming our hypothesis from the failed purge electrolysis run.

Figure 88. Zirconia Tube & Cathode Cage Post-Electrolysis

Figure 89 Offset purge cathode cage & YSZ membrane

Slotted Cathode Cage

The next cathode cage design tested was a slotted cathode cage. The objective of this new design was to compare electric field effect versus purge effect on the zirconia surface. The cathode cage was fabricated a cathode cage with six slots. This design allows the same tube purge action as the offset purge test; however, the electric field effect, if there, would be in a linear vertical pattern. This design would also improve mass transport issues. (Figures 89, 90)

All cathode design tests concluded that the degradation mechanism resulted from gas flow rather than electric field.

The fourth cathode cage revision was a bubbling cathode cage, consisting of a double wall with finely perforated inner surface to disperse the argon bubbles. The objective was to bubble argon at the site of Mg production location thereby lowering Mg activity in the salt. Stainless mesh 0.02" (0.5mm) holes and 30% open area was used, as shown in Figure 91.

Figure 90 Slotted cathode cage & YSZ membrane

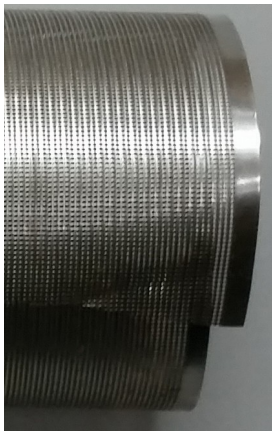

Figure 91 Bubbling Cathode Cage

Zirconia Tubes

After static testing zirconia samples last quarter, it was discovered that there are often, but not always, three layers within the membrane are formed: A) A dissolution layer in which the grains appear to be dissolving and then eventually dislodge), B) A dense region typically starting at approximately 100um from the surface, C) A porous region. (This region was not evident in all samples.) See Figure 92.

Results suggest a correlation between firing temperature and penetration depth, i.e., the higher the firing temperature, the less the penetration. As mentioned in Task 2, INFINIUM reported the highest current efficiency, 85-95%, after conducting electrolysis with Vendor C tubes fired at 1575 °C instead of 1500°C.

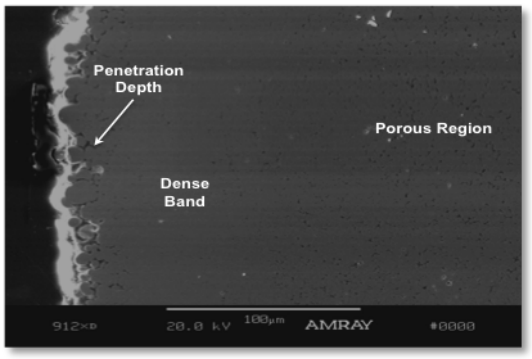

Figure 92. Changes within zirconia membrane after static exposure testing

Additionally, in order to improve current efficiency and create space for new current collector designs, INFINIUM has the process to manufacture 1” (25 mm) and 1.25”(32 mm) outer diameter tubes. Stainless steel master molds have been produced, and new firing trays are on order. Mold production began the last week of January 2013, and green tube production started in February. Fired tube production began with receipt of the firing trays in March.

The objective of this task is to continue maximizing anode assembly performance in an economically viable manner and to acquire onsite manufacturing capability.

Additionally, in order to improve current efficiency and create space for new current collector designs, INFINIUM begun manufacturing green 1” (25 mm) and 1.25” (32 mm) outer diameter tubes. See Figure 93. Diameter was increased to 1.25 inches.

Fused Alumina Silver Displacer

In order to reduce the amount of silver within the anode assembly, INFINIUM chose fused alumina as a starting material to cast thimbles for testing. Fused alumina is less reactive than other forms of alumina, providing more control over microstructure porosity during sintering.

We procured fused alumina powder with three different particle sizes and fired each at three different firing temperatures. See Figure 94. All samples prevented silver infiltration with the second coarsest performing best. Gas permeability was tested, the one with best performance was used in an electrolysis test. However electrolysis proved to unsuccessful with this spacer, possibly because the pressure drop was too large across the displacer.

Figure 93 1" Outer Diameter YSZ Tube

Figure 94. Fused Alumina Powder Samples

Make and Test Parts from the Recipient Magnesium

INFINIUM shipped 9 kg of Mg-46.5-50%Nd hardener to our alloying partner. From this hardener, the alloying partner cast 123 kg of AE42 alloy. The goal of this was to test this alloy in an automotive component in order to evaluate INFINIUM master alloy for this application.

Vehma, and its parent corporation Cosma, have long been involved in research projects to include the use of Mg metal in automotive lightweighting applications. Commercial use of Mg in vehicles is dependent on a stable, domestic supply of Mg which is cost competitive relative to existing lightweighting materials. This project provided a promising approach to commercial Mg production.

INFINIUM shipped all 30 kg of the hardener produced during this project, plus 12.7 kg of Mg-30%Nd, to the alloying partner where 263 kg of AE42 was cast and shipped back to INFINIUM: 123 kg in the form of 5.8 kg ingots, and 140 kg as 1 kg ingots. Five random ingots where removed from the second lot to be analyzed via ICP-OES. The COA generated from the lot can be seen below in Table 7. Note a total of 7.4 kg Nd was contained in the hardener shipped to the alloying partner, but due to casting issues, only 1.8 kg was in the product.

Table 7: COA for INFINIUM AE42 (second 140 kg lot)

Elements	***Concentration (%)***
Aluminum	3.070
Neodymium	1.177
Manganese	0.092
Iron	0.003
Copper	0.004
Nickel	0.001
Zinc	0.060
Lanthanum	0.073
Cerium	0.140
Praseodymium	0.008
Samarium	0.002
Magnesium	Balance

Once the material was verified, the material was packaged on a pallet. The poor form factor of the small ingots made it necessary to package the material within a heavy duty bag to prevent any material from being lost during shipping. Figure 95 illustrates the metal as packaged for shipment to Vehma.

Figure 95 507lbs AE42 shipped to Vehma. Figure 96: MMLV Front Kick Down Rail. .

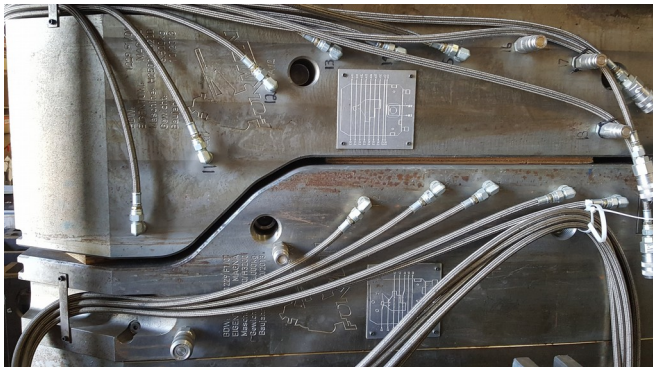

Figure 97: MMLV Front Kick Down Rail casting die: detail (above), with related tooling (right).

INFINIUM and Vehma decided on the Multi-Material Light-weight Vehicle (MMLV) Mach I Front Kick Down Rail (a.k.a. torque box) as the candidate part for testing AE42 alloy made with INFINIUM Mg-Nd master alloy, as shown in Figure 96, with its casting die and related tooling shown in Figure 97. The timing of the project allowed Vehma to utilize the tooling for two projects – the INFINIUM project and a Multi-Material Lightweight Vehicle (MMLV) prototype developed with financial assistance from the US and Canadian governments. This part showcases the ability of die casting to achieve geometrical complexity, resulting in part consolidation and reduced mass and assembly cost. Utilization of the AE42 would result over 30% mass savings over the Aural 5S aluminum alloy ($AlSi_7Mg$) used in the Canada-funded portion of the MMLV prototype.

Unfortunately, when the AE42 alloy was ready to cast, INFINIUM and Vehma were unable to find a die casting company with a machine that was compatible with the Magna die for this part. Vehma had sold its die casting machine when it decided not to produce magnesium die castings, and after an extensive search we were not able to locate a current user of this die casting machine type. Other die casting machines did not have rails compatible with the die.

Model Lifecycle Costs, Energy Use and Emissions

INFINIUM conducted four sets of modeling studies. Thermodynamic studies estimated equilibrium behavior of gases interacting with magnesium in the argon recycling system, and magnesium oxide solubility. Finite element analysis focused on the magnesium condenser, and anode system electrical current and heating. Technical cost modeling investigated capital and operating costs of magnesium production using this technology. And a report was prepared on Energy, GHG and Other Emissions.

Thermodynamic Modeling

A thermodynamics model of equilibrium gases with magnesium indicated that all but one of the argon impurities expected to be present in a MagGen™ system react with magnesium, resulting in their removal at the condenser. The oxides, nitrides and halides form inclusions which sink in liquid magnesium, enabling their removal from the product. The model predicts that the one gas remaining is hydrogen, which is that identified in the Argon Sampling Experiment above, showing good agreement.

The other thermo modeling study was a thermodynamic estimate of the liquidus surface in the reciprocal system (Ca,Mg)(O,F_2) conducted by subcontractor Kingston Process Metallurgy (KPM) using FactSage. As described on p. 27, that model predicted very low MgO solubility, much lower than the observed 10-15 wt%.

Finite Element Analysis

Extensive multi-physics modeling was performed for the design of the condenser for the first alpha prototype, in order to avoid flow issues such as dead zones and pressure differences. Temperature and velocity profiles were evaluated as the Ar and Mg vapor travel from the crucible through piping and into the condenser. Results shown for example in Figure 98 were used to refine the design prior to fabrication.

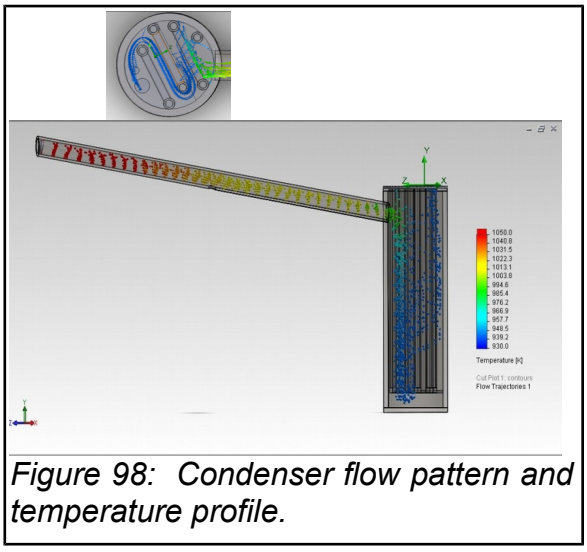

Figure 98: Condenser flow pattern and temperature profile.

INFINIUM completed a Finite Element Analysis (FEA) study of the anode assembly including the zirconia tube, liquid metal anode, and LSM-capped current collector, in two stages. The purpose of this model was to assess potential for problems such as uneven electrolysis performance or thermal stress in the system. The first stage included temperature dependence of material properties: for example, copper electrical conductivity varies by about a factor of five from room temperature to its melting point. This study indicated that the LSM and lower current collector core can be the hottest parts of the system, due to the high resistance of the LSM cap. Figure 99 shows these results.

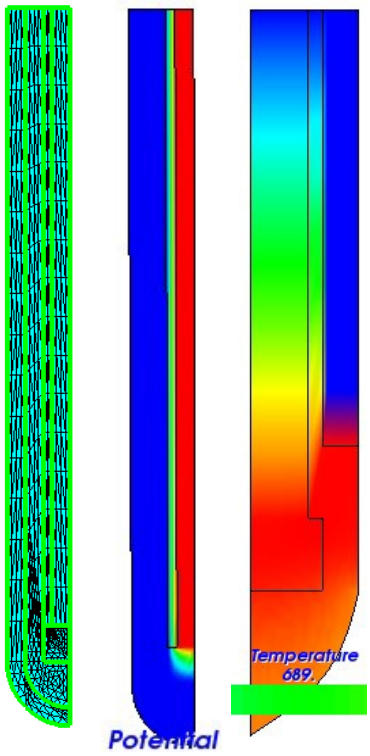

Figure 99: FEA anode assembly model: mesh (left), calculated electrical potential field (center) and calculated temperature field (right).

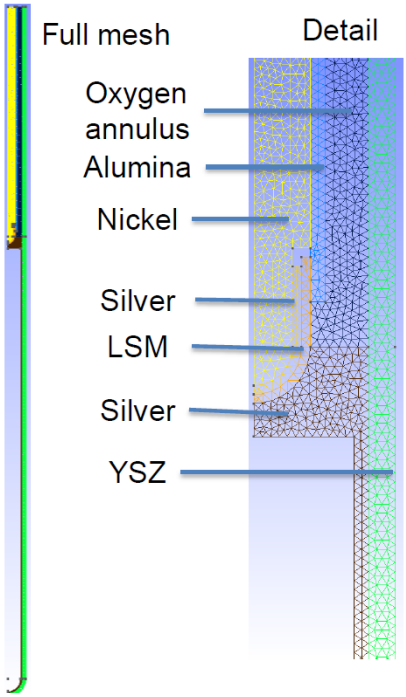

Figure 100 FEA anode assembly model geometry and mesh.

The second stage expanded the model to a high-current anode assembly design, with the goals of optimizing lead geometry for minimal energy use (resistance and heat losses) including oxygen flow, understanding trade-offs in the silver displacer design, and estimating thermal stress in the zirconia tube. This is an axisymmetric model with parameterized geometry, making it very efficient at rapidly conducting many simulations in order to search the design space. Initial geometry and parameters correspond to a future industrial 300 A tube design, but the model can also examine the tube geometry used in laboratory experiments. It includes temperature-dependent properties, including zirconia, silver, LSM and nickel electrical conductivities.

Figure 100 shows the model geometry and mesh. It has a 1.5 mm thick silver layer behind the 3 mm thick zirconia tube. The mesh does not include the silver displacing solid, as it should have roughly uniform temperature and electrical potential, due to very low electrical and thermal conductivity. The

current collector includes a nickel conducting core in an alumina sheath with LSM conducting tip and liquid silver contact. The figure shows geometry and mesh detail near the interface between the liquid silver and current collector. Mesh spacing is a uniform 1 mm throughout.

Figure 101 shows the computed electrical potential field. Overall potential drop is approximately 2.5 V. The steepest potential gradients are in the zirconia solid electrolyte tube and LSM current collector end, due to their relatively low electrical conductivities. There is also a noticeable potential gradient in the nickel conducting core, indicating its resistance is not insignificant. This is a good indicator, as the mild electrical insulation indicates some thermal insulation and the current collector is not a cold finger. In contrast, there is almost no potential gradient in the liquid silver anode, indicating very low resistance, which results in very uniform current density over the length of the zirconia tube.

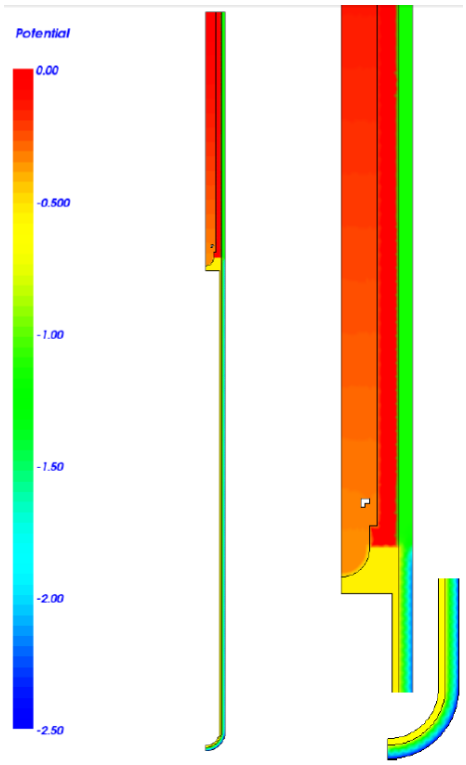

Figure 101 Computed electrical potential field.

Figure 102 shows the computed temperature field. The inset detail indicates that as before, the hottest part of the anode assembly is the LSM closed-end tube at the end of the current collector, due to the high current density and relatively low conductivity of that component. There is also noticeable resistance heating in the zirconia tube near the silver anode. Again the nickel conducting core shows a temperature gradient indicating that it does not act as a cold finger.

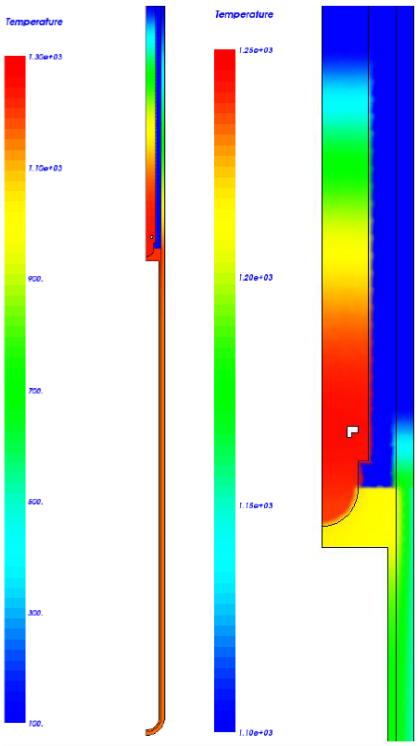

Figure 102 Computed anode assembly temperature field.

Cost Model

The cost model, which runs in a spreadsheet, includes a full mass balance which solves a linear system to determine for a given raw material assay what is the precise mixture of raw material inputs required to maintain a favorable steady-state chemistry in the molten salt. The raw material mixture then feeds back to the cost stack, so one can very easily test the precise impact of a change in, for example, raw material CaO or SiO_2 concentration on product cost. This mass balance can also account for the exact mixture of salts removed in selective salt freezing described above (see "Salt Recycling" above).

The cost model also calculates cell crucible dimensions, allowing it to return results such as salt volume, mass, residence time in the cell. And it uses temperature and other parameters to estimate metal vapor pressures and anode mass change over time. In particular, it has helped to quantify the reduction in cost due to a low-silver anode invention (see "Low-Silver Anode" above). These and other technical calculations make this a true techno-economic model of the MagGen™ process.

Capital Cost Model

INFINIUM built two capital cost models. The first begins with a full manifest-based exact cost accounting of the Beta Magnesium Prototype, and expands its part count for various furnace scales. The second is based on a new narrative for a complete plant, drawn up by an experienced magnesium, titanium and rare earth plant manager and designer, as described in the next section. Both of these cost models estimate

that MagGen™ capital cost should be lower by a factor of 4-6 than today's chloride electrolysis plants, and by a factor of 2-3 than our initial capital cost estimates.

Detailed Heat Balance

INFINIUM also developed a detailed heat balance, shown in Figure 103, in order to determine more precisely the acceptable thermal insulation losses and necessary performance of each heat exchanger in the system in order to reach our energy targets. Prior to this, we only had a coarse overall energy balance for the system.

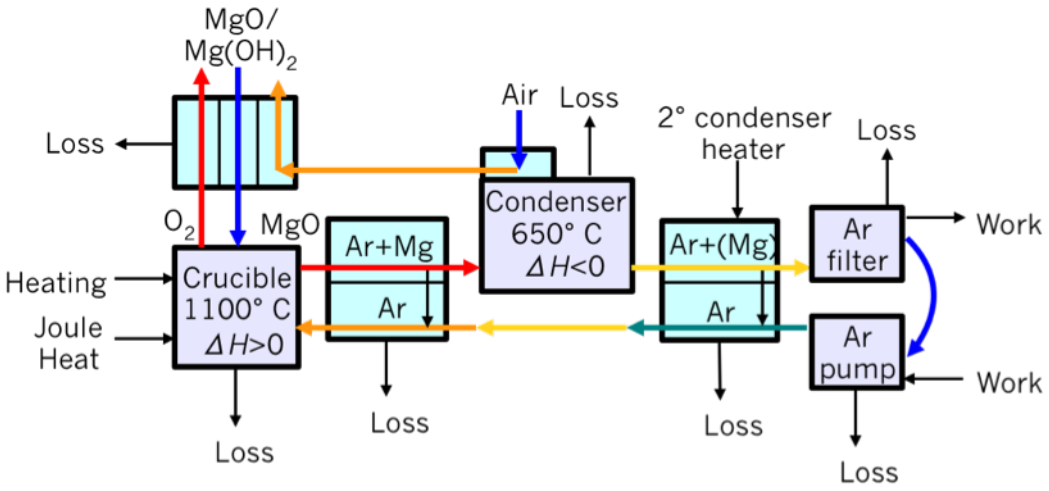

Figure 103: Detailed heat balance of the MagGen™ cell showing material flows (heavy arrows with temperature indicating color) and heat flows (thin black arrows). Grey boxes indicate reactors, cyan boxes indicate heat exchangers.

To start, a simple heat balance model was created for the process to determine the size of an electrolytic cell operating in an iso-thermal condition. In the iso-thermal condition the heat generated by the resistance by the electrical current passing through the bath and zirconia membrane is balanced by the heat losses due to the endothermic reaction to produce magnesium, loss of magnesium vapor and anode gas, heat loss through the sides and top of the cell, and heat necessary to bring the feed MgO up to operating temperature. Several insulation designs were tested using a model, it was found that the best design is to use a hot wall crucible or cell (that is a cell that does not have external insulation) because the heat generated in the process is significant. This has a secondary advantage in that the cell then can be heated externally to bring the cell to temperature were the electrolyte is molten and the cell can operate. It also means that the cell can be idled if necessary (by applying insulation or using external direct fired equipment or electrical heaters), an advantage in plant operations.

The heat balance model in this case was developed by linearization of the heat losses of a rectangular cell (length to width ratio of 3:1) and necessary depth to accommodate the electrodes. The lid of the cell was insulated so that its surface should react about 140˚F, similar to the conditions of the lid of an Alcan IV cell. The heat input was estimated from previous work described in the last quarter's report. The solution of the heat balance suggested that cell should operate at about 89kA, with 675 anode cathode pairs. As the heat balance model is improved these values

will likely change slightly.

The biggest area of uncertainty in the overall heat balance model is the disposition of heat generated in the zirconia and anode. That is, when the zirconia heats up due to its electrical resistance to oxygen ion conduction, how much of that heat goes into the molten salt vs. the anode gas or conduction up the current collector? The anode assembly FEA model above is a design tool to optimize component geometry and approach the theoretical minimum energy required for a bipolar electrolysis cell.

Electrolysis Energy Balance Model

The energy balance model begins by estimating the overpotential (voltage) of each component in the series from anode lead, to anode, to zirconia, etc. to the cathode lead. This sum plus the MgO dissociation potential represents the total applied voltage required to achieve the desired current density. Multiplying this result by *nF/M* (electrons per mole, Faraday constant, molar mass) gives the total energy consumption passed as ionic current through the system per kilogram of magnesium product. Dividing this result by the current efficiency adds energy losses due to electronic current, which essentially acts as a resistance heater, to give the total energy consumed in the cell per unit of magnesium product.

The model then takes this total energy input and subtracts known energy consumption values, such as the dissociation enthalpy of MgO, enthalpy of heating input materials to the cell temperature, and energy losses through the anode and cathode leads. In order to avoid double counting, it uses a reference temperature of the cell temperature, and includes enthalpy required to heat inputs to that temperature, but not heat “loss” by material outflows to the environment.

Figure 104 shows the results with both the total overpotential and energy disposition. The voltage stack on the left indicates zirconia resistance is the largest overpotential in the system, at nearly 1.5 V. That said, it uses a model of 3 mm thick Vendor A 6YSZ tubes, whereas 8 YSZ has significantly higher conductivity. In the heat energy stack on the right, out of 12.5 kWh/kg total energy use, MgO dissociation enthalpy is 8.5 kWh/kg or 68% of that total, indicating 68% efficiency – at creating Mg vapor. Assuming no recovery of 1.5 kWh/kg vaporization energy, this corresponds to 56% efficiency at creating Mg liquid. Accounting for all known heat losses leaves just 0.01 kWh/kg side wall losses, which is very small. But it may be feasible, as this cell can be insulated, *cf.* the Hall-Héroult cell which requires heat removal to maintain a frozen bath side-wall.

Note that this assumes no heat exchange between outputs and inputs. In particular, exiting Mg-Ar vapor can heat incoming argon in a heat exchanger, reducing the incoming argon heating required. It may also be possible to use outputs to heat incoming magnesia.

The spreadsheet estimates each resistance in the series as accurately as possible. At this point, without FEA modeling of larger-scale or industrial cells, we do not have more refined estimates of IR drop in the cathode or molten salt, nor the oxygen ion mass transfer overpotential.

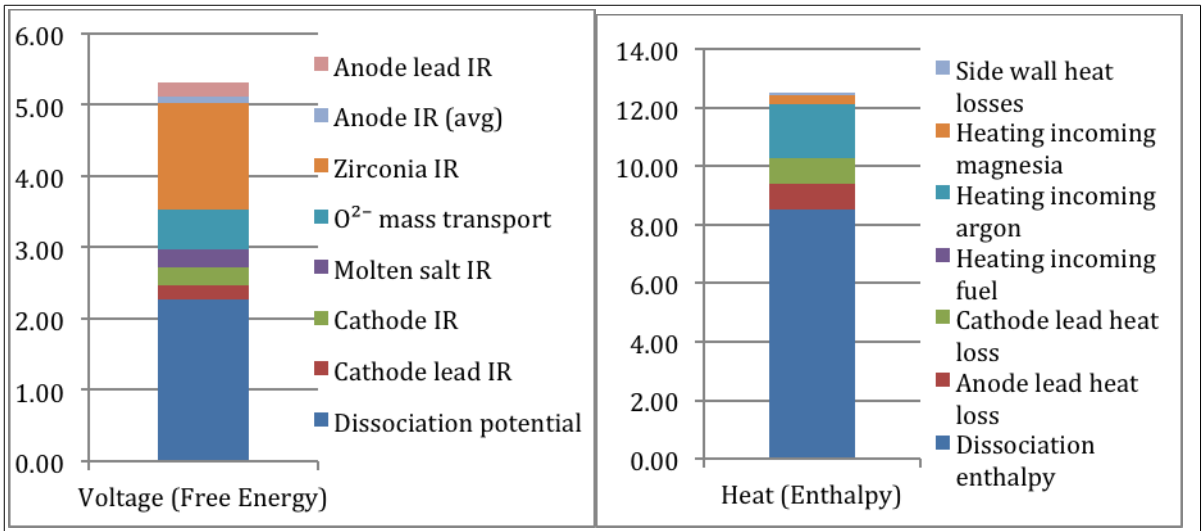

Figure 104: Voltage and thermal energy stacks in the magnesium cell energy balance.

The **silver thickness calculation** merits particular attention. Figure 99 shows the oxygen-generating anode with silver between the outer zirconia tube and an inner oxygen transport membrane, such as a porous ceramic or mixed ionic-electronic conductor. Our assumption has been that thinner is better for the silver layer, e.g. 0.25 mm thickness resulting in 0.17 V overpotential at 0.33 A/cm², and 0.62 V at 1.06 A/cm². Here we quantify the silver resistance, evaporation, and leasing cost, and estimate the optimal thickness.

Expressed in terms of dollars per kilo-amp-hour (kAh, roughly one lb Mg), silver leasing cost C_1 is given by:

$$C_1 = \frac{SRt\rho}{JU}, \tag{1}$$

where S is the silver cost per kg, R is the silver lease rate, t its layer thickness, ρ is its density, J cell current density, and U the anode utilization rate. Cost of silver lost to evaporation C_2 is:

$$C_2 = \frac{p_{v,Ag}}{p_{O_2}} \frac{M_{Ag}}{n_{O_2} F} S, \tag{2}$$

where $p_{v,Ag}$ is silver vapor pressure, p_{O2} is oxygen pressure generally 1 atm, M_{Ag} is silver molar mass, n_{O2} is number of electrons transferred per oxygen molecule i.e. 4, and F is Faraday's constant. Cost of electrical resistance C_3 is:

$$C_3 = \frac{HL^2 J}{2\sigma t}, \tag{3}$$

where H is electricity rate in $/kWh, L is the anode immersion depth in the salt, and σ is silver electrical conductivity. Figure 105 shows these three costs as a function of thickness in graphical form in terms of cost per kAh of charge passed through the cell, which corresponds to about one lb of magnesium production.

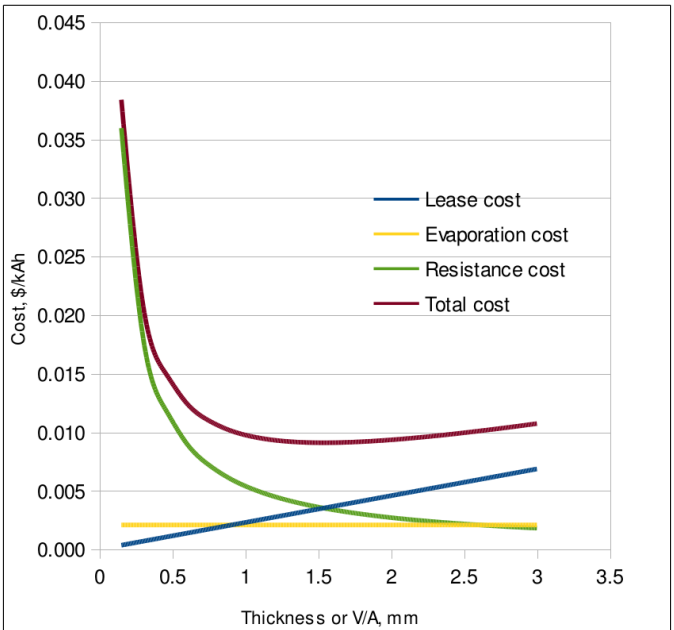

Figure 105: Costs of silver vs. layer thickness.

Setting the sum of the cost derivatives to zero gives the optimal silver layer thickness as:

$$t = \frac{LJ}{2}\sqrt{\frac{2\,HU}{SR\rho\,\sigma}}. \tag{4}$$

In this case, that cost-minimizing silver thickness is about 1.5 mm.

A further note on silver leasing is warranted here. Precious metals lease at far lower rates than convectional bank loans due to the collateral of a valuable asset, with lease rates determined by futures markets. Furthermore, the difference between current and futures prices often leads to strange results. For example, on June 25, the one-year lease rate for gold was 0.40%, platinum 0.49%, palladium 0.77%, and silver negative 0.06%! [Source: www.kitco.com/market/lfrate.html June 25, 2014.] It is not anticipated that anyone will pay INFINIUM to hold onto silver for them, so our model sets a minimum lease rate of 3%.

Turning next to anode (zirconia tube inner surface) **current density**, the model estimates various changes in total cost as a function of that parameter. Figure 106 shows that functionality with the current model. Note that it reaches a minimum around 3 A/cm^2, based on the trade-off between increasing energy loss at higher current density vs. higher productivity and decreasing capital and consumables costs.

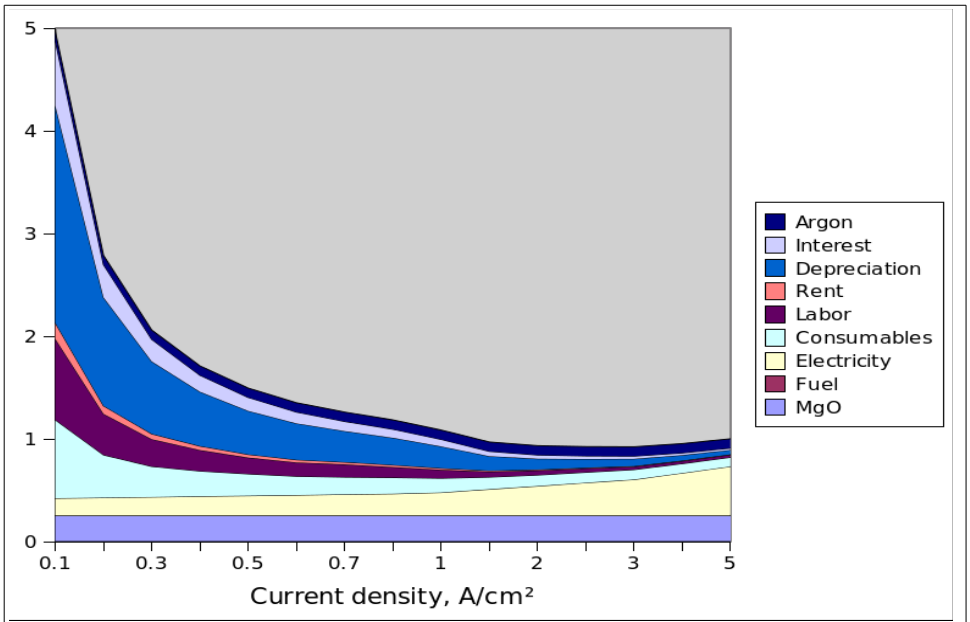

Figure 106: Total operating cost of magnesium production vs. anode current density. (Note the non-linear horizontal axis scale.)

This result is problematic in two ways. First, current density above about 1-1.5 A/cm^2 leads to rapid zirconia tube fracture due to thermal stress. Second, high current density correlates with high corrosion rate, which is not yet in the model. Including that relationship and resulting zirconia lifetime in the model would likely show a considerably lower optimal current density.

Figure 107 shows the effects of temperature and zirconia thickness and type on cost of resistance losses, again in cost per kAh. That figure shows a strong effect of zirconia type, with advanced firing methods producing dramatic increases in conductivity. Achieving similar results will result in dramatically lower zirconia overpotential (Figure 99) and system energy consumption. That figure also shows monotonic decrease in cost with increasing temperature and decreasing zirconia thickness.

As with the current density result, this illustrates a limitation of the current model, which is that it is missing information. For example, increasing temperature requires use of more costly materials for the entire electrolysis cell, and decreasing zirconia thickness reduces tube lifetime and increases longitudinal stress in the tube due to anode liquid weight. Building these into the model to generate a truly optimal result would take considerable time, and the noisy nature of such relationships as materials costs with temperature may make this better settled manually rather than by an analytical global optimization exercise.

That said, the model can get a first rough cut at this result by assuming a functional form for corrosion rate vs. current density and temperature, and refining that as we gain more data on those relationships.

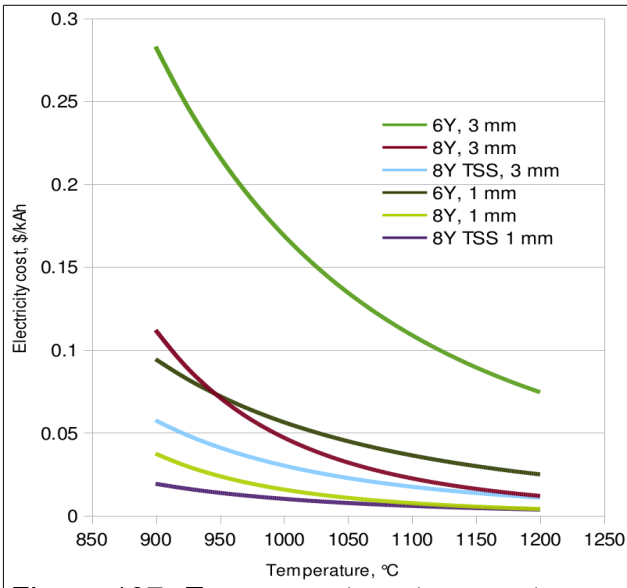

Figure 107: Energy cost vs. temperature and zirconia thickness for three YSZ types.

Magnesium Plant Design Narrative

INFINIUM has begun detailed design of a 40,000 ton/year magnesium plant. The design covers scales from thickness and size of each zirconia tube, all the way up to numbers of cells per row and rows in the plant. The design narrative includes balance of plant issues such as raw material distribution and feeding to the cells and hot metal off-take from each cell condenser. It includes about 25 design parameters.

The design narrative is the product of an experienced manager and designer of magnesium, titanium and rare earth plants, and covers scales from thickness and size of each zirconia tube, all the way up to numbers of cells per row, power supplies, raw material distribution and feeding to cells, and building layout. The electrolysis cell house component of the narrative calls for multiple buildings each with 3000-8000 tons/year capacity, indicating ability to scale down to that level of production without per-unit cost increase. Other components such as cast house for ingot production scale differently, though in an on-site “magnesium minimill” facility at a mine or customer site, some components such as administration can be shared.

The optimization exercise is showing that the internal models have uncertainty, and is informing the modeling work. It is also informed the design of the beta prototype and its experimental program. For example, when the optimal zirconium tube size is determined, then the beta prototype can use tubes of that size, and determine performance.

The heat balance determined the size of a magnesium cell that would operate in an iso-thermal manner. Based on the known current efficiency of the electrolytic cell and a goal of production of 40,000 MT of magnesium, a preliminary design of the cell house and plant was developed. Since the cell was estimated at 675 anode/cathode pairs, given the production rate of each, a total of 121 cells would be necessary. This was rounded to 120 cells, with a result of 10 buildings of 12 cells each, or five buildings of 24 cells each. The 5 building design provides for a central aisle where metal can be collected. Building size of about 200 ft x 47 ft was found, this then could

be used to determine the cost of the building. Each building has one DC rectiformer power supply, with the power bus going down one row of cells and back the other.

The number of buildings and production rate of magnesium was used to develop a process flow diagram for the process. Process streams were then estimated, necessary MgO bunker size, cooling water flow rates, argon flow rate, and argon make up then were calculated. Also calculated were the oxygen production rate, and the vaporization rate or transport of silver fume. Silver fume evaporation rates were found to be a strong function of cell temperature.

Metal tapping was to be collected of each cell; the cells would be located on a second floor, so that the metal collection cart would be located on the ground level. This frees up traffic in the cell house so that there is no interference with metal collection and any running repair or zirconia tube replacement that occurs on the second floor. Metal collection carts have been successfully automated so as not to put operators at risk during cart movement.

The process flow model was constructed in Excel, so that changes in production rates of magnesium result in a new calculation of the other flow rates in the process. Zirconia tube replacement rate and consumption of tube materials are also estimated based on production rate.

The narrative includes quoted costs for the power supply, copper electrical buss components, raw material distribution and cell feeding system, electrolysis crucible, and some of the most complex instrumentation components. It does not yet include systems for safely tapping metal from condensers and transporting it to the cast house. And it is not yet as fine-grained as the beta scale-up capital cost model. That said, it will be the most comprehensive model of capital cost which can be practically assembled without a detailed drawing of the final industrial cell, which we do not yet have.

Finally, INFINIUM has begun to explore opportunities for on-site generation using natural gas combined heat and power to generate electricity for this process and use the excess heat for raw material pre-treatment such as drying or calcining. This would increase energy efficiency, and potentially reduce costs and greenhouse gas (GHG) emissions in regions which use fossil fuels to produce electricity.

Energy, GHG and Other Emissions

The U.S. magnesium die casting market has been growing very rapidly in the short term,[i] as shown in Figure 108, and if more stringent fuel emissions standards were to cause the automotive industry to follow the recommendations in the report *Magnesium Vision 2020,*[ii] then magnesium adoption may increase from 5 kg/vehicle when the report was written in 2005 to as much as 160 kg/vehicle, a compound annual growth rate (CAGR) of 26% per year – and displacing 286 kg of steel and aluminum. A domestic secure supply of magnesium was the motivation for this project, and early on the investigators conducted this study to examine its potential impact.

Magnesium's natural abundance can easily support enormous growth: it is the third most abundant structural metal in the earth's crust, the U.S. produces about ½ million tons of magnesium oxide annually, and inflation-adjusted oxide prices have been

stable since the late 1940s.[iii] World resources are estimated at 12 billion tons; the oceans are 0.13% magnesium by weight,[iv] or 1.8×10^{15} tons, and sea water extraction of MgO is commercially viable.

Since the release of *Magnesium Vision 2020,* although the price of magnesium has nearly doubled in the U.S., several automakers have been committed to extensive magnesium use. Magna (Vehma) has been working on a 50% magnesium alloy small vehicle body and frame,[v] and Ford has been working on a magnesium alloy frame for its F-series pickups[vi] which are the best-selling vehicles in North America. That said, technical, economic, regulatory, and other political factors will affect the growth rate of die-cast magnesium, so estimating INFINIUM technology impact requires evaluation of several scenarios of magnesium market growth and recycling fraction.

In particular, if the INFINIUM primary production process could lower the cost of producing automotive magnesium, this change of economics could help spur a sizable growth of the magnesium market. In order to compare magnesium market scenarios, we will estimate long-term demand elasticity, and then compare fast-growth and slow-growth scenarios based on the INFINIUM cost advantage.

This Benefits Assessment consists of four parts: (1) transportation energy and greenhouse gas (GHG) modeling; (2) industrial economic, energy, greenhouse gas (GHG) and other environmental modeling; (3) market scenarios and the effect of the INFINIUM processes on the market, (4) resulting economic, energy and GHG impact of INFINIUM process deployment based on those scenarios.

Transportation Energy and GHG Emissions

Transportation energy and GHG impacts are based on weight savings. The Department of Energy is evaluating the impact of weight savings in detail, so this report will use a simple model based on a published estimate for the effect of weight.

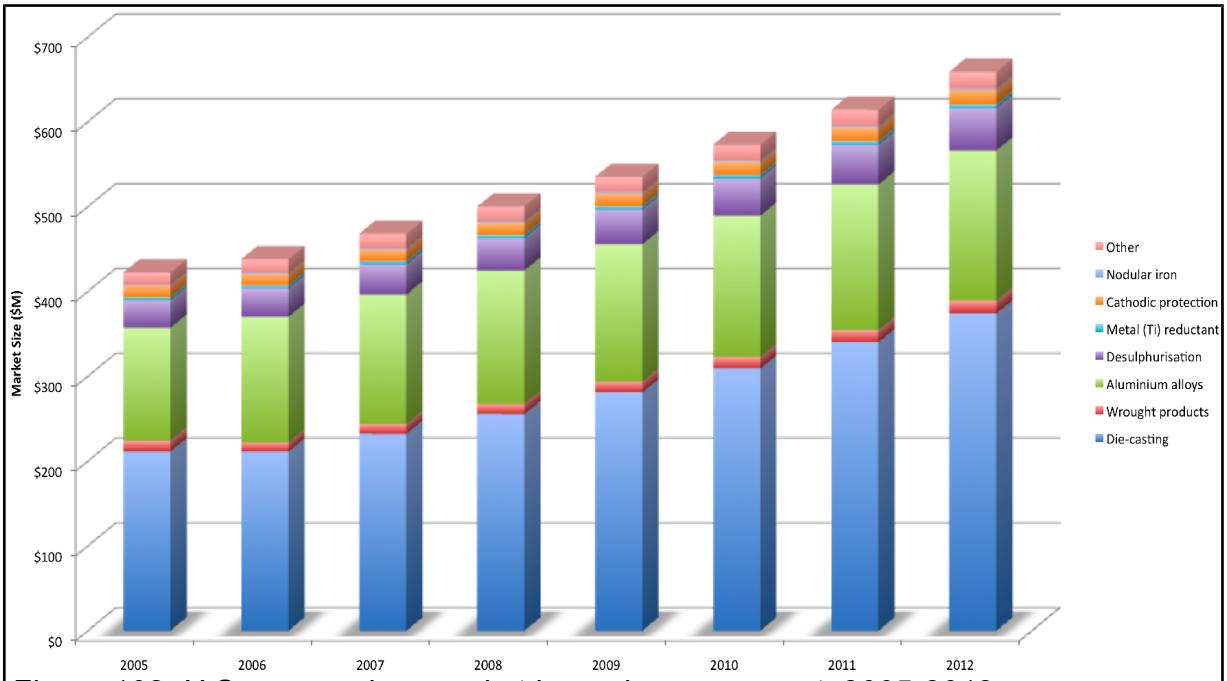

Figure 108: U.S. magnesium market by end-use segment, 2005-2012.

- Koffler and Rohde-Brandenburger have estimated fuel savings of 0.35 liters gasoline saved per (100 km driven×100 kg weight reduction).[vii]
- Multiplying this estimate by the *Magnesium Vision 2020* number of 131 kg/vehicle of weight savings gives 0.46 liters/100 km driven, or 1.95 gallons/1000 miles – about 6% fuel savings for a 30 mpg vehicle.
- Multiplying this specific savings by 2.96×10^{12} vehicle miles (4.77×10^{12} km) driven per year in the US[viii] gives 2.19×10^{10} liters (5.79×10^{9} gallons) per year gasoline savings.
- Multiplying the total gasoline savings by 0.125 MBTU/gallon[ix] gives 724 TBTU/year energy savings.
- Multiplying the total gasoline savings by 8.92×10^{-3} metric tons CO_2/gallon[x] gives 51.6 million metric tons CO_2 emissions reduction.

Note that this savings only reflects the pump-to-wheels energy and GHG savings and it does not include well-to-pump energy use and emissions. This is also the total impact of all of the work required to reach 131 kg/vehicle weight savings by magnesium adoption, a transformation which would benefit greatly from lower-cost primary processing *i.e.* MagGen™ technology. In the long term, more magnesium use would also require new recycling technology, and likely could spur use of new alloys and casting methods as well.

Industrial Energy, GHG Emissions, Economics and Other Wastes

MgO Electrolysis for Primary Production and Oxidized Scrap Recycling

Energy Use

For a self-heated electrolysis cell, energy modeling begins with two energy balances: one for free energy, the other for heat. This is similar to the analysis in Figure 104 on p. 78. The Nernst equation: $\Delta G = -nFV$ indicates that voltage and free energy are equivalent but use different units: free energy is the energy per mole of reaction extent, and voltage is the energy per coulomb of charge passed. For recycling of oxidized magnesium, the reaction is: $MgO \rightarrow Mg + \frac{1}{2}O_2$ with two moles of electrons per mole of reaction extent. At the process temperature of 1150° C, its enthalpy and free energy are 735 kJ/mol (8.41 kWh/kg) and 439 kJ/mol (5.02 kWh/kg) respectively,[x] corresponding to 3.81 V and 2.27 V respectively.

The reaction proceeds and current flows if applied voltage is above the 2.27 V dissociation potential, corresponding to reaction free energy. This and other overpotentials in the cell sum to the total voltage, as shown on the left side of Figure 109. The free energy budget consists of the following components:

- Cathode and anode resistances are minimum possible energy losses through the leads.[2]
- 1.5 V for the zirconia tube is based on 1 A/cm^2 current density through a 3 mm thick YSZ tube with conductivity 0.2 S/cm.

[2] The Wiedmann-Franz law indicates that good electrical conductors are good thermal conductors, so low-resistance leads lose a lot of heat and vice versa. There is thus an unavoidable minimum energy loss due to leads. At the process temperature, this minimum is ~0.21 V (0.46 kWh/kg) I-R drop in each lead lost to the environment as heat, plus an additional 0.46 kWh/kg heat conducted from the crucible through each lead to the environment.

- The molten salt has 20 times the conductivity of YSZ, but the anode-cathode distance is roughly 20 times the zirconia thickness (6 cm), and effective area is roughly twice that of the YSZ, making for half the resistance and voltage drop.
- The oxygen ion mass transfer number is based on its concentration (roughly 1/10 of the anions) and boundary layer thickness (roughly 1/12 of the anode-cathode distance), making it about 70-80% of the molten salt resistance.
- MgO dissociation $V = \Delta G/nF$ (see above).

The thermal energy budget on the right side of Figure 109 sums thermal energy use of the cell. The enthalpy ΔH of MgO dissociation to Mg vapor and oxygen consumes most of the heat. If one supplies sufficient free energy but not sufficient enthalpy, then the reaction proceeds but cools the cell and shuts it down. Resistance in the cell or an external heater provides this heat, and excess heat beyond the enthalpy leaves the cell through the cell leads and vessel walls. The thermal energy budget consists of the following:

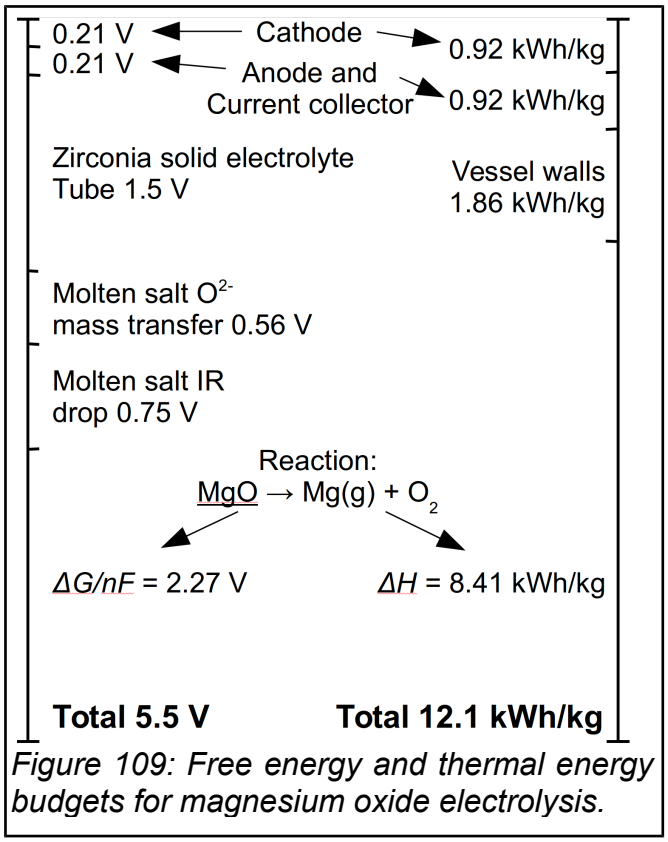

Figure 109: Free energy and thermal energy budgets for magnesium oxide electrolysis.

- Losses through cell leads mentioned above.
- Furnace vessel walls and gas flows, which we estimate will lose about as much heat as the total through electrical leads. With good insulation and heat exchangers, this could be as low as half of this value (0.8 kWh/kg), or various contingencies could increase it up to 3.8 kWh/kg.
- Enthalpy of magnesium oxide dissociation ΔH as mentioned above.

Based on these energy balances and the range of heat loss values, INFINIUM believes that operating at a cell potential of 5-6.5 V, corresponding to 11-14 kWh/kg, can achieve self-heating and 1 A/cm² zirconia tube current density. Overall energy

efficiency of Mg vapor generation (*ΔH*/input energy for the reaction in Figure 2) would then be between 63% and 76%. Because the enthalpy of dissociation to liquid magnesium is lower, with no condenser heat recovery, liquid Mg energy efficiency can get to between 52% and 63%.

Greenhouse Gas Emissions

There are no direct greenhouse gas emissions for MgO electrolysis, so Table 1 uses the U.S. average 0.688 kg CO_2e/kWh.

Economic Benefits

Economic benefits begin with the potential energy savings described above. This process is potentially similar to the Hall-Héroult cell in its low labor utilization and modular cell deployment for flexible capital cost. With these advantages, Sujit Das of Oak Ridge National Laboratories estimated total costs for this process would be well below those of alternatives.[xi] The Pidgeon silicothermic reduction process used in China, and development-stage carbothermic reduction process, both use much more energy than MagReGen™ and MagGen™, but burn coal with lower unit energy cost.

In terms of automotive materials changes, this would substitute higher-priced magnesium for lower-priced aluminum and steel. Manufacturing benefits of magnesium, such as lower part count due to easier die casting, could offset some of this cost, e.g. Field *et al.* showed that a magnesium automotive instrument panel beam die-cast in one piece can be less expensive than the equivalent steel part made from 27 stampings welded together.[xii] But much more than this, the biggest economic impact will be approximately 732 trillion BTUs of gasoline energy saved in the transportation sector and greenhouse emissions by 51.6 MMT CO_2e/year.[3]

Solid and Liquid Waste

For this process there is minimal solid or liquid waste. For each 1000 kg of magnesium production from refractory-grade MgO, the MagGen™ process makes:

- ~10 kg of mixed iron, aluminum, silicon and other more electronegative oxide impurities, which the steel industry can potentially use to reduce porosity of ingot castings;
- ~5 kg of $MgCl_2$ in the condenser, which separates from the product by flotation;
- ~50 kg process salt with slightly elevated levels of chlorides and less electronegative impurities *e.g.* KF, BaF_2. INFINIUM investigated recycling this stream with subcontractor Kingston Process Metallurgy as a subtask in this contract. If this salt recycling process uses any water, this will constitute the only liquid waste of this system.

Magnesium Metal Recycling

The post-consumer magnesium recycling rate is around 30-40% due to the difficulties involved in separating aluminum from magnesium. This is particularly true for automotive scrap. Today's recycling system efficiently separates steel, nonferrous metals, and other materials; and then within the nonferrous metals stream, separates them using X-ray fluorescence (XRF). Unfortunately, magnesium-aluminum

[3] Source: http://www.epa.gov/greenpower/pubs/calcmeth.htm#gasoline – see also endnote ix.

separation is very difficult because their XRF spectra are very close, and they occur in each other's alloys.

To help solve this problem, INFINIUM and partner Boston University conducted an 18-month Concept Definition study of a new magnesium recycling technology based on distillation mediated by molten salt and argon.[xiii,xiv,xv,xvi] A series of experiments discovered and demonstrated a new chemical separation mechanism in two stages: magnesium in a scrap metal charge preferentially dissolves into a molten salt, and argon bubbling through the salt accelerates its evaporation. Other metals have lower solubility and/or lower evaporation rate. Experiments demonstrated close to 100% yield and near-perfect separation. Two new electrical measurement techniques also provide new in-line process control signals for the process. And mathematical modeling and cost modeling indicate the process will likely be cost-effective.

The outcome of that Concept Definition study is a recycling process for recycling magnesium from mixed post-consumer sources, including heavily-oxidized material such as die casting dross and machine chips. This section describes the energy, GHG, economic, and other waste impacts of this recycling process, and the resulting data play a role in the overall impact analysis for INFINIUM magnesium primary processing and recycling technologies.

Note that since the Concept Definition study, INFINIUM has conducted a separate study on a simpler and more efficient magnesium recycling technology with ARPA-E funding.

Energy Use

The magnesium refining process requires much less energy than the electrolysis circuit. Its reaction is Mg (liquid in solution) → Mg (vapor), for which the enthalpy of vaporization ΔH_v at the 1090° C boiling point is 128 kJ/mol (1.46 kWh/kg), and the free energy of demixing to 1% Mg solution in Al is 48 kJ/mol (0.55 kWh/kg). Then again, advanced designs can recover most of the vaporization enthalpy, so the lower bound of this process energy use is as low as 48 kJ/mol (0.55 kWh/kg). To be conservative, we estimate the process energy use at 10% above twice the vaporization enthalpy or 3.3 kWh/kg, (12.1MJ/kg), also corresponding to the demixing free energy plus 2.8 kWh/kg heat losses. [The newer recycling technology would use less energy.]

The only Mg-Al separation technology in use today bubbles chlorine through a liquid metal mixture, producing Al but very impure $MgCl_2$. Full reduction to magnesium metal then requires a further 28 kWh/kg (100 MJ/kg). As the Mg:Al ratio in motor vehicles increases from 1:20 to above 1:1, as expected per *Magnesium Vision 2020*, this scales to 16 GJ/vehicle, or 192 PJ/year (181 TBTU/year). In contrast, the MagReGen™ process would use under 2 MJ/vehicle, or 24 PJ/year (22 TBTU/year).

Greenhouse Gas Emissions

As with MagGen™ MgO reduction, Table 8 uses GHG emissions of 0.688 kg CO_2e/kWh.

Economic Benefits

Process cost is expected to be very low, as it recycles its argon, uses very little energy, and has the same low labor cost and capital deployment flexibility of the

primary production process.

Solid and Liquid Waste

INFINIUM expects that this recycling process will net negative solid and liquid waste emissions because it will reduce landfilling of magnesium dross and the magnesium component of automotive recycling. That said, waste stream chemical composition may lead to higher solid waste production than the figures above for primary production.

Summary

INFINIUM estimates the energy use of MgO electrolysis energy consumption for primary magnesium production at about 13 kWh/kg, and magnesium recycling at 3.3 kWh/kg, as calculated above. These assume zero energy recovery in the magnesium condenser, which could yield up to 1.5 kWh/kg for raw material treatment and other uses. Energy use and GHG emissions estimates are presented as Table 8.

The above summarizes the calculations for energy use by the MagGen™ primary production and MagReGen™ oxide/metal recycling processes. Today most of the world's magnesium comes from the Pidgeon silicothermic process in China or magnesium chloride electrolysis in the US and Israel, the numbers in Table 8 reflect the mean of those two as presented by Sujit Das.[xi] Aluminum and steel data are from the literature as indicated by table foot/endnotes.

Per kg metal	Mg today	MagGen™	MagReGen™	Primary Al	Scrap Al	Primary steel
Energy use, kWh	64[xvii]	13-14[4]	3.3-3.4	24[xviii]	11[5]	9.5[xix]
GHG, kg CO_2	32[6]	8.9[7]-9.4	2.3-2.35	16.5	7.6	2.1[xviii]

Table 8: Energy use and GHG emissions per kilogram of metal production.

Magnesium Market Scenarios and Effect of INFINIUM Processes

Changes in energy use and GHG emissions due to MagGen™ and MagReGen™ adoption depend strongly on the growth of demand for magnesium and the change in magnesium production technology penetration. The demand component of the market balance assumes that the automotive industry is the main driver of growth, and the question is to what extent they will realize growth from 5 kg/vehicle in 2005 to the projected 160 kg/vehicle. Starting with that projection, one can envision three magnesium demand growth scenarios:

1. Low magnesium growth: with new fuel economy standards, the automotive

---

[4] The high number reflects energy use and GHG emissions for INFINIUM processes with fueled anodes.

[5] J.A. Pomykala *et al.*, "Automotive Recycling in the United States: Energy Conservation and Environmental Benefits," *JOM* 59(11):41-45 (November, 2007), p. 44: recycling saves 13 kWh/kg aluminum.

[6] Based on 50% U.S. Magnesium chloride electrolysis at 21 kg CO_2e/kg Mg (source: www.epa.gov), 50% Chinese Pidgeon process at 42 kg CO_2e/kg Mg (source: Gao Feng, *Trans. Nonferrous Met. Soc. China* 18:749, 2008).

[7] Using the 0.688 kg CO_2e/kWh from http://www.epa.gov/greenpower/pubs/calcmeth.htm#kilowatt ; this overestimates direct emissions because primary metal production plants tend to locate near hydroelectric power sources, though primary metal energy consumption makes that low-GHG power unavailable to the rest of the grid.

industry is likely to increase magnesium use by at least 7% CAGR, which would over 15 years would result in use of about 14 kg/vehicle.
2. Moderate magnesium growth: improved economics and stringent fuel economy requirements lead to changes in vehicle platforms amounting to 14% CAGR, and 36 kg/vehicle over 15 years.
3. High magnesium growth: dramatically increased demand for light-weight materials in internal combustion engine as well as plug-in hybrid electric vehicles (PHEV) and/or battery electric vehicles (BEV) lead to magnesium growth at 26% CAGR to average 160 kg as projected in *Magnesium Vision 2020*.[5]

These consumption changes, particularly in scenario 3, could lead to enormous increases in industrial energy use if today's processes continue to dominate production. But if INFINIUM is successful, our extraction or recycling process, or both, could meet this entire demand using much less energy.

Although MagReGen™ can recycle die casting dross or post-consumer scrap, process growth is somewhat constrained by the availability of post-consumer scrap. Again, this is not meant to replace remelting of prompt or primary scrap generated at the production facility, the die-caster, or the automobile assembly plant. Market penetration therefore will be defined in terms of the fraction of parts shipped in automobiles several years earlier. *For example, if the 2014 model year includes 23 kg/vehicle of magnesium, with 12 million vehicle sales in North America, then at end-of-life approximately 276 million kg, or 276,000 tonnes, of new post-consumer scrap will enter the market, of which the MagReGen™ process will claim and recycle some fraction.*

We can therefore posit the following supply technology scenarios for the magnesium market:

1. No technology change: continue to produce magnesium using 50% chloride electrolysis and 50% Chinese Pidgeon process, and no new recycling, including no post-consumer recycling – only remelting of prompt and primary scrap as happens today.
2. INFINIUM extraction: technology change for automotive parts from current methods to this primary production process, but also with no new recycling.
3. INFINIUM extraction with moderate recycling: use our recycling process to produce 40% of the motor vehicle magnesium in 2015 vehicle production, and primary production for the rest.
4. INFINIUM extraction with high recycling: use our recycling process to produce 70% of the motor vehicle magnesium in 2015 vehicle production, and primary production for the rest.

The impact of process deployment thus depends on actual consumption and technology penetration in the above scenarios. That said, the above scenarios imply that supply technology and consumption are independent. But the present technology mix is not economical, nor acceptable from a GHG standpoint, for production at the highest consumption level described above. And the penetration of INFINUM technologies could significantly improve magnesium price, to the point where markets move from one consumption scenario to another.

Demand for magnesium is a strongly nonlinear function of its price: a price below the density-adjusted price of aluminum enables widespread substitution. With aluminum at $2.20/kg, and an Al:Mg density ratio of 1.55:1, and the prospect of a steady supply of magnesium at that price, large markets may switch from Al to Mg at a price below $3.10/kg in a matter of just a few years.[8] (Current US Mg price is $4.50-5.00/kg.)

Based on this, lower prices due to INFINIUM extraction and recycling could change consumption patterns from scenario 1 to 2 or 3 over time. Indeed, successful scale-up of these processes and concrete plans to build capacity could cause vehicle makers to commit to very significant growth within as little as 5 years. Furthermore, automakers are reluctant to make a large materials change if it will jeopardize the recycling industry by increasing landfill costs, and the recycling process provides a profitable private sector path to very high recycling rates.

Overall INFINIUM Primary and Recycling Process Deployment Impact

The framework above allows us to estimate the impact of INFINIUM magnesium extraction and recycling process adoption on industrial energy use and GHG emissions according to a matrix of demand and supply technology scenarios. This analysis assumes a steady 12 million vehicles/year, and a 2005 baseline of 5 kg magnesium per vehicle. This matrix is given in Table 9 below.

Table 9: Changes in industrial energy use (TBTU/year) and GHG emissions (MMT CO_2e/year) vs. today for magnesium consumption and supply technology scenarios.

		Magnesium consumption scenario		
		Low	Medium	High
Magnesium use, kg/vehicle		14	36	160
Aluminum use change, kg/vehicle[9]		-3.4	-11.8	-59
Steel use change, kg/vehicle		-13.2	-45.4	-227
1. No technology change	Δ Energy, TBTU/yr	15.6	53.9	269
	Δ GHG, MMT/yr	2.56	8.80	44.0
2. INFINIUM extraction	Δ Energy, TBTU/yr	-3.16	-10.9	-54.4
	Δ GHG, MMT/yr	-0.07	-0.22	-1.12
3. INFINIUM extraction, moderate recycling	Δ Energy, TBTU/yr	-4.72	-13.8	-62.3
	Δ GHG, MMT/yr	-0.25	-0.37	-0.49
4. INFINIUM extraction, high recycling	Δ Energy, TBTU/yr	-5.89	-16.0	-68.4
	Δ GHG, MMT/yr	-0.49	-0.81	-1.70

As Table 9 indicates, the first technical scenario of no technology change leads to an

[8] Source: interviews with two midwest die casting companies.

[9] Assumes each 155 kg of magnesium replaces 59 kg of aluminum and 227 kg of steel, per *Magnesium Vision 2020,*[5] and that 30% of automotive aluminum and no steel comes from post-consumer scrap.

increase in industrial energy use and GHG emissions across the board.

INFINIUM extraction by itself could lead to a dramatic reduction in industrial energy use and GHG emissions, which one can readily see by comparing technology scenarios 1 and 2. Recycling can further increase the energy and GHG savings, but not by extraordinary amounts. This is because of the constraint on recycling mentioned above: in 2020, post-consumer scrap will be generated from earlier primary production, so only 40% (supply scenario 3) or 70% (scenario 4) of the much-lower production year will be available for recycling. The benefits would become much greater in subsequent years as the increasing magnesium usage in 2020 vehicles progresses through consumer use and into the recycling stream.

Based on the above presentation, one can envision the following three primary scenarios in 2020, shown in light gray cell backgrounds in Table 9 above:

1. No technology change and low magnesium growth: U.S. auto industry magnesium use grows at 7% CAGR to 14 kg/vehicle (30 lbs), contributing minimally to meeting fuel economy standards. Industrial energy use increases by 15.6 TBTU/year and GHG emissions by 2.56 MMT CO_2e/year vs. today.
2. MagGen™ extraction, no magnesium recycling, and medium magnesium growth: With a new domestic source of low-cost magnesium, the industry expands magnesium use at 14% CAGR to 36 kg (~80 lbs), but no more than this out of concern for the recycling ecosystem. Industrial energy use falls by 10.9 TBTU/year, and GHG emissions by 0.22 MMT CO_2e/year, but substantial quantities of post-shredder magnesium is landfilled as Al-Mg scrap and/or $MgCl_2$.
3. MagGen™ extraction, high MagReGen™ recycling, and high magnesium growth: Abundant domestic supply and a path to 100% magnesium recycling convince industry to build some 50% magnesium vehicle body-in-white (frame and body panels) platforms and follow Magnesium Vision 2020 to 160 kg/vehicle average magnesium intensity. Industrial energy use falls by 68.4 TBTU/year, and GHG emissions by 1.70 MMT CO_2e/year.

If these three scenarios hold, then the INFINIUM extraction and recycling processes move the industry from scenario 1 to scenario 3, and this project's impact would be **industrial energy savings of 84 TBTU/year and GHG emissions reduction of 4.3 MMT CO_2e/year.** If fuel economy regulations or fuel prices force the auto industry into consumption scenario 3 with inelastic demand, **industrial energy savings due to INFINIUM technologies would approach 340 TBTU/year and GHG emissions reductions will exceed 45 MMT CO_2e/year.** And this is well before these magnesium-intensive vehicles enter the recycling stream, which would further increase the industrial energy and GHG savings.

Indeed, assuming the “High” consumption scenario represents a long-term steady-state, the moderate and high recycling supply scenarios save 79.8 and 98.9 TBTU/year vs. today (cf. 62.3 and 68.4 TBTU/year in Table 2), and reduce GHG emissions by 4.00 and 7.84 MMT/year vs. today (cf. 0.49 and 1.70 MMT/year in Table 2).

This also does not include the **approximately 732 trillion BTUs of gasoline energy saved and greenhouse emissions reductions of 51.6 MMT CO_2e/year in the transportation sector** (see above).

Project Products and Technology Transfer Activities

Publications & Presentations

- Soobhankar Pati: “Scaling Up Solid Oxide Membrane Electrolysis Technology for Magnesium Production”, TMS Annual Meeting, March 12, 2012. (Q2)
- Adam Powell: “Multi-Physics Modeling of Molten Salt Transport in Solid Oxide Membrane (SOM) Electrolysis and Recycling of Magnesium”, TMS Annual Meeting, March 12, 2012. (Q2)
- Adam Powell: “Zirconia Solid Electrolyte Application to Metal Production and Recycling: Theory and Practice”, Seventh Annual MIT-University of Tokyo Reactive Metal Workshop, March 16, 2012. (Q2)
- Adam Powell: “SBIR Phase II: Low-Cost Low-Impact Magnesium Production by Solid Oxide Membrane Electrolysis,” Poster presented at NSF SBIR Grantees Workshop May 6-9, 2012. (Q3)
- Steve Derezinski and Lou Spiridigliozzi: “Scale-Up of Magnesium Production by Fully Stabilized Zirconia Electrolysis,” DOE Annual Merit Review Presentation May 17, 2012. (Q3)
- Adam Powell: “Zero-Emissions Energy-Efficient Magnesium Primary Production and Recycling Technologies at MOxST,” International Magnesium Association: *Proc. 69th Annual World Magnesium Conference* pp. 116-121, Presentation May 22, 2012. (Q3)
- Adam Powell: “Magnesium and Rare-Earths: Primary Production and Recycling of Automotive Metals of the Future,” Poster presented at University of Tokyo Critical Metals Colloquium September 28, 2012. (Q4)
- Adam Powell: “Clean Metal Production for a Clean Energy Future,” Presentation to ARPA-E Program Managers December 4, 2012. (Q5)
- Adam Powell, “Computer Modeling for Materials Science and Sustainability,” Presentation to National Research Council Network for Emerging Leaders in Sustainability (NELS) December 4, 2012. (Q5)
- Xiaofei Guan, Uday B. Pal and Adam Powell, "Application of COMSOL Multiphysics in the Simulation of Magnesium Refining and Production," *Proc. COMSOL Conference 2012 Boston;* oral presentation of the same title was presented on Oct. 4, 2012. (Q5)
- Adam Powell, “Magnesium in Transportation: Unlocking Limitless Potential Through Primary Production and Recycling,” ARPA-E A-TEME Workshop January 31, 2013. (Q6)
- Adam Powell, “Modeling Electrodeposition in Materials Process Operations,” TMS Annual Meeting Short Course, March 3, 2013. (Q6)
- Uday Pal, “Electrolytic Production of Metals from Oxides Dissolved in Molten

Salts," TMS Annual Meeting High Temperature Electrochemistry Symposium, March 4, 2013. (Q6)

- Adam Powell, "Systems Engineering for Scale-Up of the INFINIUM™ MagGen™ Primary Magnesium Production System," Reactive Metal Workshop March 8, 2013. (Q6)
- Uday Pal, "Low Carbon Footprint Process for Metals Production," Reactive Metal Workshop March 8, 2013. (Q6)
- Xiaofei Guan, Uday B. Pal and Adam C. Powell, "An Environmentally Friendly Process Involving Refining and Membrane Based Electrolysis for Magnesium Recovery from Partially Oxidized Scrap Alloy," accepted for publication in *JOM. (Q7)*
- Xiaofei Guan, Uday B. Pal, Srikanth Gopalan and Adam C. Powell, "LSM ($La_{0.8}Sr_{0.2}MnO_{3-\delta}$)-Inconel Inert Anode Current Collector for Solid Oxide Membrane (SOM) Electrolysis," submitted to *J. Electrochem. Soc. (Q7)*
- J. Milshtein, E. Gratz, S. Pati, A.C. Powell and U. Pal, "Yttria Stabilized Zirconia Membrane Stability in Molten Fluoride Fluxes for Low-Carbon Magnesium Production by the SOM Process," J. min. Metall. Sect. B--Metall. 49(2):183-190 (2013), doi: 10.2298/JMMB120809005M . (Q8)
- X. Guan, U. Pal, S. Gopalan and A.C. Powell, "LSM ($La_{0.8}Sr_{0.2}MnO_{3-\delta}$)-Inconel Inert Anode Current Collector for Solid Oxide Membrane (SOM) Electrolysis," *J. Electrochem. Soc.* 160(11):F1179-F1186 (2013), doi: 10.1149/2.016311jes . (Q9)
- E. Gratz, X. Guan, J.D. Milshtein, U.B. Pal and A.C. Powell, "Mitigating electronic current in molten flux for the magnesium SOM process," submitted to Metall. Mater. Trans B October, 2013. (Q9)
- A. Powell, M. Earlam and S. Barriga, "Pure Oxygen Anodes™ for Low- or Zero-Carbon Energy Efficient Metal Oxide Reduction," submitted to Cong Wang, ed., *Energy and Carbon in Metal Production* (TMS Annual Meeting 2014 Proceedings). (Q9)
- X. Guan, U. Pal, S. Gopalan and A.C. Powell, "Electrochemical Characterization and Modeling of a Solid Oxide Membrane-based Electrolyzer for Production of Magnesium and Oxygen," submitted to *Celebrating the Megascale: An EPD Symposium in Honor of David G.C. Robertson* (TMS Annual Meeting 2014 Proceedings). (Q9)
- A. Powell, M. Earlam and S. Barriga, "Pure Oxygen Anodes™ for Low- or Zero-Carbon Energy Efficient Metal Oxide Reduction," presented at *Energy and Carbon in Metal Production* Symposium at the TMS Annual Meeting (Q10)
- X. Guan, U. Pal, S. Gopalan and A.C. Powell, "Electrochemical Characterization and Modeling of a Solid Oxide Membrane-based Electrolyzer for Production of Magnesium and Oxygen," presented at *Celebrating the*

Megascale: An EPD Symposium in Honor of David G.C. Robertson Symposium at the TMS Annual Meeting. (Q10)

- Eric S. Gratz, Xiaofei Guan, Jarrod D. Milshtein, Uday B. Pal and Adam C. Powell, "Mitigating Electronic Current in Molten Flux for the Magnesium SOM Process," *Metall. Mater. Trans.* B March 29, 2014. (Q11)
- Xiaofei Guan, Uday B. Pal and Adam C. Powell, "Energy-Efficient and Environmentally Friendly Solid Oxide Membrane Electrolysis Process for Magnesium Oxide Reduction: Experiment and Modeling," *Metall. Mater. Trans.* 1E(2):132-144 April 15, 2014. (Q11)
- Xiaofei Guan, Shizhao Su, Uday B. Pal and Adam C. Powell, "Periodic Shorting of SOM Cell to Remove Soluble Magnesium in Molten Flux and Improve Faradaic Efficiency," *Metall. Mater. Trans.* 45B:2138-2144 (December 2014). (Q13)
- Uday Pal, "Green Technology for Metals Production," TMS Annual Meeting Extraction and Processing Division Distinguished Lecture, Orlando, Florida, March 16, 2015. (Q14)
- Xiaofei Guan, Uday Pal and Shizhao Su, "A Method for Improving Faraday Efficiency of Magnesium Production Employing Solid Oxide Membrane (SOM) Based Electrochemical Cells," TMS Annual Meeting High Temperature Electrochemistry Symposium, Orlando, Florida, March 16, 2015. (Q14)
- Steve Derezinski, "Scale-Up of Magnesium Production by Fully Stabilized Zirconia Electrolysis," DOE VTO Annual Merit Review, Arlington, Virginia, June 11, 2015. (Q15)
- S. Derezinski and A. Powell, "Scale-Up of Magnesium Production by INFINIUM Electrolysis," DOE Vehicle Technologies Office Annual Merit Review, Washington, DC, June 8, 2016. (Q19)

Technologies/Techniques

- In molten salt electrolysis with zirconia solid electrolyte, ability to hot-swap zirconia tubes in and out of a ≥1050°C bath with low breakage, despite the low thermal shock resistance of zirconia
- Integrated anode-cathode assembly to introduce Mg vapor-diluting argon at the cathode while facilitating hot-swap and contained any tube breakage
- Liquid magnesium condenser with high yield despite 10:1 argon dilution
- Anode current collector assembly which conducts high current from the liquid silver anode at ≥1050°C
- Porous displacer to minimize liquid silver use in the anode
- Up to 170 hours of continuous run time in a single zirconia tube
- Up to 2448 hours of high-temperature electrolysis apparatus lifetime
- Up to 85-9590% current efficiency (oxygen flow basis) over 90+ hours of continuous run time
- In direct molten salt reduction of Mg-Nd master alloy from mixed oxides, high current, up to 450 A, producing over 200 g/hour master alloy

- Steel dam and ceramic liner for floating alloy product collection with 85-95% current efficiency (reduced metals basis)
- Automatic oxide feeding for reduced downtime and operator interaction;
- Low iron and other impurities when using a tungsten cathode

Patents and Patent Applications

- Adam C. Powell and John Strauss, “Primary Production and Molten Salt-Assisted Recycling of Metals with Inert Gas Purification,” U.S. Provisional Patent Application 61/646,343 filed May 13, 2012. (Q3)
- Adam C. Powell, Soobhankar Pati, Steve Derezinski, Garrett Lau, Uday Pal, Xiaofei Guan and Srikanth Gopalan, “Conductor of High Electrical Current at High Temperature in Oxygen and Liquid Metal Environment,” U.S. Non-Provisional Patent Application 11/600,761 filed August 31, 2012. (Q4)
- Uday B. Pal, Eric Gratz, Xiaofei Guan, Peter Zink, Soobhankar Pati, Adam C. Powell, John Strauss, Aaron Tajima and R. Steve Tucker, “Methods and Apparatuses for Metals Production, Separation, and Recycling by Salt- and Argon-Mediated Distillation with Oxide Electrolysis, and Sensor Device Related Thereto,” U.S. Patent Application Number 13/645,867, PCT Application PCT/US12/58882, filed October 5, 2012. (Q5)
- INFINIUM filed US Provisional Patent Application 61/834,180 “Low-Metal Inert Anode for High-Temperature Oxygen Separation” on June 12, 2013. (Q7)
- INFINIUM filed US Provisional Patent Application 61/899,013 “Method to Remove Soluble Metal in the Flux (molten salt electrolytes), Increase Electrolysis Process Efficiency and Prevent Membrane Degradation” by Uday Pal, Xiaofei Guan and Adam Powell on November 1, 2013. (Q9)
- Adam Powell, John Strauss, R. Steve Tucker and J. Brodie Voellinger, “Improved Liquid Metal Electrodes for Gas Separation,” PCT Application PCT/US14/42163 filed June 12, 2014. (Q12)
- Adam C. Powell, Uday B. Pal and Xiaofei Guan, “Methods and Apparatuses for Increasing Energy Efficiency and Improving Membrane Robustness in Primary Metal Production,” PCT Patent Application PCT/US14/62743 filed November 3, 2014. (Q13)

Computer Modeling

Model Description, Key Assumptions, Version, Source, Intended Use

Computer models are described in the section beginning on page 72. The molten salt-oxide thermodynamics modeling by KPM used FactSage.[10] Finite Element Analysis at INFINIUM used the open source Elmer code developed by the Finnish Center for Science (CSC).[11] Other modeling such as cost models used Microsoft Excel or similar spreadsheet software such as LibreOffice.

Model Performance Criteria

There were limited opportunities for direct observation of model predictions, such as electrical potential distribution or temperatures. These models were mainly used to determine whether designs would likely encounter significant problems with non-uniform anode current distribution or excessive localized heating.

Test Results

Results are shown in the section beginning on page 72.

Model Theory

There were two thermodynamics models and two finite element models used in this project.

Thermodynamic models generally estimated equilibrium compositions of species present in the gaseous or liquid state. Activities of all species in all phases are set equal, as are pressure and temperature, subject to total mole fractions of species set as model conditions.

Finite Element Analysis estimated first fluid flow velocity distributions in compressible argon-magnesium vapor, and then electrical potential and temperature distributions in the anodes. Anode models calculated the flow of electricity through the anode assembly, taking into account the very different conductivities of its different components.

Mathematics Used

Compressible fluid flow involved the Navier-Stokes Equations of conservation of mass and momentum:

$$\frac{D\rho}{Dt} + \rho\nabla \cdot u = 0$$

$$\rho\frac{Du}{Dt} - \nabla \cdot \bar{\sigma} = F$$

[10] See the FactSage website: http://www.factsage.com/ .

[11] See the ElmerFEM website: https://www.csc.fi/web/elmer .

In the above equations, D/Dt is the substantial time derivative $\frac{\partial}{\partial t} + u \cdot \nabla$, u is fluid velocity, ρ is density, $\bar{\sigma}$ is the stress tensor, and F is body force.

Anode models used static current conduction, which solved for current distribution based on electrical conductivity distribution assuming zero charge accumulation:

$$\nabla \cdot \sigma \nabla \phi = \frac{\partial \rho}{\partial t} = 0$$

where σ here is electrical conductivity, ϕ is electrical potential, and ρ is electric charge density. This was coupled with heat conduction through Joule heating:

$$\rho c, \partial T \text{-} \partial t. = \nabla \cdot k \nabla T + \nabla \phi \cdot \sigma \nabla \phi$$

where ρ is density, *c* heat capacity, *T* temperature, *k* thermal conductivity, ϕ is electrical potential, and σ electrical conductivity. All of these equations are peer-reviewed and used in numerous finite element analysis software packages.

Hardware Requirements

All of the modeling software in this project ran on contemporaneous hardware, mostly on a 2007 Dell laptop.

Documentation

Documentation can be found at the websites linked in the FactSage and ElmerFEM footnotes.

References

[i] Roskill, *The Economics of Magnesium Metal,* October, 2008.

[ii] U.S. Automotive Materials Partnership, *Magnesium Vision 2020,* Technical Report, USCAR, Nov. 2006.

[iii] U.S. Geological Survey, *Magnesium Compounds Statistics,* last modification August 11, 2011, http://minerals.usgs.gov/ds/2005/140/ds140-mgcom.pdf .

[iv] A. Dickson & C. Goyet eds., *Handbook of methods for the analysis of the various parameters of the carbon dioxide system in sea water; version 2,* ORNL-CDIAC-74 Chapter 5 table 6.2.

[v] Department of Energy Advanced Vehicle R&D Award Announcement and List of Projects, August 10, 2011.

[vi] "Ford Could Use Magnesium for Truck Frame," *Magnesium Monthly Review* 39(10) Nov. 30 2010 p. 2.

[vii] Christoph Koffler and Klaus Rohde-Brandenburger, "On the calculation of fuel savings through lightweight design in automotive life cycle assessments," *Int. J Life Cycle Assess.* 15:128-135, 2010.

[viii] U.S. Bureau of Transportation Studies National Transportation Statistics 2010 published at: http://www.bts.gov/publications/national_transportation_statistics/html/table_04_09.html .

[ix] U.S. Environmental Protection Agency Green Power Equivalency calculator published at: http://www.epa.gov/greenpower/pubs/calcmeth.htm#gasoline .

[x] Source: http://webbook.nist.gov/chemistry/ → Formulas "MgO" "Mg" (condensed and gas) and "O_2".

[xi] Sujit Das, "Primary Magnesium Production Costs for Automotive Applications," *JOM* 60(11):63-69 (November 2008).

[xii] Frank Field, Randolph Kirchain and Richard Roth, "Process Cost Modeling: Strategic Engineering and Economic Evaluation of Materials Technologies," *JOM* 59(10):21-32, 2007.

[xiii] US Department of Energy Contract DE-EE0003454.

[xiv] Adam Powell and Soobhankar Pati, "Multi-Physics Modeling of Molten Salt Transport in Solid Oxide Membrane (SOM) Electrolysis and Recycling of Magnesium," in Laurentiu Nastac, Lifeng Zhang, Brian Thomas, Adran Sabau, Nagy El-Kaddah, Adam Powell, Hervé Combeau, eds., *CFD Modeling and Simulation in Materials Processing* (Warrendale, PA: TMS), 2012, p. 57.

[xv] Xiaofei Guan, Peter Zink and Uday Pal, "Magnesium Recycling of Partially Oxidized, Mixed Magnesium-Aluminum Scrap Through Combined Refining and Solid Oxide Membrane (SOM) Electrolysis Processes," in Suveen N. Mathaudhu, Wim H. Sillekens, Neale R. Neelameggham and Norbert Hort, eds., *Magnesium Technology 2012* (Warrendale, PA: TMS), 2012, pp. 531-536.

[xvi] Adam C. Powell, "Zero-Emissions Energy-Efficient Magnesium Primary Production and Recycling Technologies at MOxST," in *Proceedings 2012 World Magnesium Conference* (Chicago, IL: International Magnesium Association), pp. 116-121.

[xvii] Based on 50% U.S. Magnesium chloride electrolysis at 43.6 kWh/kg, 50% Chinese Pidgeon process at 102 kWh/kg (source: Sujit Das, DOE Lightweight Materials Annual Merit Review Presentation 2011).

[xviii] William Choate and John Green, "U.S. Energy Requirements for Aluminum Production: Historical Perspective, Theoretical Limits and New Opportunities," U.S. Department of Energy, February 2003, p. 24.

[xix] John Stumbles, "Energy Use in the U.S. Steel Industry: An Historical Perspective and Future Opportunities," U.S. Department of Energy, September 2000, Tables 2, 5, 17.